UNITED KINGDOM • CHINA • MALAYSIA

Preparation and Characterisation of Hyperbranched Poly Divinyl Benzene and Star Branched Poly Lactic Acid Blends and Their Composites

By

Sumaya Farhana Kabir

(BSc., MS.)

Thesis submitted to the University of Nottingham
for the degree of Doctor of Philosophy

July 2017

This thesis is dedicated to my parents
Aziza Begum & Md. Humayun Kabir Khan

My Husband
Shaki Ahmed
&
My little Princess
Suhaima Fiona Ahmed

ABSTRACT

This thesis explored the use of hyperbranched poly divinyl benzene and star shaped polylactic acid polymers as blend constituents with their respective linear analogues and also explored the use of those blends as matrices for E glass fibre composites. Investigations into their effects on the composite mechanical properties were conducted.

Hyperbranched poly divinyl benzene (HB2) with reactive (-vinyl; $-CH=CH_2$) and hydrogenated hyperbranched polyl divinyl benzene (H-HB2) with non-reactive (ethyl; $-CH_2-CH_3$) functional groups were used in this study as blend constituents with linear polystyrene (LP), since HB2 materials were too brittle to produce films. HB2 with reactive functional groups were crosslinked at high temperature which increased the glass transition temperature (T_g), thermal stability, viscosity and the tensile modulus (only after heat treatment at 200°C) of HB2 blends (LP-HB2) in comparison to LP. On the other hand, for blends with H-HB2 (LP-H-HB2), lower T_g, higher thermal stability, lower viscosity and lower tensile modulus (even after heat treatment at 200°C) was observed in comparison to LP. However, for heat treated LP-H-HB2 80-20 (containing 20wt% of H-HB2 in blend with LP) chain end crystallisation was observed which significantly ($p<0.05$) increased the tensile modulus and strength of the blend in comparison to its value at room temperature.

From the rheological studies LP-HB2 blend was suggested to have been crosslinked across the whole temperature region, whereas LP-H-HB2 blend showed flow behaviour at lower temperature (~175°C) in comparison to LP (~190°C). Composites were then prepared using LP-HB2 and LP-H-HB2 blends as matrices and E-glass fibre

as reinforcement. No significant ($p<0.05$) improvement was observed for the composites using LP-HB2 blend due to the poor wettability of crosslinked LP-HB2 with fibre. However, a significant ($p<0.05$) improvement in flexural modulus and strength for composites prepared using LP-H-HB2 80-20 as matrix was observed in comparison to composites prepared using LP as matrix.

Six arm star PLA (SPLA) of four different mol. wt. (3,6,9 and 12 kDa) was used in this study as blend constituents with linear PLA and the blends were also used as matrices for composites manufacture with E-glass fibre as reinforcement. Blending SPLA with linear PLA decreased the T_g, T_m and T_c properties, thermal stability, % crystallinity and viscosity of the blends both at room temperature and also after heat treatment (at 175°C), however, increase in their hydrolytic degradation rate was observed. These blends when used as matrices for composites revealed significantly increased flexural moduli and strength profiles in comparison to linear PLA, which was attributed to the better wettability of the blend matrices due to their lower viscosity and crystallinity. The highest flexural modulus and strength profiles (which increased by 57% and 77% respectively) were found for composite samples prepared using blends of linear PLA with highest mol. wt. (M_n) SPLA (PLA-12 80-20-GF) in comparison to the composite with linear PLA as matrix. Moreover, increased hydrolytic degradation rate was observed for SPLA blended composites due to their lower crystallinity and also due to the presence of hydroxyl (-OH) groups at the chain ends of SPLA which promoted hydrolytic degradation rates.

ACKNOWLEDGEMENT

First of all I would like to express my gratitude to Almighty Allah for every single thing I have in my life.

My heartfelt thanks goes to Dr Ifty Ahmed, my principal supervisor who trust me and open this door for me. Without his endless support and guidance I wouldn't be able to make this journey. His utmost support and encouragement gave me the strength and courage to deal with all difficulties and to submit my thesis within the shortest possible time of my baby's birth. I would also like to hugely thank Professor Derek Irvine (my second supervisor) who showed me the pathway in this tough journey. His guidance and valuable advice helped me to decide where to go with the research. Dr Andrew Parsons aka 'Andy' helped me with advice to solve many lab problems and his suggestions helped me out of some crucial issues with my research. Many thanks to Andy. I would like say a big thanks to Professor Chris Rudd who encouraged and guided me throughout this journey.

I would also like to express my gratitude to Adlington Kevin for supplying me the polymer. I really appreciate your unconditional help and support.

I am so thankful to Gabriel Choong, Zakir Hossain and Reda Felfel for their guidance and valuable suggestions.

Huge thanks to Greaves Jason, Keith Dinsdale, Tom Buss, Johns Paul, Nigel Neate, Martin Roe, Max Mason for being supportive with every single instruments I used to collect data for my research. Special thanks to Greaves Jason for all the kind consideartions while booking schedule(s) without which I won't be able to complete my research on time.

I would also like to thank my colleagues and friends Nusrat Sharmin, Towhidul Islam, Braz De Sousa Ana, Uresha Patel, Madhavie Perera, Chenkai Zhu, Fernando Barerra Betanzos, Menghao Chen, Yunqi Wang, Fey, Simon, Ward Michael, Sabrin Samad, Anik Arafat. They were always there for me when I needed support, suggestions and companionship. It was really great working with all of them.

I am so greatful to Commonwealth Scholarship Commission for funding my studentship.

My heratiest thanks goes to Meem, Tauseef, Mou, Mithila, Towhid, Borna, Munni apu, Suheli apa, Sanchita apu, Shoma di, Tania, Sabrin, Anik, Moina bhabi, Sahrif bhai, Rabiul bhai for their unconditional love, time and support during my PhD life.

Finally, those without whom I can't just think about my existance; my mother, father, younger brother Fahim and especially my husband Shaquie, my father & mother in laws and last but not the least my lil princess Fiona, this thesis is dedicated to all of them.

ABBREVIATIONS

ASTM	American Society for Testing and Materials
BS	British Standards
DMA	Dynamic Mechanical Analysis
DSC	Differential Scanning Calorimetry
DTRT	Dynamic Temperature Ramp Test
DVB	Divinyl benzene
FTIR	Fourier Transform Infrared Spectroscopy
GPC	Gel Permeation Chromatography
HB	Hyperbranched polymer
H-HB	Hydrogenated hyperbranched polymer
ΔH_m	Enthalpy of melting
ΔH_c	Enthalpy of crystallisation
IFSS	Interfacial Shear Stress
ISO	International Standards Organisation
kDa	KiloDalton
LP	Linear Polystyrene
LF	Linear functional Polystyrene
L_0	Gauge length
M_n	Number Average Molecular weight
M_w	Weight Average Molecular weight
M_L	Mass loss
m_i	Mass of sample before degradation
m_d	Mass of sample after drying
PDI	Polydispersity Index
PBG	Phosphate Based Glass
PBS	Phosphate Buffered Saline
PCL	Poly-ε-caprolactone
PGF	Phosphate Glass Fibre
PDLLA	Poly(D,L-lactide)
PLA	Poly(lactide)

PLLA	Poly(L-lactide)
SPLA	Star shaped Poly(lactide)
SEM	Scanning Electron Microscopy
T_g	Glass transition Temperature
T_m	Melting Temperature
T_c	Crystallisation temperature
TGA	Thermo-gravimetric analysis
THF	Tetrahydrofuran
V_f %	Fibre Volume Fraction
wt%	Weight percentage
XRD	X-ray Diffraction
$\%X_c$	Percentage Crystallinity

TABLE OF CONTENTS

LIST OF FIGURES

LIST OF TABLES

CHAPTER 1

1 INTRODUCTION

1.1 Overview

Polymer matrix composites are comprised of fibres (short or long chain fibre) dispersed in an organic polymer matrix. The function of the matrix is to bond the fibres together and to efficiently transfer loads between them. To obtain desirable properties in composite materials, the applied load should effectively be transferred from the matrix to the fibres via the interface. This means that the interface must provide strong adhesion between the fibres and matrix. To achieve this strong adhesion, the fibres should be well impregnated by the matrix material. Failure of achieving a strong interface can result in loss of mechanical integrity.

The Biocomposite group at the University of Nottingham have conducted a number of studies [1-4] to address different challenges associated with resorbable polymer matrix composites. Examples have included, ensuring uniform distribution of fibres in matrices, to investigate dry fibre bundle problem, to enhance the fibre matrix interface and also reducing composite processing time to minimise the loss of polymer molecular weight due to thermal degradation. Furthermore, more recent processes currently under investigation to address these issues include in situ polymerisation [1, 4] and use of coupling/sizing agents.[3, 5]

An alternate potential solution to the issues proposed was via the use of branched polymers as matrices for preparing polymer fibre composites. The most common branched shape polymers are referred to as star-shaped, comb, hyperbranched, dendrimers etc. (please see Figure 1.1).[6, 7]

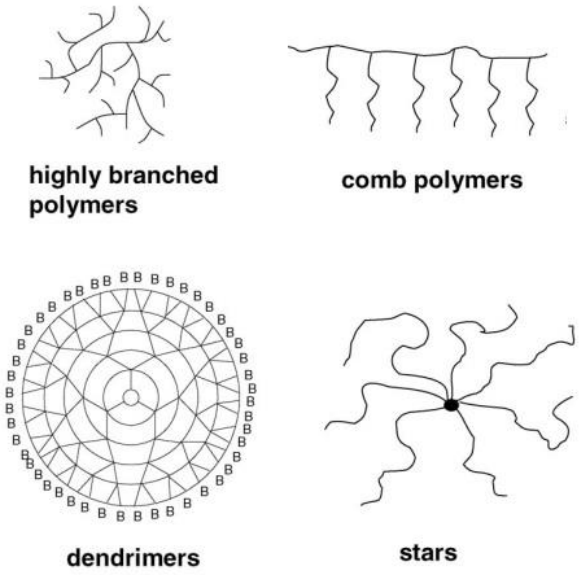

Figure 1.1: *Schematic representation of different branched polymer shapes*

Branched polymers contain more and shorter polymer chain ends than their linear counterparts of equal molecular weight.[8] The compact structure, enhances branching density and multiple tailorable functional groups can produce polymers which exhibit significantly different physico-chemical properties in comparison to linear polymers.[9, 10] For instance, these polymers possess good solubility in various organic solvents and have lower melt viscosities in comparison with their linear analogues.[9]

So, inclusion of these branched polymers was expected to provide a plasticising effect using what is essentially the same material (same chemical structure), rather than using a potentially non-compatible third party plasticiser, such as paraffin oil. This plasticising effect could help to reduce the brittleness of the composite and make melt processing easier, for example; inclusion of a filler could increase viscosity considerably and a plasticiser could help counter this effect. Additionally, branched polymers could be made to be either reactive or non-reactive by controlling their

functional groups – this provides potential for matrix crosslinking or a better matrix/fibre bonding effect during or via post-processing.

1.2 Aim and Objectives

Aim

The overall aim of this PhD project was to investigate the effects of including branched biopolymer structures as matrix components for use in composites. This project considered the effect of increasingly branched materials, from lightly branched/linear functional to hyperbranched and star structures. Furthermore, studies also investigated if the effects of branched structures could be translated between non-biopolymer and biopolymer systems.

Objectives

The objectives were as follows

1. Investigate initially polystyrene (PS)/divinyl benzene (DVB) hyperbranched materials and their properties.
2. Produce blends of hyperbranched (Poly divinyl benzene) and linear polystyrene through the solvent casting method.
3. Investigate the thermal, thermo- mechanical, mechanical and rheological properties of the above polymer blends.
4. Investigate the literature for development of hyperbranched biopolymer structures.
5. Investigate star PLA structure and their effect as blend components with linear PLA.
6. Investigate the thermal, thermo- mechanical, mechanical and rheological properties of these biopolymer blends.

7. Produce and characterise composites using both hyperbranched DVB and star biopolymer blends as matrices and E-glass fibre as reinforcement.

1.3 Thesis Structure

The objectives listed above have been divided into respective chapters as follows:

Chapter 1 Introduction and Overview

Chapter 2 Review of the literature for hyperbranched (HB) polymers, blends and composites developed utilising HB polymers and star Poly lactic acid (SPLA) polymer, blends and composites with SPLA.

Chapter 3 Describes all the materials and methods used in this study.

Chapter 4 This chapter investigated the thermal and thermomechanical characterisation of linear polystyrene (LP) and blends of LP with hyperbranched polymers of two different mol. wt. HB1, HB2, hydrogenated hyperbranched (H-HB2) and linear functional LF poly divinyl benzene.

Chapter 5 This chapter describes the rheological and mechanical properties (at room temp. and heat treated) of LP and its blends and the mechanical properties of the composites developed using these polymer materials.

Chapter 6 The thermal, thermomechanical, crystallinity and hydrolytic degradation of linear polylactic acid (PLA) and blends of linear PLA with star PLA (SPLA) of four different mol. wt. (both at room temperature and heat treated) were investigated in this chapter.

Chapter 7 This chapter describes the rheological, mechanical properties SPLA blends (both at room temperature and heat treated). The mechanical, crystallisation and hydrolytic degradation of composites were also investigated in this chapter.

Chapter 8 This chapter presents a synergistic summary bringing together the main conclusions and recommended areas for further research.

1.4 References

1. *Habeb, R., et al., Fabrication effects on properties of composites for medical applications: 1. composite preparation and characterization. Journal of Reinforced Plastics and Composites, 2010.* ***29****(1): p. 112-122.*

2. *Haque, P., et al., Influence of compatibilizing agent molecular structure on the mechanical properties of phosphate glass fiber-reinforced PLA composites. Journal of Polymer Science Part A: Polymer Chemistry, 2010.* ***48****(14): p. 3082-3094.*

3. *Hasan, M.S., et al., Investigating the use of coupling agents to improve the interfacial properties between a resorbable phosphate glass and polylactic acid matrix. Journal of Biomaterials Applications, 2013.* ***28****(3): p. 354-366.*

4. *Habeb, R., et al., Fabrication effects on properties of composites for medical applications: 2-retention of composite mechanical properties. Journal of Reinforced Plastics and Composites, 2010.* ***29****(12): p. 1804-1813.*

5. *Haque, P., et al., Interfacial properties of phosphate glass fibres/PLA composites: Effect of the end functionalities of oligomeric PLA coupling agents. Composites Science and Technology, 2010.* ***70****(13): p. 1854-1860.*

6. *Seiler, M., Hyperbranched polymers: Phase behavior and new applications in the field of chemical engineering. Fluid Phase Equilibria, 2006.* ***241****(1): p. 155-174.*

7. *Klok, H.A., et al., Synthesis and solid state properties of novel fluorescent polyester star polymers. Macromolecular Bioscience, 2003.* ***3****(12): p. 729-741.*

8. *Helminen, A., Branched and crosslinked resorbable polymers based on lactic acid, lactide and ε-caprolactone. 2003, PhD thesis. Helsinki University of Technology.*

9. *Aloorkar, N., et al., Star polymers: an overview. Int. J. Pharm. Sci. Nanotechnol, 2012.* ***5****(2): p. 1675-1684.*

10. *Mulkern, T.J. and N.C. Tan, Polystyrene/hyperbranched polyester blends and reactive polystyrene/hyperbranched polyester blends. 1999, DTIC Document.*

CHAPTER 2

2 LITERATURE REVIEW

2.1 Hyperbranched Polymers

The unique structure of hyperbranched (HB) polymers can be characterised by a core with a high local concentration of branching points with chain ends at the periphery (Figure 2.1).[1-3] Due to their unique architecture, HB macromolecules can possess unusual properties.[3] For instance, HB polymers exhibit extremely high solubility in various organic solvents and low intrinsic viscosities in comparison with their linear counterparts.[3, 4]

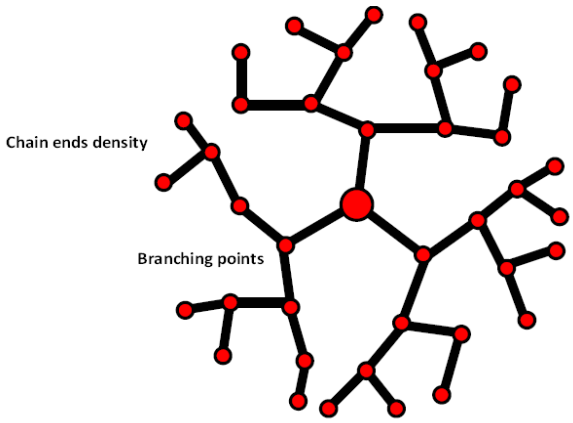

Figure 2.1: *Schematic configuration of a hyperbranched (HB) polymer.*

2.2 Properties of HB polymers

2.2.1 Thermal properties

HB polymers are mostly referred to as amorphous polymers (unless the polymers have been modified to induce crystallinity) since branching reduces their ability to crystallise as linear polymers.[5] In this regard, glass transition temperature (T_g) is one of the most important thermal properties of HB polymers.

In comparison to linear polymers, the T_g of a HB polymer is dependent on many factors, for instance, the number and chemical nature of its end groups, branching points, the compactness of the structure etc.[1, 6] The T_g of HB polymers has been reported to decrease with increasing end-group free volumes and to increase with increasing polarity of end groups and branching density.[7]

Kim and Webster [8] proposed that the T_g of HB polymers depended more on the chain length between the branching points rather than the molecular weight. On the contrary, Frechet *et al.* [9] stated that the T_g of HB polymers is mainly affected by the chain end structure and molecular weight. Voit [6] demonstrated that the T_g of HB polymers was independent on the molecular architecture and dependent mainly on the nature of the end groups. Their observation was supported by the study of Hawker and Chu [10] who investigated the influence of chain end groups on the T_g of HB polymers. They prepared HB poly(ether ketones) with different degree of branching and end groups such as fluoro, hydroxy, and benzophenone groups. They demonstrated that the T_g of HB polymers were independent of macromolecular architectures, and instead strongly depended on the nature of the chain end groups. Voit [11] also investigated the effect of the chemical nature of the end groups on T_g and revealed that an aliphatic polyester generally had a much lower T_g than an aromatic one.

Elrehim *et al.* [12] studied the thermal properties of HB poly(urea urethane)s modified with aliphatic, aromatic chain end groups. For HB polymers of the aromatic chain end group, they observed higher T_g value at 93°C than the HB with aliphatic

chain end group (T_g at 73°C) and stated that the bulky phenyl groups hindered the polymer chain motions and thus increased the T_g.

They also studied the thermal stability of aliphatic and aromatic chain ended HB polymers and found lower thermal stability (10% weight loss was observed at 207°C) for HB with aromatic chain end group than the HB polymer with aliphatic chain end group (with 10% weight loss observed at 234°C).

Effect of chain end group on the thermal properties of HB was also studied by Shanmugam *et al.*[13] They prepared HB aromatic poly(ether-ester) with terminal benzyl alcohol groups and then modified the chain end groups with benzyl carbamate and decyloxy benzoate. For the HB polymer with benzyl carbamate and decyloxy benzoate chain end group they found lower T_g values at 155°C and 118°C respectively than the T_g of HB with a benzyl alcohol chain end group at 245°C. They attributed this low T_g value to the flexible alkyl chains at the surface of the HB polymer.

Shanmugam *et al.*[13] also measured the thermal stability and found higher thermal stability for the end group modified HB polymer in comparison to the unmodified polymer. Both the modified end group and unmodified HB polymer underwent thermal decomposition in two distinct stages. The first stage started around 255°C and 288°C, and the second stage started around 389°C and 416°C for HB with benzyl carbamates and decyloxy benzoate respectively whereas for the unmodified HB, these values were 218°C and 350°C respectively.

The effect of polar (hydroxyl; -OH) and non-polar (aliphatic n-alkyl) chain end group on the thermal properties of aromatic HB polyesters was studied by Schmaljohann *et al.* [14] They observed a decrease in T_g value for HB with non-polar chain end group

than the HB with polar one. They suggested that the decreases in T_g for non-polar chain end HB were due to the reduced intermolecular interactions from hydrogen bonding of polar -OH chain end groups. For HB polyester with polar -OH functional group the T_g was reported to be at 218°C which then decreased to 160°C and 180°C via C12 and C16 alkyl chain end modification.

However, no complete model has been presented to predict the T_g of HB polymers. As such, it can be summarised that the T_g of HB polymers is a function of mol. wt., the number, nature (polarity) and the steric hindrance of chain end-groups, the degree of branching and amount of cross-links. All of these properties in combination have been shown to play an important role on the glass transition temperature of HB polymers.[15]

2.2.2 Glass Transition Temperature (T_g) of HB polystyrene

Akabori *et al.* [16] carried out a study to see the effect of chain end and mol. wt. on the T_g value of hyperbranched polystyrene (HBPS). They compared the T_g value of HB polymer with two different end groups; HB with dithiocarbamate (DC) end groups (HBPS–DC) and HB with hydrogen (H) termini (HBPS-H) and obtained much lower T_g values for the HBPS–DC at 335K than that of the HBPS-H at 364K of similar mol. wt. To study the effect of mol. wt. they prepared HBPS-H of two different mol. wt. (M_w; 47 and 157 kDa) by substituting HBPS–DC and compared their T_g value to the linear polystyrene (LPS) of equivalent mol. wt. They observed lower T_g value at 364K for HBPS-H of low mol. wt. than the LPS of equivalent mol. wt. at 375K. However, they also reported higher T_g values at 376K for HBPS-H of high mol. wt. than the lPS of equivalent mol. wt. at 375K. They explained that the lower T_g of HBPS-H was expected

due to the large number of chain end groups. However, they attributed the higher T_g value of HBPS-H to the development of a cyclic (crosslinked) structure in the high mol. wt. HBPS. They concluded that the T_g value of HB polymers was determined by not only the chain end and branching effects, but also the presence of intramolecular cyclisation.

2.2.3 Rheological properties

One of the more interesting properties of HB polymers is their low viscosity in comparison to their linear analogues.[17-19] This low viscosity was reported to be due to less entanglement of the HB polymer chains.[18]

The relationship between melt viscosity and molecular weight of linear and HB polymers is shown schematically in Figure 2.2. The viscosity of linear polymers is known to increase linearly up to a certain molar mass, called critical molar mass, M_c. However, for HB polymers, the increase in viscosity was less pronounced and levelled off at a certain higher molecular weight (see Figure 2.2 below).[20]

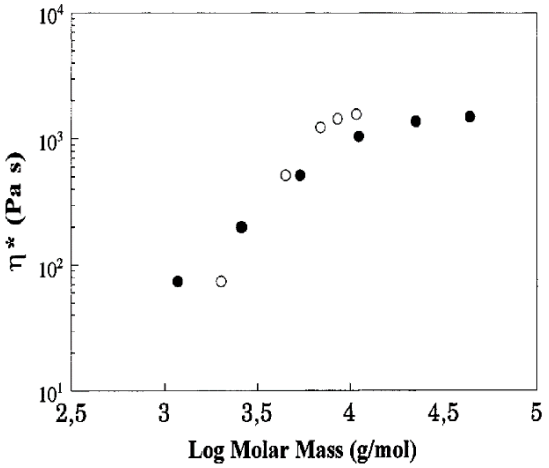

***Figure 2.2**: Schematic diagram for the relationship of melt viscosity at 85°C vs log molar mass for hydroxyl functional HB aliphatic polyesters based on bismethylol propionic acid (o) linear and (●) HB polymers. [21]*

The nature of the end-groups was also reported to affect the melt behaviour of HB polymers. It has been reported that an increase in the polarity of the end-groups increased the viscosity of HB polymers due to the interaction between the polar chain end group.[14, 22, 23] Schmaljohann *et al.*[14] studied the melt rheology of the HB polymer with polar (-OH group) and non-polar (aliphatic n-alkyl) chain end group. They found a strong decrease in the complex viscosity for HB polymer with non-polar chain end group (2800 Pa.s at 1 rad/s) than the HB polymer with polar group (20,000 Pa.s at 1 rad/s).

Hsieh *et al.*[24] studied the rheological behaviour of a series of aliphatic HB polyesters, with different molecular weights (2.1, 3.5, 5.1 and 7.5 kDa named as H20, H30, H40 and H50 respectively) in the molten state. They observed shear-thinning behaviour for low mol. wt. H20 and H30 polymers and Newtonian behaviour for high mol. wt. H40 and H50 in both oscillatory and steady shear measurement. They explained that although HB polymers were reported to show Newtonian behaviour due to the lack of polymer chain entanglement, for H20 and H30 polymer shear thinning behaviour was observed which was not due to polymer chain entanglement but rather the presence of polar interactions between the numerous peripheral hydroxyl groups.

On the other hand, for H40 and H50 they observed Newtonian behaviour due to the absence of strong polar interactions since high mol. wt. HB polymer contained lower concentration of hydroxyl units. They explained that for high mol. wt. HB polymers, with increasing mol. wt. the polymer branches were more flexible and folded back

into less polar end groups which were exposed to other molecules and caused less polar interactions.

Shanmugam *et al.* [13] also measured the viscosity of end group modified (with benzyl carbamates and decyloxy benzoate) HB aromatic poly(ether-ester)s and reported higher viscosity for these HB polymers than for the end group unmodified HB polymer (with benzyl alcohol) and stated that bulky benzyl carbamates and decyloxy benzoate groups at the polymer chain ends increased the polymer viscosity.

2.2.4 Mechanical properties

HB polymers caused poor mechanical properties and brittleness due to absence of polymer chain entanglement [25] and this property has restricted the use of HB polymers to applications where mechanical properties are of less importance.

Schmaljohann *et al.* [14] determined the mechanical properties of HB polyester modified with aliphatic C12-alkyl chain end group. From DMA analysis they reported a very low modulus of the film produced (E'< 1000 MPa) and attributed this low mechanical properties to the lack of polymer chain entanglement of HB polymer compared to linear polymer counterparts.

2.3 HB polymer blends

Exploitation of the unusual properties of HB polymers has shown their uses in a vast range of areas and applications. For example as coatings, adhesives, additives and as carriers of dye molecules.[2, 26] However, almost all of these applications require the use of HB as a polymer blend constituent due to their inevitable mechanical brittleness (due to the lack of polymer chain entanglement).[27] Therefore, blending

of HB with other conventional (linear) polymer counterparts has been investigated to achieve films with useful properties.[28]

To date, HB polymers have been used as a blend material for imparting or modifying different properties. HB polymer was reported to be blended with thermoplastic to act as lubricants, processing aids [29-31] and compatibiliser [32, 33] for thermoplastic resin, to act as additives for epoxy thermoset resins [34, 35] and as a crosslinking agent for both thermoplastic and thermoset epoxy.[30, 36]

2.4 Blends of HB polymer with thermoplastic

Diao *et al.* [33] added HB poly(amide-ester) to the blend of poly (acrylonitrile-butadiene styrene)/poly(vinylchloride) to act as compatibiliser. They reported that small quantities of HB had a significant effect on the mechanical properties (the tensile strength of the blends had increased from 41.6 MPa to a maximum value 43.2 MPa for addition of 2 phr (part per 100) HB and thus improved the compatibility of the blends.

They again prepared blends of polypropylene/poly(vinyl chloride)/hyperbranched poly(amide-ester) (PP/PVC/HB) and investigated their mechanical and rheological properties. They reported an increase in tensile strength values (from ~23.5 to ~26.5 MPa) and a decrease in the viscosity of the blends on addition of 3 phr HB poly (amide-ester). They concluded that the HB behaved as a processing aid due its molecular structure and caused lower viscosity of the melt and solution in comparison to their linear counterparts. [32]

Hong *et al.* [37] also investigated the role of HB polymers as processing aids for linear ow-density polyethylene (LLDPE). In their first attempt they prepared a blend of LLDPE and trace levels of HB (0.05%) and showed that the power requirements for extrusion processes had significantly decreased (they observed a 16.5% reduction in specific mechanical energy) as a result of reduced viscosity of the blend.

In their second study Hong *et al.* added 0.5wt% HBP as a processing aid for linear low-density polyethylene (LLDPE) in the tubular film blowing process and reported an enhanced processing rate (for extrusion process, the mass flow rate increased to 3.5kg/h on addition of 0.5wt% HBP with LLDPE whereas for neat LLDPE the mass flow rate was 2.5 kg/h). [31]

For polystyrene, Mulkern and Tan [30] used HB polyol of low viscosity as processing aid and reported a significant drop in blend viscosity on addition of trace level (2 vol%) of HB with polystyrene.

Blends of HB polymers have also been studied to increase the mechanical properties of thermoplastics. Zhang and Sun [38] investigated the mechanical properties of poly (lactic acid) (PLA) blended with 2wt% HB polymer. They reported increased tensile strength and elongation at 70.8 MPa and 5.16% respectively in comparison to than neat PLA (at 57.6 MPa and 3.33%). However, they observed a decrease in tensile strength and elongation at 38.7 MPa and 2.9% respectively for addition of 10wt% of HB. They explained that the improved mechanical properties were due to strong hydrogen bonds between HB and PLA and crystallinity produced by nucleation of HB, which decreased at higher wt% of HB due to the stereo-hindrance effect of inhomogeneous HB.

Massa *et al.* [39] investigated the blends of hydroxyl phenyl and acetoxy phenyl-terminated HB polyesters with different linear polymers such as polycarbonate, polyesters and polyamides. They reported that blending polycarbonate with hydroxyl and acetoxy-terminated HB polyesters increased the tensile modulus by 32% and 15% respectively. However, the elongation at break decreased from 82% to just below 3% for both blends. They concluded that HB polyesters acted as reinforcing agents in the blends due to their high aromaticity and stiffness.[39]

The mechanical properties of blends of polypropylene with HB polyester was investigated by Schmaljohann *et al.* [40] They conducted DMA measurements and reported lowest storage modulus *E'* (~10^3) for neat HB polyester, whereas this value increased comparatively *E'* (~10^4) for both linear polypropylene and blends. They attributed the low storage modulus of neat HB to the lack of crystallinity and the absence of entanglements in HB polymer. They [40] also measured the zero shear viscosity of neat polymers (HB polyester and polypropylene) and blends at 200°C and observed very low zero-shear viscosity for HB at 19 Pa.s whereas for polypropylene and blends (containing 10wt% of HB polyester) they found values at 800 Pa.s and 480 Pa.s respectively. They attributed this low viscosity of neat HB to its globular structure, absence of entanglements, and also the absence of polar interactions (from -OH chain end group) due to the presence of alkyl chain end group.

For melt viscosity, at 200 °C, they observed viscous behaviour for neat polymers and blends (loss modulus (*G''*)> the storage (*G'*)) rather than an elastic behaviour which indicated that the polymers and blends were extremely fluid at that temperature. Nunez *et al.*[41] measured the solution viscosity of HB polyesters and their blends

with linear polymer (poly (2-hydroxyethyl methacrylate)). They observed Newtonian behaviour for HB polyester solutions which they attributed to the absence of physical entanglements in the HB polymer.

They [41] also reported lower solution viscosity for both neat HB polyesters and blends than that of the linear polymer. They explained that the absence of chain entanglements and denser structures of the neat HB decreased the number of physical entanglements between linear polymers in blends which caused lower solution viscosity. For example the solution viscosity of linear polymer was ~40 Pa.s and on addition of 10wt% of HB the value for the blend was decreased to ~10 Pa.s and on addition of 40wt% this value decreased to ~1Pa.s. Kim and Webster [8] blended HB polyphenylene with polystyrene and reported that the melt viscosity decreased by 50% at 180°C with addition of 5wt% HB in comparison with that of the control polystyrene.

2.5 Blends of HB polymer with Epoxy/thermosets

Epoxy resins have successfully been toughened by blending them with rubbers and thermoplastics.[42] However, these blends have suffered from increased viscosity, and decreased tensile and flexural strengths.[43] In this regard, HB had proved to be a promising material due to its low viscosity (suggested to be due to lack of chain entanglements) even at high mol. wt. and tailorable functional groups which facilitated enhanced matrix adhesion and better interfacial properties.[42, 44]

Varley and Tian [42] cured epoxy/HB blends and observed two phases (an epoxy rich phase and a HB-rich phase) in the cured blends and reported increases in toughness from 0.50 $MPa(m)^{1/2}$ (for the cured neat epoxy resin) to 0.96 $MPa(m)^{1/2}$ (for the cured

blend containing 20wt% HB). They explained that HB had a greater range of interactions with the matrix and hence increased the ability to transfer stress to the particle and increased the fracture toughness. However, they also found a decrease in flexural modulus and strength with increasing HB content in the blends and stated this was due to increased plasticisation of the HB polymer on the cured network. They also studied the viscosity of the blends with temperature ramping and found a very low viscosity (~5Pa.s) at ~30°C followed by a rapid increase in viscosity (~10^4 Pa.s) when the blend was cured at~120°C.

An increase in fracture toughness to 3.20 MPa$(m)^{1/2}$ for a cured blend (containing 9wt% of aromatic HB) in comparison to the neat epoxy (fracture toughness ~1.8 MPa $m^{1/2}$) was demonstrated by Zhang and Jia.[43] They attributed this increase in toughness to the chain rigidity and intramolecular defects of the HB polymer which absorbed more impact energy. Furthermore, they found an increase in tensile strength for the cured blends at 78.24 MPa whereas the neat epoxy value was 64.74 MPa. They stated that chain rigidity and crosslinking of HB had increased the tensile strength.

To examine the effect of the polymer architecture as epoxy modifier, Wu *et al.* [45] blended epoxy with HB polyester oligomers and with a linear thermoplastic which also contained a structure similar to that of the HB. They obtained similar viscosity at 0.17 Pa.s and 0.18 Pa.s for blends containing 50wt% HB and thermoplastic respectively. They also observed similar fracture toughness at 0.7 MPa $m^{1/2}$ and 0.63 MPa $m^{1/2}$ for the HB and linear thermoplastic modified epoxy respectively and

contrary to the studies above suggested that the HB architecture did not have an advantage in viscosity or toughness over a low molecular weight linear thermoplastic.

2.6 Fibre reinforced thermoplastic composite production techniques

Fibre-reinforced polymer matrix composites consist of polymer matrices imbedded with reinforcing fibres.[46, 47] Here, fibre is the load-bearing component, which have higher strength and modulus than the matrix material [48, 49] and the matrix uniformly distribute the applied load and transfer the load to fibre.[49] The matrix used can be either thermoset or thermoplastic polymer. For thermoplastic fibre reinforced composites, fibres used are of usually made of carbon, glass and matrices used are thermoplastic polymers such as nylon, polypropylene or high performance thermoplastics, such as polyetheretherketone (PEEK), polyethermide (PEI).[48, 50]

Thermoplastic composites production techniques depend on the starting fibre length of the precursor material, i.e. short fibre, long fibre and continuous fibre (woven, braided, interlaced) thermoplastic composites. For example, for short fibres (typically ,3 mm long), processes such as injection moulding, extrusion moulding; for long fibres (3– 25 mm long), compression moulding, extrusion compression moulding and continuous fibres, pultrusion, filament winding, diaphragm forming techniques are widely used.[51, 52]

The commonly used production techniques for continuous fibre reinforced thermoplastic composites are discussed below

Pultrusion

The term “pultrusion” is the combination of the words “pull” and “extrusion”. This is an automated, highly productive process which allows for the fabrication of

continuous length composites of a constant cross-section.[47, 51] This process integrates reinforcement impregnation with composite consolidation.[53]

A thermoplastic pultrusion machine (Figure 2.3) typically consists of a creel, a guide pate, a preformer, pultrusion die (consists of hot and cold dies) and a pulling mechanism. In this process, the reinforced fibres (in the form of tape, woven, and/or mat) are pulled from a creel through a resin bath where they are wetted and impregnated with liquid resin. The wet fibres then pass through a preforming guide system where the excessive resin is squeezed out from fibres and then through the pultrusion die (consists of hot and cold dies). The composite is heated in the hot die and consolidated in the cold die.[51] A cooling system is indispensable for manufacturing of thermoplastic matrix composites to ensure stable cross-sectional dimensions in final product,[51] which is not needed for thermoset matrix composites.

Upon exiting the die, the composite is fully shaped and solidified. Finally, the finished product is cut on the desired length by the cut-off saw. A schematic of the process is shown in Figure 2.3

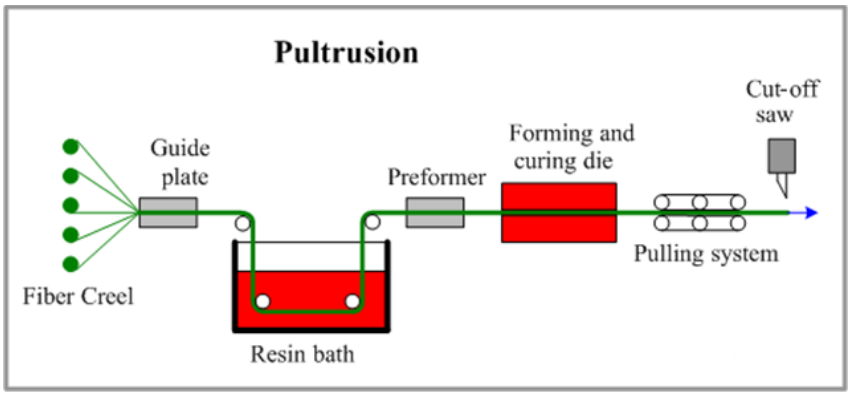

***Figure 2.3**: A schematic representation of the pultrusion process [54]*

Composites with thermoset and thermoplastic matrices can both be pultruded. Pultrusion of thermoset matrix composites is a well known and commercially established manufacturing method, whereas there has been less work on pultrusion of thermoplastic composites.

Advantages:

- Thermoplastic resin pultrusion is more advantageous in comparison to the thermoset resin, since no further chemical reactions are needed and as a result the processing steps are fewer in numbers.[50]
- Pultruded thermoplastic composites can be post-formed or joined, e.g. by welding, making further processing of profiles very much easier.[51]

Limitations:

- The limitations with thermoplastic resins are their higher melt viscosities (two to three orders) in comparison to thermoset resin, which leads to poorer fibre wetting and thus to poorer product properties.[51]
- Unlike the thermoset matrix composites dies, a thermoplastic matrix composite die assembly needs to have a cooling system to ensure the stable cross-sectional dimensions in final product. [55]

Filament winding (FW)

This is another continuous process, where a continuous filament of reinforcing material/ fibres are wrapped around a rotating mandrel in layers to obtain the desired part thickness.[51, 53] If a liquid resin is applied on the filament prior to winding, the process is called wet filament winding and if the resin is sprayed onto the mandrel with wound filament, the process is called dry filament winding.[56]

In this process, a preheater is used to heat the material to the process temperature. Moreover, a heating system is also used for heating the mandrel to avoid any preliminary thermal degradation of the matrix. The fibre rovings are pulled through a resin bath immediately before being wound onto the mandrel. The pulling tension on the continuous fibres and the heating source temperature are directly related to the impregnation and consolidation.[51] A consolidation roller is used for compaction. Heat and pressure are applied at the contact point of the roller and the mandrel for melting and consolidation of thermoplastics. The bonding between the incoming preform and the laminate is obtained by melting the matrix and applying a pressure gradient normal to the mandrel surface at the contact point.[53] A schematic of the process is shown in Figure 2.4

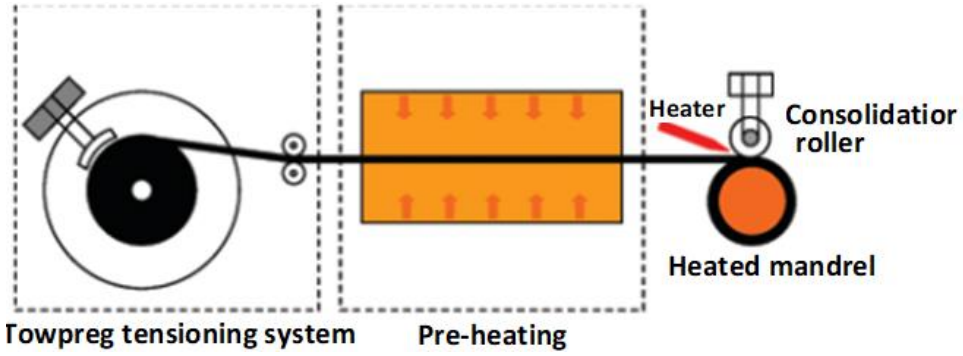

***Figure 2.4**: A schematic representation of the filament winding process*[51]

Advantages:

- Filament winding is one of the most cost effective processes used for manufacturing fibre reinforced composites.[57]
- There are some unique advantages associated with thermoplastic FW.[50] First, non-symmetrical winding patterns are possible because of the rapid solidification of the matrix after tape deposition.

Second, since no autoclave is required for curing, there is no practical limit to the size of thermoplastic filament wound structures.

- No secondary processing (e.g., oven curing) is necessary because the resin impregnated fibre bundles are continuously oriented, laid down and consolidated onto the tool surface in a single step.[57]

Limitations:

- The process is complicated because it requires a localized heat source and a consolidation roller.[51]

2.7 Techniques to probe the fibre-matrix interface

The fibre–matrix interfacial shear strength (IFSS) is defined as the amount of stress required to debond the fibre from the matrix by applying a shear force [58] and is an important criterion for selecting the fibre and matrix in making a composite.

There are three main methods used to investigate interfacial properties:

- Single fibre fragmentation test (SFFT)
- pull-out/ microbond test
- and short beam test

There are many advantages and disadvantages for each test method and the debate on which method is most effective is ongoing.[59, 60]

Single Fibre Fragmentation Test (SFFT)

The SFFT method was originally proposed by Kelly and Tyson [61] for fibre/metal composites and is one of the most frequently used methods for calculating interfacial shear stress (IFSS).[62, 63] In this method, a single fibre is embedded in a matrix in the shape of a dog bone and is axially loaded in tension as shown in Figure 2.5.[61]

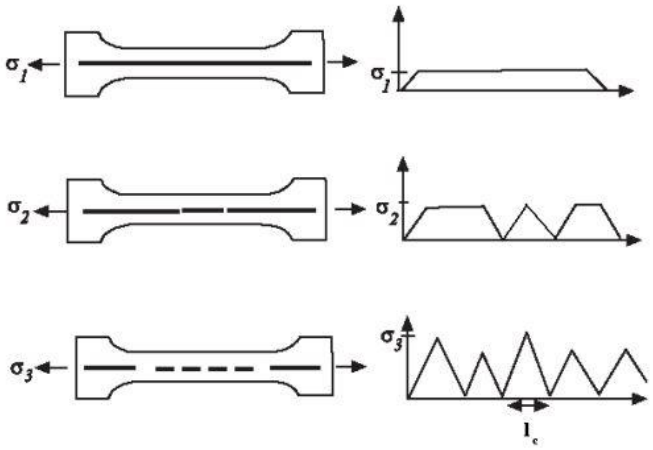

***Figure 2.5**: A schematic representation of the single fibre fragmentation test (SFFT)[63]*

During the test, the tensile stress from the matrix is transferred to the fibre and when the tensile stress in the fibre exceeds its fracture strength, the fibre fragmentation begins. As the applied load progressively increases, the fracture process repeats itself producing shorter and shorter fragment lengths until the remaining fragment lengths are no longer sufficient in size to produce additional fibre fracture through this stress transfer mechanism. The shorter the fragments are, the better the adhesion is.

When the fibre lengths become too short, the shear stress along their lengths can no longer causes any further failures. The shortest fragment length is known as the critical fibre length and is used to calculate the IFSS, τ_i, using the following equation developed by Kelly-Tyson in 1965.[61]

An average shear strength τ_i can be determined from a simple balance of force as shown in equation 2.1

$$\tau_i = \frac{d\sigma_f}{2L_c} \qquad (2.1)$$

where σ_f is the fibre strength, d is the fibre diameter and L_c is the critical fibre fragment length. The stress distribution along the fibre-matrix interface is assumed to be constant and the fibre strength assumed to have negligible variability. [63, 64]

Advantages:

- Direct observation of interfacial events
- State of stress is similar to that in the composite
- Many data points with few specimens
- Sensitive to interfacial conditions

Limitations:

- Difficult and time consuming to prepare samples
- Matrix strain needs to be greater than three times that of fibre strain, so this method can only be used for certain fibre-matrix combinations

Pull-out/MicrobondTest

The microbond experimental test method was developed by Miller *et al.* [65] in the early stages of composite research and is considered to be the most direct method to calculate IFSS. This method consists of first applying a resin drop onto the surface of a single fibre, curing the fibre-resin system to form the droplet, and then applying a shearing force to pull the fibre out of the droplet or vice-versa. A schematic of the test set up is shown in Figure 2.6. Here, a fibre is embedded in a matrix block of known geometry that is held in place while a force is applied to the fibre to pull it from the matrix (Figure 2.6(a)).

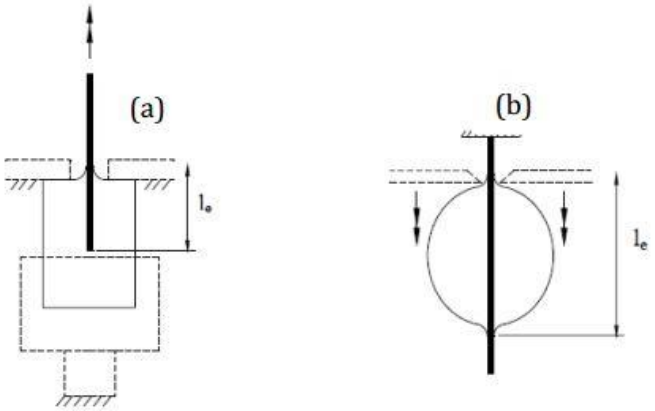

Figure 2.6: *Schematic showing a) Pull-out test from a block of matrix and b) Microbond test with polymer droplet* [66]

The fibre diameter and the embedded length are measured with an optical microscope to compute the embedded area, which is the surface area of the fibre in contact with the resin. The applied load and displacement are monitored until the fibre is pulled out of the matrix or the fibre breaks. The maximum load at which the complete debonding of the interface occurs is defined as the debonding force and is used to compute the IFSS using equation 2.2 assuming that the shear stress is constant along the embedded length,

$$\tau_i = \frac{F}{\pi d l_e} \tag{2.2}$$

where F is the debonding load, d is the fibre diameter and l_e is the fibre embedded length.

Advantages:

The sample preparation for this method is considered to be simpler than other techniques and requires smaller amounts of material.

Unlike the SFFT, this method can be used with any fibre/matrix combination

Limitations:

One of the difficulties with this method is ensuring that the droplets of polymer are similar in size and that the polymer droplet is more or less uniformly distributed around the fibre. So, a large number of samples need to be prepared for testing which can be time consuming especially considering that any sample that fails at the meniscus cannot be included in the calculation.

Short beam shear test

Short Beam Shear test is also used to determine the interlaminar shear strength of fibre reinforced composites.[67] It makes use of the fact that shear stresses always occur in a flexure test.[68]

In this test method a beam specimen is loaded in three-point bending, as shown in Figure 2.7. The term "short beam" indicates that the support span length, *s*, is a low multiple of the specimen thickness, *t.*[69] The aim is to force the beam specimen to fail in a shear mode. If the span is small in comparison to the specimen thickness, the shear stresses that occur are very large in comparison to the normal flexural stresses generated by the bending moment.[68, 69] Thus, the shorter the beam, the greater the shear stress relative to the bending stresses.[68]

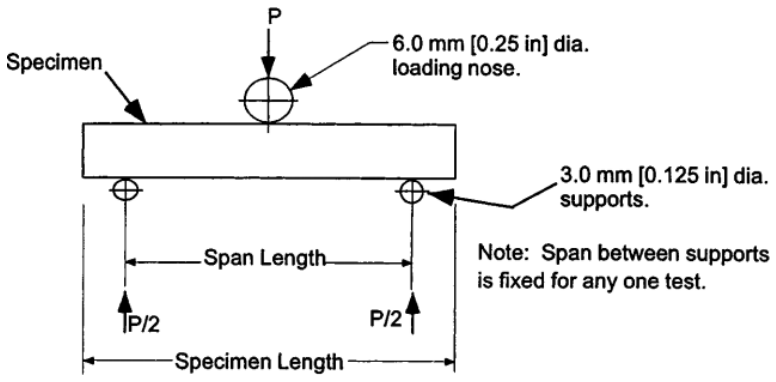

***Figure 2.7**: A Schematic representation of the short beam test*

The thickness and width of the test specimen are measured before conditioning. The specimen ends rest on two supports and the load is applied by means of a loading nose directly centred on the midpoint of the test specimen. The loading nose is then used to flex the specimen at a specified speed per minute until breakage. The onset of damage of the specimen is characterised by a sharp drop in the load-displacement curve. The maximum load is then recorded and the short-beam strength can be calculated using equation 2.3 as follows [70]

$$F = 0.75 \times \frac{P_m}{b \times h} \tag{2.3}$$

where F is the short-beam strength, P_m is the maximum load observed during the test, b is the measured specimen width and d is the measured specimen thickness.

Advantages:

This test method is relatively simple to employ.

This method requires a simple tool

Limitations:

In textile fabric composites the waviness of fibre reduces the compression strength and causes the compression failure on the loading side. [71]

The brittle matrix composites are crushed under the loading head. [72]

2.8 Composites with HB

Functionalised HB polymers were reported to be used as matrix modifiers for both thermoset and thermoplastic polymer matrix composites. For thermoset composites, the HB was used as modifiers to increase toughness [73-75] and for thermoplastic composites was mostly used to improve the fibre/matrix adhesion.[76, 77]

Gustav *et al.* [77] produced polypropylene (PP)/glass fibre composites and investigated the influence of matrix modification on the interfacial shear strength (IFSS) of the composites. To increase the interfacial strength in polypropylene composites they used two different matrices; a highly reactive HB polymer grafted PP matrix and a maleic anhydride grafted PP matrix. They reported the IFSS of composites were 20 MPa, 19 MPa and 15 MPa with HB polymer grafted PP matrix, maleic anhydride grafted PP matrix and neat PP matrix respectively. They attributed this increase in IFSS to higher diffusivity of the HB polymer grafted PP matrix which led to 22% more PP molecules located at the matrix/fibre interface and to react at the fibre surface. They explained that this higher diffusivity of HB polymer grafted PP matrix was to be due to the solubility difference between the PP matrix and HB polymer which induced a high diffusion driving force.

A HB polymer was also used as a compatibiliser for sisal fibre/polypropylene (PP) composites by Lu *et al.*[76] They reported better flexural strength (42.6 MPa) and modulus (2.13 GPa) for composites containing 2 wt% HB modifier in comparison to the neat PP composite at 35.7 MPa and 1.8 GPa respectively. They attributed this higher mechanical properties of HB modified composite to better distribution of sisal fibre in polypropylene matrix.

Wong *et al.* [78] used blends of HB polyester and polylactic acid (PLA) as matrix of PLA- flax fibre composites. They reported that the elongation of the composites (containing 50% v/v HB polyester in matrix) had increased to 0.22% and the tensile modulus decreased to 5.73 GPa whereas this value for neat PLA matrix composite was found to be 0.07% and 11.92 GPa respectively. They attributed this increase in

elongation and decrease in modulus of the HB matrix modified composite to low crystallinity of the HB. They explained that low crystallinity of HB suppressed the crystallinity of PLA and caused a plasticising effect that increased the elongation and decreased the modulus value.

For thermoset matrix composites, HB polymers were used mainly due to their varying functional groups which could be tailored with reactive and suitable functional groups so that they can be made compatible with the surrounding matrix material and thus ensure appropriate stress transfer capacity between the fibre and the matrix.[74] Verrey *et al*.[73] produced carbon/epoxy composites by resin transfer moulding (RTM) using a matrix epoxy resin and HB polymer blends. They observed that for the HB modified resin based composite the interlaminar shear strength (G_{Ic}) only increased to 750 J/m^2 in comparison to the value of the neat epoxy matrix composite at 600 J/m^2. They attributed this small increase to poor bonding between the fibre and the matrix. They argued that for carbon–epoxy composites, the usual epoxy-compatible sizing agent for the fibres contained amine groups which promoted bonding of the resin to the fibres. However, during the curing process HB consumed most of the amine and poor interfacial bonding was observed since the amine had locally depleted.

DeCarli *et al*. [75] produced carbon/epoxy composites using matrix which was a blend of epoxy and epoxy functionalised HB polymer. They observed increases in fracture toughness, however, a decrease in interlaminar shear strength, flexural modulus and strength was also observed. For example, for neat epoxy resin the flexural modulus, strength and interfacial shear strength was 107 GPa, 851 MPa and 47 MPa

respectively whereas for composites with 10wt% HB in matrix this value was found to be decreased at 96 GPa, 740 MPa and 37 MPa respectively. They suggested that there may have been some agglomeration of the HB on the surface of the carbon fibre which led to a poor fibre matrix interface and hence decrease in values.

2.9 Summary

The literature data has shown that the low viscosity and a large number of tailorable functional groups have made HB an important element for investigation of thermoplastic and thermoset polymer blends. Moreover, the blends of HB have also been reported to be used as matrices for both thermoplastic and thermoset composites.

In this thesis hyperbranched divinyl benzene containing reactive methylene ($CH=CH_2$) and non-reactive ethyl ($-CH_2-CH_3-$) functional groups (methylene was hydrogenated to ethyl group) were used as blend constituents with linear polystyrene (LP). The thermal, mechanical and rheological properties of the blends were then investigated to investigate the suitability of these blends for use as composite matrix materials. Composites were also produced using blends as matrices and woven E-glass fibre as reinforcement and the mechanical properties of composites on the basis of using different blend polymer matrices were also evaluated.

Amongst the branched structures, biopolymers such as poly lactic acid (PLA) and polycaprolactone (PCL) have been investigated mainly as star structures [79-82] , although some limited evidence of synthesising hyperbranched PCL (PCL) [83, 84] was found. However, those are not industrially viable. The work in this thesis focussed on star shaped PLA to determine if the effects of hyperbranched structures observed for

polystyrene could be translated to star branched biopolymer structures. This was followed by investigating these polymers as matrix components in composites.

2.10 Star polylactic acid (SPLA)

Poly(L-lactic acid) (PLLA) is a biodegradable thermoplastic polymer which is produced from plant-derived renewable sources such as corn starch and can be synthesised from ring-opening polymerisation of lactide monomers.[85, 86] It has a wide range of applications in the biomedical field, including pharmaceutical, environmental, industrial and other areas.[87-89] Depending on the end applications, achieving predicted degradation behaviour can be of vital importance. However, the hydrolytic degradation rate of the polymer can be dependent on various factors such as polymer chain orientation, crystallinity, fillers or additives, and molecular weight.[86, 89] For example, highly crystalline and oriented PLA products have rather low degradation rates and can maintain their shape and mechanical properties for more than a year.[86] As such in some cases it may be necessary to modify the physical properties of the polymer on a structural basis, to impart some control over the polymers physical properties. One approach used to modify the polymer properties includes introducing branched structures to decrease the polymer crystallinity and to modify its degradation properties.[90, 91]

Star polymers, are multi-armed polymeric materials with arms which radiate from a central core, and are of particular interest as they possess rheological and mechanical properties which are different from the traditional linear counterparts. [86] For example, star polymers can possess smaller hydrodynamic volume, radius of gyration

and therefore lower viscosity than the linear version of same molecular weight (M_n).[92, 93]

In general, star shaped PLA has been shown to exhibit lower glass transition temperature (T_g), crystallisation temperature (T_c) and melting temperature (T_m) than their linear counterparts. [85, 92]

2.11 Properties of star shaped polymers

2.11.1 Thermal properties

Tsuji *et al.* [94] prepared linear and 3-arm star PLLA with various molecular weights to investigate the effects of multi-arms on the physical properties and crystallisation behaviour. They reported higher T_g (at 57.5°C), T_{cc} (at 125.9°C) and lower T_m (at 167.5°C) for the 3-arm star PLLA in comparison to the linear PLLA (T_g (at 56.1°C), T_{cc} (at 114.0°C) and lower T_m (at 176.5°C)) of the same molecular weight (M_n). They explained that the higher T_g of 3-arm PLLA compared with that of linear PLLA revealed that the branching disturbed the segmental motion, whereas the higher T_{cc} and lower T_m of 3-arm star PLLA compared with those of linear PLLA indicated that the branching effected the growth of the crystallites during DSC scanning or increased the lattice disorder of the crystallites formed.

Tsuji *et al.* [94] also investigated the thermal stability of linear and 3-arm star PLLA and evaluated the starting and ending temperatures ($T_{d,S}$ and $T_{d,E}$, respectively) for thermal degradation of the polymers. They concluded $T_{d,S}$ and $T_{d,E}$, of the 3-arm star PLLA were more dependent on M_n and observed a steeper decrease in $T_{d,S}$ and $T_{d,E}$ with decreasing M_n compared to that of the linear PLLA. They suggested that the decrease in thermal stability was due to the rapid increase of terminal group density

of the 3-arm star compared with the slow increase of the terminal group density of linear PLLA. On the other hand, for 3-arm star PLA of $M_n > 2\times10^4$ g mol^{-1} they observed higher $T_{d,S}$ and $T_{d,E}$ value which contradicted their previous explanation. In this case they stated that this might be due to the reduced chain mobility of the branches which overcame the effect of the higher density of the terminal groups.

Zhao *et al.* [95] prepared star shaped PLLA of 16-21-arms with different molecular weight. They observed lower glass transition temperatures (T_g), melting points (T_m) and crystallinity for the star shaped PLLA in comparison to those of linear PLA. They attributed the low melting point (100–140°C) of star-shaped PLA to the crystalline imperfections which were present due to the increased free end groups and branching points in the star shaped polymer in comparison to the linear one.

They also investigated the effect of annealing on the thermal properties of the star-shaped PLA. They annealed star PLLA at 80°C for various time points and concluded that with increasing annealing time, the glass transition temperatures and % crystallinity of star PLLA gradually increased. For annealing time of 1 hour they reported the T_g, T_m and $\%X_c$ to be 53.6°C, 119.6 °C and 13% whereas for 10 hour annealing the T_g, T_m and $\%X_c$ obtained was 55.2°C, 122.7°C and 31% respectively and stated that annealing of PLA at temperatures above T_g was a promising way to achieve control over the crystallinity.[95]

They also studied the thermal stability of star PLLA and found that the maximum decomposition temperature (T_{max}) of star PLLA (210°C) was significantly lower than that of linear PLLA (250°C). They explained that the relatively poor thermal stability

of the star PLLA was due to the thermally unstable nature of hydroxyl terminated star PLLA, which decomposed to form cyclic monomer.[95]

Wang and Dong [96] synthesised linear PLLAs, four and six arm star-shaped PLLAs and investigated the thermal and crystallisation properties of both linear and star PLA via DSC. They reported that the melting temperature (T_m), cold crystallisation temperature (T_{cc}), and the percentage crystallinity (%X_c) of the star PLLAs decreased with increasing number of arms at a fixed number average molecular weight (M_n). For example, with increasing number of arms the percentage of crystallinity (%X_c) was reported to decrease by 58%, 52%, 41% and 31% for linear 1 arm and 2 arm, star 4 arm and 6 arm PLLA respectively. They attributed this to the decreasing molecular weight of each PLLA arm linking to the functional initiator core and the progression of imperfect crystallisation.[96]

Sakamoto and Tsuji [97] prepared linear 2-arm and branched 4-arm PLA having a wide range of number-average molecular weight (M_n) varying from 5.0 $\times10^4$ to 6.0$\times10^4$ g mol^{-1} to study the effects of branching architecture on their crystallisation and thermal properties. They found that the branching architecture of 4-arm PLA delayed or disturbed the non-isothermal crystallisation during heating compared to the linear architecture. They explained that with decreasing molecular weight, the crystallisation of both linear and star PLLA was accelerated due to the enhanced chain mobility. However, for star PLLA, at the same time, the crystallisation also decelerated (for star PLA of M_n~3.0 $\times10^4$ g mol^{-1}, T_{cc} values was 110°C whereas for star PLLA of M_n~1.2$\times10^4$ g mol^{-1}, T_{cc} value was 118°C) due to the elevated number of branching points per unit mass.

Lee *et al.* [90] prepared linear, three-arm (3OH-PL) and four-arm PLA (4OH-PL) using three kinds of initiators i.e. dodecanol, glycerol or pentaerythritol of differernt number average molecular weight. They reported lower T_m for three arm and four-arm star PLA (<160°C) compared with linear PLA (>160°C) and higher cold crystallisation temperatures (>100°C) than that of linear PLA (<100°C) and concluded that the lower melting point and higher cold crystallisation temperature were typical characteristics of star PLA.

Moreover, they also synthesised Cl-, NH_2-, and COOH- terminated four arm PLA from OH-terminated PLA. They measured the thermal stability of 4 arm PLAs of different functional groups and found that OH-terminated star-PLA started to degrade at ~210°C whereas star PLA of other functional groups thermally decomposed at temperature in excess of >300°C. They attributed this lower thermal stability of the OH-terminated star PLA to the thermally unstable nature of the hydroxyl groups, which decomposed to form the cyclic monomer and suggested that the thermal stability of star PLA could be improved by end-group modification.[90]

Wang *et al.* [98] prepared long chain branched PLA with terminal -OH group and found that the branched PLA caused fast crystallisation as the branch points acted as nucleating agents to accelerate crystallisation, however, unlike linear PLA they disturbed the perfection of crystal. On the other hand, with linear PLA, the nucleation was difficult but the regular linear structure made the crystal perfect.

2.11.2 Rheological properties of S-PLA

Kim and Kim [99] measured the intrinsic viscosity of linear and star PLLA in chloroform solution and reported that the star PLLA (~3.1 dL/g) showed lower intrinsic viscosity

than the linear ones (4.4 dL/g) of equivalent molecular weight (M_w~3.0×10^5). They attributed this behaviour to the smaller hydrodynamic volume of the star PLLA than the linear counterpart.

Kim *et al.* [86] also reported lower intrinsic viscosity of star PLLA (~2.42 dL/g) than the linear analogue (~3.57 dL/g) in dilute solution. They also ascribed this to the smaller hydrodynamic volume of the star PLLA than the linear counterpart of same molecular weight (1.97×10^3).

However, for concentrated solutions, they observed higher zero shear viscosity (>10,000 Pa.s) for star PLLA in comparison to the linear one (<1000 Pa.s) at 195°C due to the well entangled arms of star PLA. Star PLA also showed the greater dependence of viscosity (shear thinning behaviour) on temperature which they attributed to the greater compressibility of the star-shaped polymers. They explained that at low shear rate the star-shaped PLLA may produce bulkier dimensions than the linear one. That was why star PLLA deformed more readily and also stretched by shear and as a result showed more prominent shear-thinning behaviour than its linear counterpart.[86]

Wang *et al.* [98] prepared the long-chain branched poly(L-lactide)s (LCB-PLAs) with controlled branch length and reported that with increasing branch density, the zero-shear viscosity η_0 (for linear PLA the η_0 was reported to be 4.32 kPa and for 3 arm star PLA the η_0 value was 375 kPa) and shear-thinning behaviour increased. They also observed higher storage modulus value (at 0.1 rad/s) for 3 arm star PLA ~10^4 Pa whereas this value for linear PLA was found to be ~10^1 Pa and concluded that the long-chain branching due to entanglement could increase the melt elasticity and melt strength of PLA.

2.11.3 Hydrolytic degradation of star shaped polymer

Yuan *et al.* [100] hydrolytically degraded linear 1-armed poly(DL-lactide), PDLLA and poly(L-lactic acid), PLLA and star-shaped 6- armed PDLLA and PLLA of similar molecular weights (M_n value of star PDLLA 21.8 kDa and star PLLA 21.64 kDa) in PBS solution (pH 7.4) at 37°C. They found that the hydrolytic-degradation rate, as monitored by weight loss, was higher for the 6-armed PDLLA and PLLA than that of the corresponding linear PDLLA and PLLA (M_n value 22.3 kDa and 22.1 kDa respectively). They ascribed this to the much shorter chains of star-shaped PDLLA and PLLA. They also explained that the star-shaped polylactide degraded in two steps. First, the ester groups hydrolysed and PLA chains cleaved randomly, and then the shorter PLA chains became detached from the core.

On the other hand, Fu *et al.* [101] hydrolytically degraded (in PBS solution at 37°C) 1-armed PDLLA and multi-armed PDLLA and reported that multi-armed PDLLA had a lower hydrolytic degradation rate, as traced by weight loss and molecular weight decrease, than the 1-armed PDLLA. They observed the percentage weight loss of linear PDLLA was 51.2% after 10 weeks of degradation time whilst for star PLA the percentage weight loss was 28.6%.

They stated that according to conventional theory, the degradation of multi-armed PDLLA should be easier due to presence of more hydrophilic groups and much shorter polymer chains. However, they proposed two explanations for the lower degradation rate of star PDLLA. Firstly, a strong intermolecular force might be present in the star-shaped polymer due to the entangled behaviour of the long arm-chain which could prevent water erosion of the polymer. Secondly, the epoxidised soybean oil could

minimise the amount of trapped water (due to its hydrophobic nature) and, therefore, slow the permeation of water into the star polymer occurred.

Tsuji and Hayashi [89] studied the hydrolytic degradation (monitored by weight loss and molecular weight) of linear 2 arm and star-shaped 4-arm poly(L-lactide) (hydroxyl-terminated) at 37°C in phosphate buffer solution. They observed a continuous decrease in M_n value for linear PLLA whereas a very small decrease in M_n was noticed for 4 arm star PLLA samples. For example, for linear PLLA, the M_n decreased from ~10^4 g mol^{-1} to around 10^3 g mol^{-1} within 20 weeks of degradation time whereas for 4 arm PLLA, the M_n remained constant at 10^5 g mol^{-1}.

Similarly, they also observed lower hydrolytic degradation rates- for 4-armed (hydroxyl-terminated) PDLLA than that of linear 2 armed PDLLA when they performed a comparative hydrolytic degradation study (in phosphate-buffered solution at 97°C) and monitored the number average molecular weight (M_n).[102]

In both cases, they explained that for star polymer, the terminal hydroxyl groups could form hydrogen bonds with adjacent terminal hydroxyl groups. Such intra and intermolecular hydrogen bonding prevented the terminal hydroxyl groups from interacting with water molecules and the cleavage of the ester groups around the terminal hydroxyl groups which hindered the hydrolytic degradation.[89, 102] Moreover, the hydrogen bonding would increase the apparent molecular weight and thereby reduced the chain mobility. The decreased chain mobility would be another factor to restrict the diffusion of water molecules and thus delay the hydrolytic degradation.[89, 102]

Kim *et al.* [103] investigated the hydrolytic degradation of linear 1-armed and star-shaped 4-armed PLLAs and found that initially the molecular weight decreased faster for 1-armed PLLA than for 4-armed PLLA which they attributed to the higher crystallinity of star PLLA since degradation of PLLA started predominantly in the amorphous region. However, at a later stage they observed faster degradation rate for the 4-armed star PLLA than that of linear PLLA and explained that at this stage the degradation of the PLLA was influenced by the chain end concentration (the hydroxyl end groups) which was higher than the linear PLLA of equivalent molecular weight and underwent higher hydrolytic degradation at the later stage.

2.12 SPLA polymer blends

Linear PLA has been reported to be blended with star PLA to modify crystallinity, hydrolytic degradation behaviour and also to improve the rheological and mechanical properties.[104-106] For example, blending star PLA with linear PLA has been reported to improve the plasticisation effect of linear PLA since linear PLA was fairly brittle, with low impact strength due to its high crystallinity.[107] Linear PLA has also been reported to be blended with low molecular weight compounds and oligomers, however, low molecular weight plasticisers can migrate to the surface, embrittlement and also volatilise over time.[107] As such, blending linear PLA with relatively high molecular weight polymers was proposed to prevent the aforementioned problems, but the desired properties could not be achieved due to the immiscibility between the different structures.[108-110] In this regard, blending branched/star PLA with linear PLA was found to be effective as both have identical chemical structure.[105]

Phuphuak *et al.* [104] prepared four-branched PLLAs (M_n from 3370 to 12,200) initiated by a monosaccharide, i.e., methyl-a-D-glucopyranoside which they denoted as MG and 21-branched PLLA (M_n from 18,000 to 79,700) initiated by β-cyclodextrin denoted as (CD). They prepared blends of linear PLA with 1 wt% of MG-PLLA and CD-PLLA of all M_n value by solvent casting method and with 5wt%,10wt%, and 20wt% MG-PLLA and CD-PLLA of lowest M_n value (3.3 kDa and 18 kDa respectively) and evaluated both the plasticisation and crystallisation effects of the star PLA in the blends. Tsujimoto *et al.* [107] used castor oil (which contains three secondary hydroxyl groups) as an initiator to produce 3 arm star PLA. Then they prepared blends containing 5wt% of star PLA of different molecular weights (molecular weight depends on the different feed ratio of lactide) and evaluated the plasticisation effects of the branched PLA.

Khajeheian and Rosling [111] also prepared blends containing 10 and 30 wt % of star PLLAs (of different M_n) with a linear PLLA and studied the melt flow and thermal properties. Wang *et al.* [105] produced a long-chain branched PLLA and then blended this with linear PLA and studied the rheology and crystallisation properties of blends.

2.12.1 Thermal properties of blends

Khajeheian and Rosling [111] reported that the low molecular weight (M_n~2500) star PLA (SPLA) acted as a plasticiser for blends of linear PLLA with 30wt% of star PLA and the T_g of the blend was reported to be lower by 7°C (12% reduction). On the other hand, upon annealing, they observed that the crystalllinty of the blends containing 30 wt % of the high molecular weight SPLA (M_n~33,400) increased (~30%) compared with blends containing low molecular weight star PLA. The higher crystallinity was

evident from the increased heat of melting (ΔH_m) and crystallisation (ΔH_c) and the higher melting temperature for the blends containing star PLA of high molecular weight. They concluded that the high molecular weight SPLA increased the ability of linear PLA to be crystallise during the heating ramp. They explained that upon increasing temperature, the macromolecular freedom increased and the amorphous segments reorganised into crystalline part. For blends containing 10% of SPLA of different molecular weight they observed single T_g and suggested that the blends were compatible.

They also reported higher thermal stability for both neat star polymers and blends in comparison to linear PLA. They measured the thermal stability from the initial degradation temperature which they denoted as (T_i). For linear PLA they reported the T_i to be 210°C whereas for blends containing 30 wt % of low molecular weight (M_n~2500) SPLA to be 215°C and for high molecular weight (M_n~33,400) SPLA to be 222°C respectively.[111]

Phuphuak *et al.* [104] suggested good miscibility (as confirmed by a single T_g) of the blends of linear and branched PLLA. They found that the shorter the SPLA chain (lower M_n value) the more significant the reduction in T_g. For example, they reported that for PLA/MG-PLLA and PLA/CD-PLLA blends containing 1wt% of lowest molecular weight (M_n~ 3370 and 18,000) SPLA, the T_g was reported to be 28°C and 22°C respectively whereas for blends with higher molecular weight SPLA (M_n~ 12,200 and 79, 700) the T_gs increased to 47°C and 50°C, respectively. The lowering of T_g reflected the ease of segmental movements of PLA chains initiated by SPLA and concluded that the low molecular weight SPLA acted as a plasticiser.[104] They also identified dual

characteristics (both plasticiser and nucleating agent) of the SPLA and stated that addition of SPLA eased segmental mobility of the PLA chains and thus allowed the polymer chain to be rearranged and crystallised.

They also reported that for the same molecular weight of the SPLA in blends, the T_g increased with increasing wt% of S-PLA. They found that for blends containing 1wt% 5wt%, 10wt%, and 20wt% of MG-PLLA, the T_g increased to 28°C, 31°C, 33°C and 36°C respectively. They suggested that higher amount of SPLA, instead of inducing chain mobility, restricted the chain movement of PLA, thereby increasing the T_g.

Wang *et al.* [105] reported on blends of 16% long chain branched 3 arm star PLA with linear PLA. For blends containing three arm PLA, they observed that the crystallinity of linear PLA increased from 1.9% to 34.2%, indicating that blending of three arm PLA with linear PLA accelerated crystallisation of the blends.

Tsujimoto *et al.* [107] conducted DSC analysis for both linear PLLA and blends containing 5wt% of branched PLA and reported that for blends, the T_g and the crystallisation temperature (T_c) of blends decreased slightly to 54°C and 119°C compared to values for linear PLA at 58°C and 131°C respectively. Moreover, the addition of the branched PLA also suppressed the crystal growth of linear PLLA. They attributed these effects to the plasticisation effect of the branched PLA and its flexibility of the core structure of the branched polymer.

2.12.2 Effects on mechanical properties

Phuphuak *et al.* [104] also studied the mechanical properties (tensile strength and elongation at break) of the blends of linear and branched PLLA. One of the primary functions of the plasticiser is to increase the elongation at break. They reported the

tensile strength value and the elongation at break for linear PLA is about 34.6 MPa and 5.36% respectively. They found that the short-chain SPLA (low M_n value 18,000) (5wt% in the blend) acted as a plasticiser for linear PLA more significantly and resulted in an increase in the elongation at break (by 30-40%) and decreased tensile strength to ~10MPa. However, for increased amount (20wt%) of short-chain SPLA in blends, the elongation at break decreased to ~12% and the tensile strength increased to ~25 MPa. They concluded that the higher percentage of short-chain SPLA acted as nucleating agent which increased crystallinity and decreased elongation at break.

Tsujimoto *et al.* [107] also studied the mechanical properties of the blended film linear PLLA with 5wt% of branched PLA. They found that addition of 5wt% branched polymer acted as a plasticiser and increased the elongation at break. They performed the tensile testing of the blended films and reported an increase in elongation at break to 48% whereas the linear PLA film value was 18%. However, for increased amount (10wt%) of branched PLA in blends, they observed a 43% decrease for the elongation at break. They concluded that a small amount of the branched PLA was sufficient to plasticise linear PLA without a decrease in tensile strength.

2.12.3 Effects on rheological properties

Khajeheian and Rosling [111] measured the shear viscosity (η) of linear PLLA and blends at 240°C. They found the zero shear viscosity of linear PLLA at 100 Pa.s and for blends containing 30wt % of SPLAs (M_n 2.5 kDa and 12 kDa) they found that the zero shear viscosity decreased to ~20 Pa.s.

They also studied the change in dynamic storage modulus (G') and loss modulus (G'') with frequency and found that both the linear PLA and the miscible blends

(containing 30wt % of SPLAs of M_n 2.5 kDa and 12 kDa) exhibited terminal flow behaviour at low frequency which were characteristics of viscoelastic liquids. However, for all other blends containing 10wt % of SPLAs, they observed the non-terminal behaviour which was not detected for the linear PLA and miscible blends. They attributed this behaviour to the lower miscibility levels of the blends and explained that for immiscible blends an "additional" elastic response originated from the surface interaction between the SPLA in the discrete phase and linear PLLA in the continuous matrix and stated that the interface between the two polymers played an important role in the viscoelastic response of molten SPLA/ linear PLA blends.

Wang *et al.* [105] studied the complex viscosities of linear PLA and blends containing long chain branched three arm star PLA as a function of frequency. They found that the blends containing 16% three arm star PLA showed the highest frequency dependence and higher shear thinning behaviour, whilst the linear PLA showed the least. They explained that there were more chain entanglements in the blends than in linear PLA which caused much longer relaxation time than that in linear PLA.

2.12.4 Effects on hydrolytic degradation

Anderson *et al.* [112] investigated the hydrolytic degradation of blends of PLLA with star-shaped D-LA oligomers (containing four and six hydroxyl end-groups) to form a strereocomplex. They found that the stereocomplexes containing star shaped D-LA oligomers with 4 hydroxyl chain groups underwent a similar mass loss to the stereocomplex with linear D-LA oligomers. However, they observed the decrease in the degree of stereocomplexation for D-LA oligomers with 6 hydroxyl chain group which led to faster mass loss. They concluded that increasing the number of chain-

ends from four to six decreased the degree of stereocomplexation and thus increased the hydrolytic degradation.

2.13 Composites with star shaped Polymer

Although there are lot of studies using PLA as matrix for biocomposites, only very few works have been reported in the literature on using star polymers as matrix in composite materials.

Chen *et al.* [113] produced hydroxyl-terminated 4-arm star-shaped PLA end capped with methacrylic anhydride (MAAH) and crosslinked it via heating to act as a thermoset matrix. In their study besides using cross-linked SPLA matrix they also treated the ramie fabrics with 8% NaOH solution to enhance the interfacial adhesion between the fabrics and matrix. They prepared the thermoset PLA composites by hot press moulding at 150°C and 6 MPa for 15 min and studied the thermal, mechanical and water absorption of the prepared composite. They reported that the tensile strength and flexural strength increased by 39% and 35% respectively for 48% loading of treated ramie fabrics. However, they observed a decrease in tensile strength and flexural strength by ~16% and ~37% when they further increased the ramie content above 48%. They explained that further increase of ramie content resulted in a decrease of the matrix content which caused poor bonding between the fibres and matrix, as a result delamination occurred, interlayer bonding force weakened and the tensile and flexural strength decreased.

Akesson *et al.* [114] also developed a new bio based polyester resin for thermoset composite applications by end-functionalising star shaped lactic acid (LA) oligomers

of by methacrylic anhydride. They found that the resin could be completely crosslinked within a few minutes at 170°C. They suggested that this resin could be used as a thermoset resin for composite or coating applications.

On the other hand, for thermoplastic polymer resin composites several issues still need to be resolved. Thermoplastic resins are generally known for their high viscosity and the use of thermoplastic matrices in making composites can result in poor impregnation and require either prolonged impregnation times or significant processing pressures.[115] In most cases, the composite materials obtained from using these matrices may possesses non-impregnated regions of fibres by polymers [116] which can have detrimental effects on the mechanical properties and problems of delamination can arise when the material is composed of several reinforcing layers.

However, several routes have been explored to improve the polymer impregnation of the reinforcing fibres and to improve the adhesion between the fibres and the matrix. For example, using thermoplastic resin with a reduced molecular weight as matrix can increase the impregnation of fibre by polymer matrix.[117]

Generally, the use of thermoplastic polymers of low molecular weights in the matrix can detrimentally effect the mechanical properties of the composites, in particular the ultimate strength and the yield strength. This is due to the mechanical properties of the composites also depend on the mechanical properties of the matrix which transmits the stresses to the reinforcing material.

Another route to improve impregnation of the reinforcing fibres by the matrix is to employ a matrix in the form of an oligomer or of a pre polymer of low molecular weight which can be polymerised via in situ polymerisation processes.[118]

Myard and Philippo [119] investigated an alternate method of using a thermoplastic matrix. They used the star structure polymer (polyamide; nylon-6) which exhibited high fluidity in the molten state and provided good impregnation of the reinforcing fibres during composite preparation.

The composite matrix was obtained from a blend of the star and linear polyamide and used carbon and glass fibres as reinforcing agents. The temperature applied was greater than the melting point of the star polyamide-6 (230-260°C) for 1 to 3 minutes and the pressure applied was between 1 and 20 bar. They cooled the composite to 50-60°C before removing it from the mould.

They compared the mechanical properties of the prepared star polymer (thermoplastic) composites with thermosetting (Epoxy) matrix composites containing the same reinforcing agent. They reported the flexural modulus and strength of the star polymer/glass fibre composites was 21.2 GPa and 580 MPa whereas the flexural modulus and strength of epoxy polymer /glass fibre composite was 21.0 GPa and 630 MPa respectively. Similarly, for the star polymer/carbon fibre composite they reported the flexural modulus and strength to be 54.3 GPa and 536 MPa whereas for epoxy/carbon fibre composite the flexural modulus and strength was 52.0 GPa and 796 MPa respectively. They explained that the high fluidity or low viscosity of the star polymer in the molten state, despite low processing pressure caused optimum impregnation of the reinforcing fibres by the matrix without

affecting the mechanical properties of the composites in comparison to the mechanical properties of the composites produced using thermosetting matrix.

2.14 Summary

From the literature surveyed, it can be concluded that SPLA has been used as a blending constituent with linear PLA to modify (increase or decrease) the crystallisation, hydrolytic degradation and also to decrease the brittleness of linear PLA. Unlike other blend constituents, SPLA has been shown to achieve desired blend properties for linear PLA, since both have the identical chemical structure. However, the effect of using of SPLA as a blend constituent depends mainly on their number of arms, arm length, and nature of end groups.

To the best of the author's knowledge SPLA blends with neat PLA have not yet been reported to be used as matrix materials for polymer fibre laminate composites. However, other star polymer blends have been reported to be used as matrix materials for polymer fibre composites.

2.15 References

1. *Voit, B.I. and A. Lederer, Hyperbranched and highly branched polymer architectures—synthetic strategies and major characterization aspects. Chemical Reviews, 2009.* ***109****(11): p. 5924-5973.*

2. *Gao, C. and D. Yan, Hyperbranched polymers: from synthesis to applications. Progress in Polymer Science, 2004.* ***29****(3): p. 183-275.*

3. *Korolev, G. and M. Mogilevich, Properties and application of hyper-branched polymers, in Three-Dimensional Free-Radical Polymerization. 2009, Springer Berlin Heidelberg. p. 243-255.*

4. *Mishra, M. and S. Kobayashi, Star and hyperbranched polymers. Vol. 53. 1999: CRC Press.*

5. *Malmström, E., M. Johansson, and A. Hult, The effect of terminal alkyl chains on hyperbranched polyesters based on 2,2-bis(hydroxymethyl)propionic acid. Macromolecular Chemistry and Physics, 1996.* ***197****(10): p. 3199-3207.*

6. *Voit, B.I., Hyperbranched polymers: a chance and a challenge. Comptes Rendus Chimie, 2003.* ***6****(8): p. 821-832.*

7. *Liu, H. and C.E. Wilén, Extension of the chain-end, free-volume theory for predicting glass temperature as a function of conversion in hyperbranched polymers obtained through one-pot approaches. Journal of Polymer Science Part B: Polymer Physics, 2004.* ***42****(7): p. 1235-1242.*

8. *Kim, Y.H. and O.W. Webster, Hyperbranched polyphenylenes. Macromolecules, 1992.* ***25****(21): p. 5561-5572.*

9. *Wooley, K.L., et al., Physical properties of dendritic macromolecules: a study of glass transition temperature. Macromolecules, 1993.* ***26****(7): p. 1514-1519.*

10. *Hawker, C.J. and F. Chu, Hyperbranched Poly(ether ketones): Manipulation of structure and physical properties. Macromolecules, 1996.* ***29****(12): p. 4370-4380.*

11. *Voit, B.I., Dendritic polymers: from aesthetic macromolecules to commercially interesting materials. Acta Polymerica, 1995.* ***46****(2): p. 87-99.*

12. *Elrehim, M.A., et al., Structural and end-group effects on bulk and surface properties of hyperbranched poly (urea urethane) s. Journal of Polymer Science Part A: Polymer Chemistry, 2005.* ***43****(15): p. 3376-3393.*

13. *Shanmugam, T., C. Sivakumar, and A.S. Nasar, Hydroxyl-terminated hyperbranched aromatic poly (ether-ester) s: Synthesis, characterization, end-group modification, and optical properties. Journal of Polymer Science Part A: Polymer Chemistry, 2008.* ***46****(16): p. 5414-5430.*

14. *Schmaljohann, D., et al., Modification with alkyl chains and the influence on thermal and mechanical properties of aromatic hyperbranched polyesters. Macromolecular Chemistry and Physics, 2000.* ***201****(1): p. 49-57.*

15. *Inoue, K., Functional dendrimers, hyperbranched and star polymers. Progress in Polymer Science, 2000.* ***25****(4): p. 453-571.*

16. *Akabori, K.-i., et al., Glass transition behavior of hyper-branched polystyrenes. Polymer, 2009.* ***50****(20): p. 4868-4875.*

17. *Turner, S.R., et al., Hyperbranched aromatic polyesters with carboxylic acid terminal groups. Macromolecules, 1994.* ***27****(6): p. 1611-1616.*

18. *Mourey, T.H., et al., Unique behavior of dendritic macromolecules: intrinsic viscosity of polyether dendrimers. Macromolecules, 1992.* ***25****(9): p. 2401-2406.*

19. *Jikei, M. and M.-a. Kakimoto, Hyperbranched polymers: a promising new class of materials. Progress in Polymer Science, 2001.* ***26****(8): p. 1233-1285.*

20. *Malmström, E., M. Johansson, and A. Hult, Hyperbranched aliphatic polyesters. Macromolecules, 1995.* ***28****(5): p. 1698-1703.*

21. *Hult, A., M. Johansson, and E. Malmström, Hyperbranched polymers, in Branched Polymers II. 1999, Springer. p. 1-34.*

22. *Zhang, Y., et al., One-pot synthesis of a new hyperbranched polyester containing 3,6-di-acceptor-substituted carbazole chromophores for nonlinear optics. Macromolecular Chemistry and Physics, 1996.* ***197****(2): p. 667-676.*

23. *Schmaljohann, D., et al., Modification with alkyl chains and the influence on thermal and mechanical properties of aromatic hyperbranched polyesters. Macromolecular Chemistry and Physics, 2000.* ***201****(1): p. 49-57.*

24. *Hsieh, T.-T., C. Tiu, and G. Simon, Melt rheology of aliphatic hyperbranched polyesters with various molecular weights. Polymer, 2001.* ***42****(5): p. 1931-1939.*

25. *Salamone, J.C., Concise polymeric materials encyclopedia. Vol. 1. 1998: CRC press.*

26. *Yates, C. and W. Hayes, Synthesis and applications of hyperbranched polymers. European Polymer Journal, 2004.* ***40****(7): p. 1257-1281.*

27. *Kwak, S.-Y., et al., Amelioration of mechanical brittleness in hyperbranched polymer. 1. Macroscopic evaluation by dynamic viscoelastic relaxation. Polymer, 2004.* ***45****(20): p. 6889-6896.*

28. *Nunez, C.M., et al., Mechanical properties of blends of PAMAM dendrimers with poly (vinyl chloride) and poly (vinyl acetate). Journal of Polymer Science Part A: Polymer Chemistry, 1998.* ***36****(12): p. 2111-2117.*

29. *Mulkern, T.J. and N.C. Tan, Polystyrene/hyperbranched polyester blends and reactive polystyrene/hyperbranched polyester blends. 1999, DTIC Document.*

30. *Mulkern, T. and N. Tan, Processing and characterization of reactive polystyrene/hyperbranched polyester blends. Polymer, 2000.* ***41****(9): p. 3193-3203.*

31. *Hong, Y., et al., A novel processing aid for polymer extrusion: Rheology and processing of polyethylene and hyperbranched polymer blends. Journal of Rheology (1978-present), 1999.* ***43****(3): p. 781-793.*

32. *Diao, J.Z., et al., Mechanical properties and morphology of blends of hyperbranched polymer with polypropylene and poly (vinyl chloride). Iranian Polymer Journal, 2006.* ***15****(1): p. 91-98.*

33. *Diao, J., et al., Compatibilization effects of a hyperbranched polymer on acrylonitrile-butadiene-styrene/poly (vinylchloride) blends. Iranian Polymer Journal, 2006.* ***15****(11): p. 863-870.*

34. *Jackson, M.B., et al., Toughening epoxy resins with polyepichlorohydrin. Journal of Applied Polymer Science, 1993.* ***48****(7): p. 1259-1269.*

35. *Kim, D.S., et al., Effects of particle size and rubber content on fracture toughness in rubber-modified epoxies. Polymer Engineering & Science, 1996.* ***36****(6): p. 755-768.*

36. *Bhardwaj, R. and A.K. Mohanty, Modification of brittle polylactide by novel hyperbranched polymer-based nanostructures. Biomacromolecules, 2007.* ***8****(8): p. 2476-2484.*

37. *Hong, Y., et al., Film blowing of linear low-density polyethylene blended with a novel hyperbranched polymer processing aid. Polymer, 2000.* ***41****(21): p. 7705-7713.*

38. *Zhang, J.F. and X. Sun, Mechanical properties and crystallization behavior of poly (lactic acid) blended with dendritic hyperbranched polymer. Polymer International, 2004.* ***53****(6): p. 716-722.*

39. *Massa, D., et al., Novel blends of hyperbranched polyesters and linear polymers. Macromolecules, 1995.* ***28****(9): p. 3214-3220.*

40. *Schmaljohann, D., et al., Blends of amphiphilic, hyperbranched polyesters and different polyolefins. Macromolecules, 1999.* ***32****(19): p. 6333-6339.*

41. *Nunez, C.M., et al., Solution rheology of hyperbranched polyesters and their blends with linear polymers. Macromolecules, 2000.* ***33****(5): p. 1720-1726.*

42. *Varley, R.J. and W. Tian, Toughening of an epoxy anhydride resin system using an epoxidized hyperbranched polymer. Polymer International, 2004.* ***53****(1): p. 69-77.*

43. *Zhang, D. and D. Jia, Toughness and strength improvement of diglycidyl ether of bisphenol-A by low viscosity liquid hyperbranched epoxy resin. Journal of applied polymer science, 2006.* ***101****(4): p. 2504-2511.*

44. *Ratna, D. and G. Simon, Thermomechanical properties and morphology of blends of a hydroxy-functionalized hyperbranched polymer and epoxy resin. Polymer, 2001.* ***42****(21): p. 8833-8839.*

45. *Wu, H., et al., Investigation of readily processable thermoplastic-toughened thermosets. V. Epoxy resin toughened with hyperbranched polyester. Journal of Applied Polymer Science, 1999.* ***72****(2): p. 151-163.*

46. *Divya, H., L.L. Naik, and B. Yogesha, Processing Techniques of Polymer Matrix Composites–A Review.*

47. *Advani, G., Introduction to composites and manufacturing processes. Manufacturing Techniques for Polymer Matrix Composites (PMCs), 2012: p. 1.*

48. *Khanam, P.N. and M.A.A. Almaadeed, Processing and characterization of polyethylene-based composites. Advanced Manufacturing: Polymer & Composites Science, 2015.* ***1****(2): p. 63-79.*

49. *Way, C., et al., Processing Stability and Biodegradation of Polylactic Acid (PLA) Composites Reinforced with Cotton Linters or Maple Hardwood Fibres. Journal of Polymers and the Environment, 2013.* ***21****(1): p. 54-70.*

50. *Hoa, S.V., Principles of the manufacturing of composite materials. 2009.*

51. *Vaidya, U. and K. Chawla, Processing of fibre reinforced thermoplastic composites. International Materials Reviews, 2008.* ***53****(4): p. 185-218.*

52. *Thattai Parthasarathy, K.B., Processing and characterization of long fiber thermoplastics. 2008, The university of alabama at birmingham.*

53. *Allen, K.A., Processing of Thermoplastic Composites.*

54. *Kopeliovich, D.D. Closed mold fabrication of Polymer Matrix Composites. 2012; Available from: http://www.substech.com/dokuwiki/doku.php?id=closed_mold_fabrication_of_polymer_matrix_composites.*

55. *Larock, J.A., H.T. Hahn, and D.J. Evans, Pultrusion Processes for Thermoplastic Composites. Journal of Thermoplastic Composite Materials, 1989.* ***2****(3): p. 216-229.*

56. *Whelan, A., Polymer technology dictionary. 2012: Springer Science & Business Media.*

57. *Romagna, J., G. Ziegmann, and M. Flemming, Thermoplastic filament winding—an experimental investigation of the on-line consolidation of poly (ether imide) fit preforms. Composites Manufacturing, 1995.* ***6****(3-4): p. 205-210.*

58. *Slivka, M.A., C. Chu, and I.A. Adisaputro, Fiber-matrix interface studies on bioabsorbable composite materials for internal fixation of bone fractures. I. Raw material evaluation and measurement of fiber—matrix interfacial adhesion. Journal of Biomedical Materials Research Part A, 1997.* ***36****(4): p. 469-477.*

59. *Wu, H., A comparison of micromechanical evaluation on interfacial shear strength using microbond pull-out and micro-indentation tests. Journal of Materials Science Letters, 1997.* ***16****(24): p. 2039-2040.*

60. *Verpoest, I., M. Desaeger, and R. Keunings, Critical review of direct micromechanical test methods for interfacial strength measurements in composites, in Controlled interphases in composite materials. 1990, Springer. p. 653-666.*

61. *Kelly, A. and a.W. Tyson, Tensile properties of fibre-reinforced metals: copper/tungsten and copper/molybdenum. Journal of the Mechanics and Physics of Solids, 1965.* ***13****(6): p. 329-350.*

62. *Lodeiro, M., et al., Critical review of interface testing methods for composites. 1998: National Physical Laboratory. Great Britain, Centre for Materials Measurement and Technology.*

63. *Drzal, L.T., P.J. Herrera-Franco, and H. Ho, 5.05 - Fiber–matrix interface tests A2 - kelly, anthony, in Comprehensive Composite Materials, C. Zweben, Editor. 2000, Pergamon: Oxford. p. 71-111.*

64. *Piggott, M., Why interface testing by single-fibre methods can be misleading. Composites Science and Technology, 1997.* ***57****(8): p. 965-974.*

65. *Miller, B., P. Muri, and L. Rebenfeld, A microbond method for determination of the shear strength of a fiber/resin interface. Composites Science and Technology, 1987.* ***28****(1): p. 17-32.*

66. *Gohil, P.P. and A. Shaikh, Analytical investigation and comparative assessment of interphase influence on elastic behavior of fiber reinforced composites. Journal of Reinforced Plastics and Composites, 2010.* ***29****(5): p. 685-699.*

67. *Silverajah, V., et al., A comparative study on the mechanical, thermal and morphological characterization of poly (lactic acid)/epoxidized palm oil blend. International Journal of Molecular Sciences, 2012.* ***13****(5): p. 5878-5898.*

68. *Feraboli, P.J. and K.T. Kedward. In search of the true interlaminar shear strength. in Nineteenth technical conference of the joint American society for composites/American Society for Testing and Materials Committee D. 2004.*

69. *Adams, D. and J. Busse. Suggested modifications of the short beam shear test method. in Proceedings of the 49th International SAMPE Symposium and Exhibition: Materials and Processing Technology. 2004.*

70. *Standard, A., Standard test method for short-beam strength of polymer matrix composite materials and their laminates. Annual book of ASTM standards, West Conshohocken, 2007.* ***15****: p. 54-60.*

71. *Emehel, T. and K. Shivakumar, Tow collapse model for compression strength of textile composites. Journal of Reinforced Plastics and Composites, 1997.* ***16****(1): p. 86-101.*

72. *Shivakumar, K., A. Pora, and F. Abali. Interlaminar Shear Test for Laminated Textile Fabric Composites. in Proceedings of 13th International Conference on Composite Materials. 2001.*

73. *Verrey, J., et al., Interlaminar fracture toughness improvement in composites with hyperbranched polymer modified resin. Composites Science and Technology, 2005.* ***65****(10): p. 1527-1536.*

74. *Mezzenga, R., L. Boogh, and J.-A.E. Månson, A review of dendritic hyperbranched polymer as modifiers in epoxy composites. Composites Science and Technology, 2001.* ***61****(5): p. 787-795.*

75. *DeCarli, M., et al., Toughening of a carbon fibre reinforced epoxy anhydride composite using an epoxy terminated hyperbranched modifier. Composites Science and Technology, 2005.* ***65****(14): p. 2156-2166.*

76. *Lu, S., et al., Sisal fibre/polypropylene composites modified with carboxyl terminated hyperbranched polymer. Plastics, Rubber and Composites, 2013.* ***42****(9): p. 361-366.*

77. *Jannerfeldt, G., et al., Matrix modification for improved reinforcement effectiveness in polypropylene/glass fibre composites. Applied Composite Materials, 2001.* ***8****(5): p. 327-341.*

78. *Wong, S., R.A. Shanks, and A. Hodzic, Mechanical behavior and fracture toughness of poly (l-lactic acid)-natural fiber composites modified with hyperbranched polymers. Macromolecular Materials and Engineering, 2004.* ***289****(5): p. 447-456.*

79. *Zhao, Y.-L., et al., Synthesis and thermal properties of novel star-shaped poly (l-lactide) s with starburst PAMAM–OH dendrimer macroinitiator. Polymer, 2002.* ***43****(22): p. 5819-5825.*

80. *Shadi, L., et al., Preparation of electrospun nanofibers of star-shaped polycaprolactone and its blends with polyaniline. Journal of Materials Science, 2014.* ***49****(14): p. 4844-4854.*

81. *Finne, A. and A.-C. Albertsson, Controlled synthesis of star-shaped L-lactide polymers using new spirocyclic tin initiators. Biomacromolecules, 2002.* ***3****(4): p. 684-690.*

82. *Turunen, M.P.K., et al., Synthesis, characterization and crosslinking of functional star-shaped poly (ε-caprolactone). Polymer International, 2002.* ***51****(1): p. 92-100.*

83. *Yang, H., et al., One-step synthesis of hyperbranched biodegradable polymer. RSC Advances, 2013.* ***3****(19): p. 6853-6858.*

84. *Trollsås, M., et al., Hyperbranched poly (ε-caprolactone) s. Macromolecules, 1998.* ***31****(11): p. 3439-3445.*

85. *Cameron, D.J. and M.P. Shaver, Aliphatic polyester polymer stars: synthesis, properties and applications in biomedicine and nanotechnology. Chemical Society Reviews, 2011.* ***40****(3): p. 1761-1776.*

86. *Kim, E.S., B.C. Kim, and S.H. Kim, Structural effect of linear and star-shaped poly (L-lactic acid) on physical properties. Journal of Polymer Science Part B: Polymer Physics, 2004.* ***42****(6): p. 939-946.*

87. *Han, L., et al., Exclusive stereocomplex crystallization of linear and multiarm star-shaped high-molecular-weight stereo diblock poly (lactic acid) s. The Journal of Physical Chemistry B, 2015.* ***119****(44): p. 14270-14279.*

88. *Tsuji, H. and Y. Yamashita, Highly accelerated stereocomplex crystallization by blending star-shaped 4-armed stereo diblock poly (lactide) s with poly (d-lactide) and poly (l-lactide) cores. Polymer, 2014.* ***55****(25): p. 6444-6450.*

89. *Tsuji, H. and T. Hayashi, Hydrolytic degradation and crystallization behavior of linear 2-armed and star-shaped 4-armed poly (l-lactide) s: Effects of branching architecture and crystallinity. Journal of Applied Polymer Science, 2015.* ***132****(20).*

90. *Lee, S.H., et al., Synthesis and degradation of end-group-functionalized polylactide. Journal of Polymer Science Part A: Polymer Chemistry, 2001.* ***39****(7): p. 973-985.*

91. *Breitenbach, A. and T. Kissel, Biodegradable comb polyesters: Part 1 synthesis, characterization and structural analysis of poly(lactide) and poly(lactide-coglycolide) grafted onto water-soluble poly(vinyl alcohol) as backbone. Polymer, 1998.* ***39****(14): p. 3261-3271.*

92. *Cameron, D.J. and M.P. Shaver, Control of thermal properties and hydrolytic degradation in poly (lactic acid) polymer stars through control of isospecificity of polymer arms. Journal of Polymer Science Part A: Polymer Chemistry, 2012.* ***50****(8): p. 1477-1484.*

93. *Aloorkar, N., et al., Star polymers: an overview. Int. J. Pharm. Sci. Nanotechnol, 2012.* ***5****(2): p. 1675-1684.*

94. *Tsuji, H., et al., Physical Properties, crystallization, and spherulite growth of linear and 3-arm poly(l-lactide)s. Biomacromolecules, 2005.* ***6****(1): p. 244-254.*

95. *Zhao, Y.-L., et al., Synthesis and thermal properties of novel star-shaped poly(l-lactide)s with starburst PAMAM–OH dendrimer macroinitiator. Polymer, 2002.* ***43****(22): p. 5819-5825.*

96. *Wang, L. and C.M. Dong, Synthesis, crystallization kinetics, and spherulitic growth of linear and star-shaped poly (L-lactide) s with different numbers of arms. Journal of Polymer Science Part A: Polymer Chemistry, 2006.* ***44****(7): p. 2226-2236.*

97. *Sakamoto, Y. and H. Tsuji, Crystallization behavior and physical properties of linear 2-arm and branched 4-arm poly(l-lactide)s: Effects of branching. Polymer, 2013.* ***54****(9): p. 2422-2434.*

98. *Wang, L., et al., Rheology and crystallization of long-chain branched poly(l-lactide)s with controlled branch length. Industrial & Engineering Chemistry Research, 2012.* ***51****(33): p. 10731-10741.*

99. *Kim, S.H. and Y.H. Kim, Biodegradable star-shaped poly-l-lactide. Studies in Polymer Science, 1994.* ***12****: p. 464-469.*

100. *Yuan, W., et al., Synthesis, characterization and degradation of hexa-armed star-shaped poly(l-lactide)s and poly(d,l-lactide)s initiated with hydroxyl-terminated cyclotriphosphazene. Polymer Degradation and Stability, 2005.* ***87****(3): p. 503-509.*

101. *Fu, C., et al., Improved hydrolytic stability of poly(dl-lactide) with epoxidized soybean oil. Polymer Degradation and Stability, 2010.* ***95****(4): p. 485-490.*

102. *Tsuji, H. and T. Hayashi, Hydrolytic degradation of linear 2-arm and branched 4-arm poly (dl-lactide) s: effects of branching and terminal hydroxyl groups. Polymer Degradation and Stability, 2014.* ***102****: p. 59-66.*

103. *Kim, S.H. and Y.H. Kim, Biodegradable star-shaped poly-l-lactide, in Studies in Polymer Science, D. Yoshiharu and F. Kazuhiko, Editors. 1994, Elsevier. p. 464-469.*

104. *Phuphuak, Y., et al., Balancing crystalline and amorphous domains in PLA through star-structured polylactides with dual plasticizer/nucleating agent functionality. Polymer, 2013.* ***54****(26): p. 7058-7070.*

105. *Wang, L., et al., Blends of linear and long-chain branched poly (l-lactide) s with high melt strength and fast crystallization rate. Industrial & Engineering Chemistry Research, 2012.* ***51****(30): p. 10088-10099.*

106. *Ouchi, T., S. Ichimura, and Y. Ohya, Synthesis of branched poly (lactide) using polyglycidol and thermal, mechanical properties of its solution-cast film. Polymer, 2006.* ***47****(1): p. 429-434.*

107. *Tsujimoto, T., et al., Synthesis of branched poly (lactic acid) bearing a castor oil core and its plasticization effect on poly (lactic acid). Polymer Journal, 2011.* ***43****(4): p. 425-430.*

108. *Phetwarotai, W., P. Potiyaraj, and D. Aht-Ong, Properties of compatibilized polylactide blend films with gelatinized corn and tapioca starches. Journal of Applied Polymer Science, 2010.* ***116****(4): p. 2305-2311.*

109. *Peesan, M., P. Supaphol, and R. Rujiravanit, Effect of casting solvent on characteristics of hexanoyl chitosan/polylactide blend films. Journal of Applied Polymer Science, 2007.* ***105****(4): p. 1844-1852.*

110. *Focarete, M.L., et al., Miscibility and mechanical properties of blends of (L)-lactide copolymers with atactic poly (3-hydroxybutyrate). Macromolecules, 2002.* ***35****(22): p. 8472-8477.*

111. *Khajeheian, M.B. and A. Rosling, Preparation and characterization of linear and star-shaped poly L-lactide blends. Journal of Applied Polymer Science, 2016.* ***133****(2).*

112. *Regnell Andersson, S., et al., Customizing the hydrolytic degradation rate of stereocomplex PLA through different PDLA architectures. Biomacromolecules, 2012.* ***13****(4): p. 1212-1222.*

113. *Chen, X., et al., Preparation and properties of ramie fabric-reinforced thermoset poly lactic acid composites. Journal of Reinforced Plastics and Composites, 2014.* ***33****(10): p. 953-963.*

114. *Åkesson, D., et al., Synthesis and characterization of a lactic acid-based thermoset resin suitable for structural composites and coatings. Journal of Applied Polymer Science, 2010.* ***115****(1): p. 480-486.*

115. *Kim, J.W. and J.S. Lee, The effect of the melt viscosity and impregnation of a film on the mechanical properties of thermoplastic composites. Materials, 2016.* ***9****(6): p. 448.*

116. *Balasubramanian, M., Composite materials and processing. 2013: CRC Press.*

117. *Oswald, H.J. and L. Segal, Glass fiber filled polyamide composites. 1975, Google Patents.*

118. *Gerard, P., M. Glotin, and G. Hochstetter, Composite material via in-situ polymerization of thermoplastic (meth) acrylic resins and its use. 2012, Google Patents.*

119. *Myard, P. and F. Philippon, Composite materials comprising a reinforcing material and a star polyamide as a thermoplastic matrix, the precursor compound article of said materials and the products obtained using same. 2008, Google Patents.*

CHAPTER 3

3 Materials and Methodology

3.1 Summary

This chapter details the materials and methods used to prepare the blends of linear polystyrene (LP) with hyperbranched (HB), hydrogenated hyperbranched (H-HB) and linear functional (LF) poly divinyl benzene and also the blends of linear poly lactic acid (PLA) with star shaped poly lactic acids (SPLAs). Composites were manufactured using E glass fibres and both polystyrene and poly lactic acid blends as matrix. Neat polymers and blends were characterised using FTIR, DSC, TGA, DMA. and the mechanical properties (tensile strength and modulus) of linear polymer films and blends were also obtained. Rheological test (dynamic temperature ramp test, DTRT) of linear polymer films and blends were carried out to determine the temperature at which the polymer and blends started to show the flow behaviour. The viscosity measurement was conducted to find the viscosity of linear polymer films and blends at the temperature of making composites. The flexural strength and modulus of composites were measured. Degradation studies were carried out in deionised water for linear PLA, blends and the composites prepared using linear PLA and the blends as matrix.

3.2 Materials

Linear polystyrene (LP) (Grade 430102) (M_w ~192 KiloDalton (kDa)) was purchased from Sigma Aldrich, UK. The hyper-branched poly divinyl benzene of two different mol. wt. (*HB1*) and (*HB2*) of (M_w~ 20.8 kDa and 60 kDa respectively), hydrogenated hyperbrached poly divinyl benzene (*H-HB2*) (M_w~60 kDa) and the linear functional poly divinyl benzene (*LF*) (M_w~10 kDa) was manufactured and supplied by Adlington kevin, PhD student, Department of Chemical and Environmental Engineering, University of Nottingham, UK. Woven E-glass fibre was purchased from Plastic Direct (U.K.), weave style: plain woven, thickness: 0.2 mm, overall weight: 200g/m^2, sizing type: silane and chloroform (10% w/v) was purchased from Fisher Scientific (UK).

Polylactic acid (PLA) beads were purchased from NatureWorks LLC (IngeoTM Grade 3251D average Mw~90 -120 kDa, Density=1.24 g cm^{-3}). The star shaped poly lactic acid of four different molecular weights M_n~ 3, 6, 9 and 12 kDa was prepared and supplied by Alexander, postdoctoral research associate, Department of Chemical and Environmental Engineering, University of Nottingham, UK.

3.3 Synthesis of polymers

3.3.1 Synthesis of Hyperbranched poly divinylbenzene (HB), hydrogenated Hyperbranched poly divinylbenzene (H- HB) and linear functional poly divinylbenzene (LF)

The HB (monomer 100% DVB), H-HB (monomer 100% DVB) and LF (monomer 99% styrene and 1% DVB) was synthesised according to the synthesis process described in literature.[1] The required quantities of degassed DVB, cyclohexanone and CoPhBF were placed into a dry Schlenk flask equipped with a magnetic stirrer bar and containing an inert nitrogen atmosphere. The reaction flask was then immersed in a preheated oil bath and the reaction was conducted at 150°C for 22 mins under inert atmosphere. Upon completion of the reaction, the vessel was immediately quenched in liquid nitrogen to prevent further reaction and hence gelation. The mixture was then diluted using chloroform and then precipitated three times using cold (0°C) methanol. The precipitation was filtered using a büchner funnel filter and kept under vacuum at room temperature (25^{o}C) for 48 hours. The GPC data of the HB1, HB2, H-HB2 and LF is presented in Table 3.1. Figure 3.1 is representing the functional groups presented in LP, HB1 &HB2, H-HB2 and LF polymers.

Table 3.1: *GPC data for the HB1 &HB2, H-HB2 and LF polymers used in this study*

Polymer	M_n (kDa)	M_w (kDa)	Polydispersity (M_w/M_n)
HB1	4.3	20.8	4.77
HB2	2.8	60	21.42
H-HB2	2.8	60.1	21.46
LF	5.6	10.3	1.822

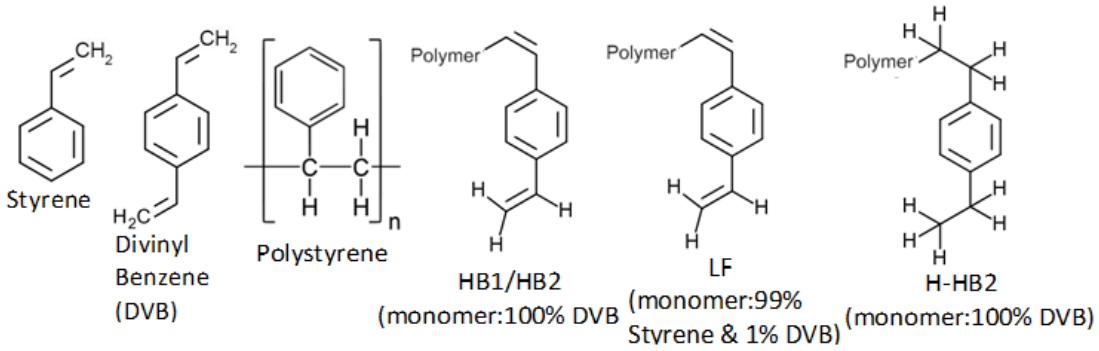

Figure 3.1: *Structural groups predicted to be present in LP, HB1 &HB2, H-HB2 and LF polymers*

3.3.2 Synthesis of star poly lactic acid

Sorbitol and L-lactide of a specific molar ratio were placed in a 25 mL round bottom flask. The flask was purged with Argon for several minutes. The sample was inserted into an oil bath that was pre-heated to 180°C. After 5 minutes, 100 µL of catalyst stock solution was injected and the reaction was allowed to proceed for 20 minutes. Once complete, the reaction vessel was opened and the reaction mixture was spurged with air for 1 minute. A still head with a reflux condenser was attached and the residual monomer was removed at 175°C under vacuum. The reaction mixture was then poured into a petri dish lined with aluminium foil. The GPC data of SPLA is presented in Table 3.2. The schematic representation of 6-arm star shaped PDLLA is presented in Figure 3.2.

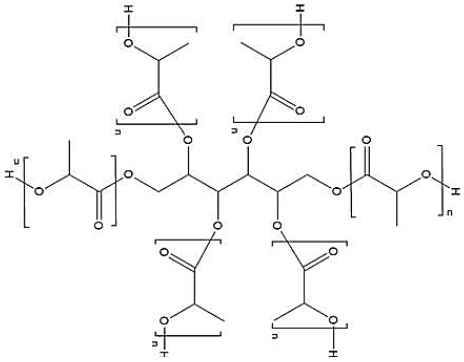

Figure 3.2: *Schematic representation of 6-arm star shaped PDLLA*

Table 3.2: *GPC data for the star polylactic acid (SPLA) used in this study*

Polymer	M_n (kDa)	M_w (kDa)	Polydispersity (M_w/M_n)
SPLA-3	3.11	3.3	1.06
SPLA-6	6.02	6.35	1.05
SPLA-9	8.86	9.26	1.04
SPLA-12	11.6	12.1	1.04

3.4 Preparation of Blends

3.4.1 Preparation of blends of linear polystyrene with hyperbranched, hydrogenated hyperbranched and lightly branched poly divinyl benzene

The blends of linear polystyrene (LP) with hyperbranched (HB1 and HB2), hydrogenated hyperbranched (H-HB2) and linear functional (LF) poly divinyl benzene of two different compositions (90-10 and 80-20) were prepared by dissolving specific amounts of the polymers in chloroform (4% w/v). The solution was stirred at room temperature (~25°C) for 3 hours using a magnetic stirrer for homogenisation and poured into a PTFE mould. The mixture was then allowed to evaporate at room temperature (25°C) for 24 hours. A slow evaporation rate was maintained by covering the mould with perforated paper which restricted the escape of the volatile solvent. The film of linear polystyrene (used as control) was also prepared following the same procedure as above. The neat polymers and all the blends (thickness ~0.3 mm) were

further dried in an oven at 50°C for 3 days to remove any residual solvent. However, the films of neat branched polymers could not be tested due to their inherent brittle nature.

LP film and all blends except LP-LF 90-10 and 80-20 were heat treated at 200°C for 20 min and then cooled down below the glass transition temperature (T_g) (~101°C) at ~10°C per min. LP-LF blends were heat treated at 140°C for 20 min and also cooled down below the T_g (~80°C) at ~10°C per min to study the change in properties of the LP film and blends after heat treatment. The polymer sample codes are represented in Table 3.3.

Table 3.3**:** *Sample codes used with their respective polymer forms and blends investigated*

Sample codes	LP (wt%)	HB1 (wt%)	HB2 (wt%)	H-HB2 (wt%)	LF (wt%)
Linear LP film	100		-	-	-
LP-HB1 90-10	90	10	-	-	-
LP-HB1 80-20	80	20	-	-	-
LP-HB2 90-10	90		10		
LP-HB2 80-20	80		20		
LP-H-HB2 90-10	90		-	10	-
LP-H-HB2 80-20	80		-	20	-
LP-LF 90-10	90		-	-	10
LP-LF 80-20	80		-	-	20

3.4.2 Preparation of blends of linear poly lactic acid with star shaped poly lactic acid

The blends of linear with star shaped poly lactic acid (of four different molecular weights; M_n: 3 kDa, 6 kDa, 9 kDa and 12 kDa) (Table 3.4) of 80-20 composition were also prepared by following the same procedure as mentioned in section 3.4.1. However, unlike LP-HB blends, blends of linear PLA and SPLA was cast in glass petri

dishes and covered fully to ensure slowest solvent evaporation so that air didn't trap in the casted films.

However, linear PLA and blends were heat treated at 175°C for 20 mins and also cooled down below the T_g (~50°C) at ~10°C per min to observe the effect of heat treatment on the thermal, crystallisation and degradation properties of the samples. The polymer sample codes are represented in Table 3.5.

Table 3.5: *Sample codes with their respective polymer forms and blends investigated*

Sample codes	PLA (wt%)	SPLA-3 (wt%)	SPLA-6 (wt%)	SPLA-9 (wt%)	SPLA-12 (wt%)
Linear PLA film	100		-	-	-
PLA-3 80-20	80	20	-	-	-
PLA-6 80-20	80		20	-	-
PLA-9 80-20	90			20	-
PLA-12 80-20	80				20

3.5 Preparation of composites using polymer blends as matrix

3.5.1 Preparation of polystyrene blends composites

The LP film, LP-HB1, LP-HB2, LP-H-HB2 and LP-LF blends (~0.3 mm thick) were prepared as mentioned before. The composites were prepared via a film stacking process. The polymer films were stacked alternately with woven E-glass fibre mats in a 1mm thick mould cavity between two metallic plates (see Figure 3.3). The width and length of the mould was 60 mm x 60 mm respectively. For composites with LP, blends of hyperbranched (LP-HB1 and LP-HB2) and hydrogenated hyperbranched (LP-H-HB2) divinyl benzene the entire stack was then heated in the press for 10 min at 200°C and pressed for 10 mins at 40 bar. For composites with lightly branched divinyl

benzene (LP-LF-GF) the polymer fibre stack was heated at 140°C for 10 min and then pressed for 10 min at 40 bar pressure. After pressing the composites were cooled immediately under the same pressure at a rate ~10°C/min to below T_g of LP (~101°C) for LP-HB1-GF, LP-HB2-GF and LP-H-HB2-GF composites and T_g of LP-LF (~80°C) for LP-LF-GF composites. The LP-GF composite was prepared to use as control. The resulting laminated composites were cut into 25mm length × 10 mm width for flexural test method using a Diamond cutter. The composites prepared in this study with their respective sample codes, polymer blends and volume fractions of polymer blends and fibres are presented in Table 3.6 below.

***Table 3.6**: Composite codes, polymer matrices and volume fractions of polymer matrices and fibres*

Composite code	Polymer films	E-Glass fibre (vol^m %)	Polymer films (vol^m %)
LP-GF	LP	40±0.07	60±0.05
LP-HB1 90-10-GF	LP-HB1 90-10	39.0±0.1	60.98±0.09
LP-HB1 80-20-GF	LP-HB1 80-20	37.8±0.05	62.12±0.2
LP-HB2 90-10-GF	LP-HB2 90-10	38.7±0.2	61.21±0.09
LP-HB2 80-20-GF	LP-HB2 80-20	38.1±0.1	61.86±0.1
LP-H-HB2 90-10-GF	LP-H-HB2 90-10	40.5±0.09	59.45±0.07
LP-H-HB2 80-20-GF	LP-H-HB2 80-20	40.3±0.08	59.62±0.08
LP-LF 90-10-GF	LP-LF 90-10	37.8±0.3	62.11±0.2
LP-LF 80-20-GF	LP-LF 80-20	37.8±0.1	62.17±0.1

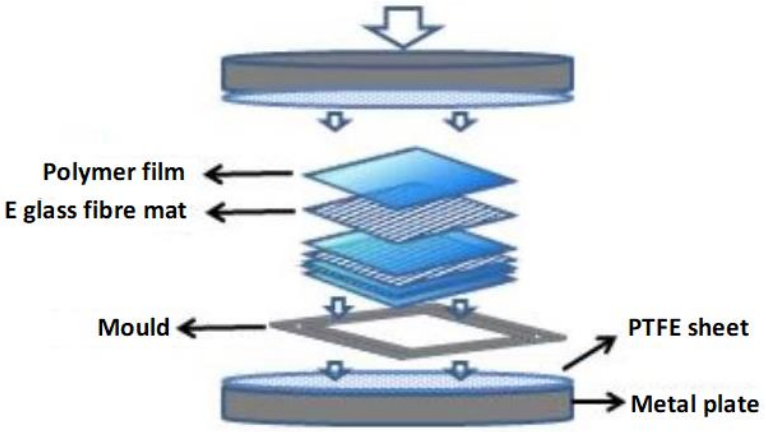

***Figure 3.3**: A Schematic diagram of the stacking arrangement of the prepared composites [2]*

3.5.2 Preparation of poly lactic acid blends composites

The PLA film, PLA-3 80-20, PLA-6 80-20, PLA-9 80-20 and PLA-12 80-20 blends (~0.3 mm thick) were prepared as mentioned in 3.4.1. Unlike LP composites, for PLA composites the whole stack was heated in the press for 10 min at 175°C and pressed for 10 mins at 40 bar. After pressing the composites were cooled immediately under the same pressure at a rate ~10°C/min to below T_g of SPLA (~50°C). The composites prepared in this study with their respective sample codes, polymer blends and volume fractions of polymer blends and fibres are presented in Table 3.7 below.

***Table 3.7:** Composite codes, polymer matrices and volume fractions of polymer matrices and fibres*

Composite code	Polymer films	E-Glass fibre (vol^m %)	Polymer films (vol^m %)
PLA-GF	PLA	39.4±0.1	60.6±0.2
PLA-3 80-20-GF	PLA-3 80-20	38.9±0.1	61.0±0.1
PLA-6 80-20-GF	PLA-6 80-20	39.0±0.3	60.9±0.3
PLA-9 80-20-GF	PLA-9 80-20	39.4±0.09	60.5±0.2
PLA-12 80-20-GF	PLA-12 80-20	40.0±0.1	59.9±0.1

3.6 Characterisation Techniques

3.6.1 Gel Permeation Chromatography (GPC)

GPC was performed using a refractive index (RI) detector with HPLC grade THF as the eluent. Analysis of branched and star shaped polymers was performed at 40°C with a flow rate of 1 ml/min through gel Mixed-C columns with a calibration range set was 580 – 377,400 Da calibrated using polystyrene standards. Sample concentration was ca. 1 mg/ml. The GPC data were analysed using the ASTRA GPC offline software (Version 6.1)

3.6.2 Fourier Transform Infrared (FTIR) Spectroscopy

Functional groups of the linear, branched and star shaped polymers were identified using FTIR spectroscopy (Tensor-27, Bruker, Germany). Opus^{TM} software version 5.5 was used for analysing the spectra and the scanning was done in transmittance mode in the region of 4500 to 550 cm^{-1} (wave numbers) using a standard Pike attenuated total reflectance (ATR) cell (Pike Technology, UK). The experiment was repeated with three times for each polymer.

3.6.3 Differential Scanning Calorimetry (DSC)

The linear, branched, star shaped polymers and the blends of different compositions were investigated using a DSC (Q2000, TA instruments, UK) to investigate their glass transition temperatures. Samples (approximately 5 mg) were heated from 25°C to 300°C at a heating rate of 10°C min^{-1} under nitrogen gas flow (100 mL min^{-1}). After heating, the samples were subsequently cooled down to 25 °C at 20°C min^{-1} before ramping again to 300°C at the same heating rate. After completion of each heating cycle the samples were isothermally held for 5 min. Data acquisition and processing

was performed using TA Universal analysis 2000 software. A blank pan measurement was also conducted for background correction and at least three tests were conducted for each material to ensure repeatability. Glass transition temperature was determined from the middle of the incline of the initial heat flow curve. The percentage crystallinity (%X_c) of linear, star PLA and the blends of linear and SPLA was calculated according to Equation 3.4

$$\%X_c = \frac{\Delta H_m - \Delta H_c}{93.1} \times 100 \quad (3.4)$$

Where, ΔH_m and ΔH_c are the enthalpy of melting and crystallisation (J g^{-1}) respectively, of the polymers and the heat of fusion of a 100% crystallinity is 93.6 J g^{-1}.

3.6.4 Thermogravimetric Analysis (TGA)

A SDT Q600 thermogravimetric analyser from TA instruments (USA) was used to analyse the thermal stability of the linear, branched, star shaped polymers and the blends. Samples (approximately 5 mg) were heated from room temperature (25°C) to 600°C at a heating rate of 10°C min^{-1} under 100 mL/min air flow. A blank analysis was conducted for background correction. The mass loss (%) and its derivative with respect to temperature of the pure polymers and the blends were determined. Data acquisition and processing was performed using TA Universal analysis 2000 software. The experiment was repeated three times for each sample.

3.6.5 Dynamic Mechanical Analysis (DMA)

The dynamic mechanical analysis was performed for both blends and films of linear polymers using a DMA (Q-800 from TA Instruments, USA) in multi frequency strain

mode to investigate the tensile storage modulus (*G'*), loss modulus (*G''*) and tan delta of the polymer films. The dimensions of the samples were 5 mm in width and 25 mm in length and heated from room temperature (25°C) to maximum 120 °C at a rate of 3 °C min^{-1}, 15 mm gap distance, 0.05% strain, 0.01 N preload force, 125% force track and 1 Hz constant frequency. Q series (Q-800) software was used for the characterisation.

3.6.6 X-Ray Diffraction (XRD)

XRD diffraction patterns of linear PLA, blends and composites prepared using linear PLA and blends as matrix were recorded using a D500 diffractometer (SIEMENS) operated at 40 kV and 25 mA, utilising a CuKα- radiation source (λ=0.154). The scans were controlled by the Diffrac-AC software program. For XRD analysis, samples were scanned using a step-scanning method with a step size of 0.05° and 2s intervals in the range from 2° to 50° of the diffraction angle (2θ)

3.6.7 Rheological Characterisation

3.6.7.1 Dynamic Oscillatory measurement

Rheological experiments were conducted using an Anton-Paar 302 rheometer. Films of linear polymers and blends of 0.6 mm thickness were prepared using solvent casting process and were placed between two parallel plates (25 mm). For linear polystyrene and LP-HB1, LP-HB2 and LP-H-HB2 blends the plates were then heated to 100°C and for LP-LF blends to 90°C to ensure even distribution of the sample within two parallel plates. Whereas for linear PLA and blends, the plates were heated to 80°C. In both case the parallel plate gap was adjusted between 0.5-0.6 mm. The heating and cooling rate was 7°C min^{-1} at an angular frequency of 6.283 rad s^{-1} and

strain was maintained within the linear viscoelastic regime, typically 0.1%. Temperature-dependent changes in elastic (storage) modulus, G' and viscous (loss) modulus, G'' were recorded in the dynamic temperature ramp test (DTRT). The analysed temperature interval range was from 100 °C to 200°C for LP, LP-HB1, LP-HB2 and LP-H-HB2 blends and from 90°C to 150°C for LP-LF blends. Similarly, for linear PLA and blends the analysed temperature interval range was from 80 °C to 180°C.

3.6.7.2 Dynamic viscosity measurement

The dynamic viscosity was also determined using Anton-Paar 302 rheometer. Measurements were performed using a 25 mm parallel plate gap which was adjusted to between 0.5-0.6 mm. All tests were done with a logarithmically increasing shear rate range between 0.01 s^{-1} and 100 s^{-1}. Viscosity of LP, LP-HB1, LP-HB2 and LP-H-HB2 blends were measured at 200°C and LP-LF was measured at 140°C. The linear PLA and blends were measured at 175°C.

3.6.8 Burn off tests

The fibre volume fraction of the composites was determined via the standard test method (BS 2782-10: Method 1002:1977 EN 60) for ignition loss of cured reinforced resins. The mass of the metal sample tray was measured with and without the composite sample. Triplicate samples were then placed into a furnace at 500°C (below the glass T_g) for an hour, ensuring complete combustion of the polymer. The mass of the trays and residues were measured after removal from the furnace. Then the fibre volume fractions were calculated according to the following equation 3.5)

$$P = \frac{m_2 - m_3}{m_2 - m_1} \times 100 \quad (3.5)$$

where, P is the percentage loss on ignition

m_1 is the mass of the container

m_2 is the initial total mass of the container plus the specimen

m_3 is the final total mass, after combustion, of the container and the residue.

3.6.9 Mechanical testing

3.6.9.1 Tensile tests

The linear polymer films and blends of the different compositions investigated were cut into dog bone shapes (width ˜ 4mm, thickness˜ 0.3mm) (see Figure 3.4) using a dog bone cutter and the tensile properties were determined using an Instron tensile test machine 5969 (Software-QMAT) with a cross head speed of 0.5 mm min^{-1}, gauge length 25 mm and a 1 kN load cell. Also in conjugation with an Imetrum video gauge, values were collected from at least five repeat specimens. The tensile strength and modulus were calculated from experimental data according to the standard (ISO/DIS 527-1).

***Figure 3.4**: Representative image of the dog bone shape polymer films tested*

3.6.9.2 Flexural test:

The flexural strength and modulus of the composite samples (10mm×25mm) were evaluated by flexural (three-point bending) tests using an Instron 5969 testing machine (Software-QMAT). These measurements were done according to the standards BS EN ISO 14125:1998. A crosshead speed of 0.5 mm/min and a 5 kN load cell was used. Flexural studies were conducted using three repeat specimens.

3.6.10 Scanning Electron Microscopy

Scanning electron microscope images were taken to examine the cross section of the freeze-fractured composite plates. The specimens were carbon coated prior to examination and viewed with a JEOL 6400 SEM scanning electron microscope operated at 10 kV in secondary electron mode (SE).

3.6.11 Statistical analysis

Statistical analysis on a sample group (more than two specimens) was performed using Tukey's Multiple Comparison Test (95 % confidence intervals) through a one-way analysis of variance (ANOVA), employing Graph Pad Prism software (version 5.01).

3.6.12 Solution degradation studies

3.6.12.1 Percentage Mass Loss

The linear PLA films, blends and composites prepared using PLA and blends as matrix of dimension 10×25×1 mm^3 (length× width× height) were immersed in deionised water (50 mL) according to standard ISO 10993-13:2010. The vials were then placed in an oven at 50°C. At various time points (7 days, 14 days, 21 days, 28 days and 35 days) the samples were taken out and then dried for two days at 50°C to remove any trace amounts of water. The mass of the samples was taken prior to immersion, m_i and the dry mass of the sample was measured, m_d. The percentage mass loss was calculated according to the following equation 3.6)

$$\%M_L = \frac{(m_d - m_i)}{m_i} \times 100 \qquad (3.6)$$

3.6.12.2 pH measurements

The pH of the deionised water was measured before sample immersion and at each time point during the degradation study. Measurements were taken using Hanna Instruments pH 211 Microprocessor pH meter.

3.7 References

1. *Barker, I.A., et al., Catalytic Chain Transfer Mediated Autopolymerization of Divinylbenzene: Toward Facile Synthesis of High Alkene Functional Group Density Hyperbranched Materials. Macromolecules, 2012.* ***45****(23): p. 9258-9266.*

2. *Liu, X., Surface modification of bioresorbable phosphate glass fibres for biomedical applications. 2014, PhD thesis.The University of Nottingham. p. 163.*

CHAPTER 4

4 Comparison of thermal and thermo-mechanical properties for styrene based hyper, hydrogenated hyper and linear functional divinyl benzene polymers and their blends with linear polystyrene

4.1 Introduction

In recent years there has been an increasing level of interest in the use of non-linear polymer structures within the polymer using communities. This is because their three dimensional structures have been demonstrated to exhibit both physical and material properties that are differentiated for conventional, linear chain polymers. Polymer structures types that are routinely synthesised include graft, star, dendrimers and hyperbranched polymers. Dendrimers have a well-defined structure, however, they are usually prepared by multi step reactions and expensive routes. Consequently, HB polymers are prepared by one step and relatively inexpensive approaches, however, they possesses same but a less well-defined structure than dendrimes.[1, 2] In the specific case of hyperbranched (HB) polymers, these produce what are referred to “globular” structure which are characterised by a high concentration of inter-chain branching points and a high level of chain ends per molecular proposed to be located at the periphery.[3-5] Due to their unique architecture, HB macromolecules possess some unique properties.[5] For example, HB polymers exhibit high solubility in various organic solvents and low intrinsic viscosities in comparison with their linear analogues.[6] Such that they have been exploited in a broad range of application areas including coatings, adhesives, modifiers, additives and as carriers of dye molecules.[4, 7]

However, in practice almost all of these applications have utilised HB polymers as a constituent within a polymer blend. This is mainly because HB homopolymers exhibit mechanical brittleness and as a result the production of free viable polymer films cannot be produced from these polymers.[8] The brittleness of HB polymers are mainly due to the lack of polymer chain entanglement within the bulk.[9] Therefore, blending of HB with other more conventional, typically linear polymers is a route to overcoming these issues and achieving the manufacture of materials with useful properties.[10, 11]

The typical target of a polymer blending is to produce a polymeric material with overall material properties beyond that exhibited by the individual polymer components that make up that blend.[12-14] The material properties exhibited the blend developed polymer usually depend on the degree of interaction between the two pure polymers and hence the level of compatibility within the blend system.[13-15] For example, a poor degree of interaction or immiscibility can result in high interfacial tension and thus lead to poor mechanical properties.[16, 17] The miscibility within a blend is usually determined by comparing the glass transition temperature (T_g) of the blend versus those of its pure polymer components. For example, a miscible polymer blend will exhibit a single T_g between the T_g values of the pure individual polymers.[18] In contrast immiscible blends will exhibit distinct T_g values at the temperatures characteristic of the T_g of the pure homopolymers.

Consequently, because blending produces materials that are a composite of those of the its constituents, blends of HB polymers with linear polymers should provide a route to produce novel materials with enhanced properties.[19] To date, literature

reports have detailed the use of HB polymers as a blend component to impart or modify properties such as increasing toughness,[20] and enhancing the thermal decomposition of a microbial polyester.[10] Kim and Webster reported a decrease in the melt viscosity and improved modulus with the blend of HB poly(phenylene) and polystyrene when compared to pure polystyrene.[21]

HB polymers have already proved to be effective additives for epoxy thermoset resins.[22, 23] The addition of HB polymers has been shown to increase the toughness of epoxy resin whilst exerting little or no effect on the viscosity.[24-27] For example, Zhang and Jia blended HB poly(trimellitic anhydride-diethylene glycol) ester epoxy resin (molecular weight 3,400 g mol^{-1}) with an epoxy amine resin system (diglycidyl ether of bisphenol-A) (DGEBA) in presence of a curing agent. They reported twice the fracture toughness (3.20 MPa $m^{1/2}$) for cured systems when compared to that of the of DGEBA alone.[28] Liu *et al.* also cure DGEBA with different wt% HB (hyperbranched polyethers) functionalised with epoxy with a curing agent and reported the impact strength, tensile strength and T_g increased to 41.2 kJ/m^2, 72.1 MPa, and 150.7°C, respectively for 5wt% HB loading than pure DGEBA.[29]

In this study we used a range of HB polymers prepared by Catalytic Chain Transfer (CCT) Mediated Autopolymerisation method [2] and the structures are defined in the experimental sections. CCT is a very efficient control strategy for free radical polymerisation of divinyl monomers to form hyper-branched materials of controlled molecular weight.[30, 31] The main products of catalytic chain transfer polymerisation are of unsaturated carbon-carbon double bonded terminated polymer chains.[2, 32] The polymers prepared in this study were hyper-branched

poly divinyl benzene (HB), hydrogenated hyper-branched poly divinyl benzene (H-HB) (the end vinyl group was hydrogenated) and the linear functional polymer (LF). The polymers produced were blended with linear polystyrene LP of two different compositions (90-10 and 80-20) via solvent casting method and characterised. The thermal and thermo-mechanical properties of these polymer blended films were also evaluated to investigate the effect of introducing HB polymers containing different functional groups and exhibiting differing degrees of branching into blends with linear polystyrene.

4.2 Results

4.2.1 FTIR Analysis

Functional groups of the neat polymer samples (LP, HB1, HB2, LF, H-HB2 - see Figure 4.1) were identified using FTIR-ATR spectroscopy (Chapter 3 section 3.6.2) and this data is presented in Figure 4.1 .

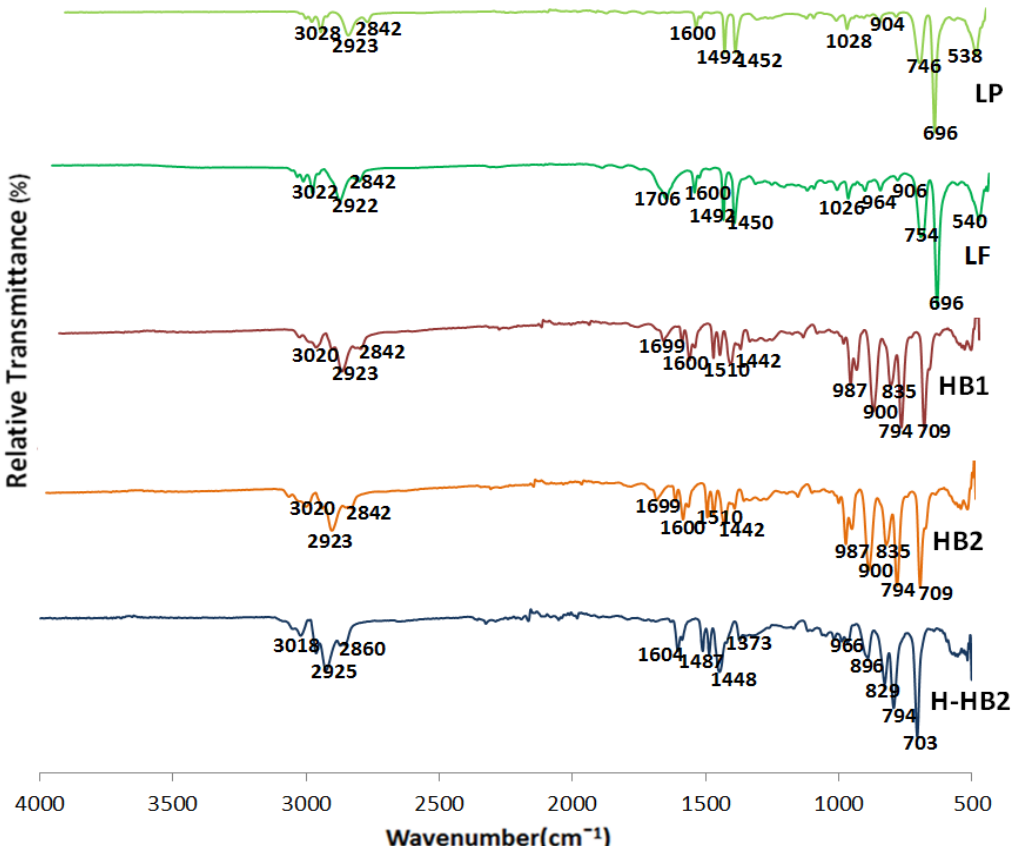

***Figure 4.1**: Comparison of the FTIR-ATR spectrum of LP, LF, HB1, HB2 and H- HB2 polymers*

Common peaks were identified for all styrene based polymers (LP, HB1, HB2, LF, H-HB2) in the region from 3018 cm^{-1} to 3028 cm^{-1} for aromatic C-H stretching vibrations and from 1440 cm^{-1} to 1700 cm^{-1} for phenyl C=C and C-C stretching.[33-35] Moreover, the bands for symmetric and asymmetric C-H stretching were observed for each of the polymers at ~2842 and ~2923 cm^{-1}. [36]

4.2.2 DSC Analysis

DSC analysis was conducted (as stated in Chapter 3 section 3.6.3) to investigate the thermal properties of the neat polymers (LP, LF, HB1, HB2 and H-HB2) and LP-HB1, LP-HB2, LP-H-HB2 including the LP-LF blends of 90-10 and 80-20 compositions (see Figure 4.2a and b respectively).

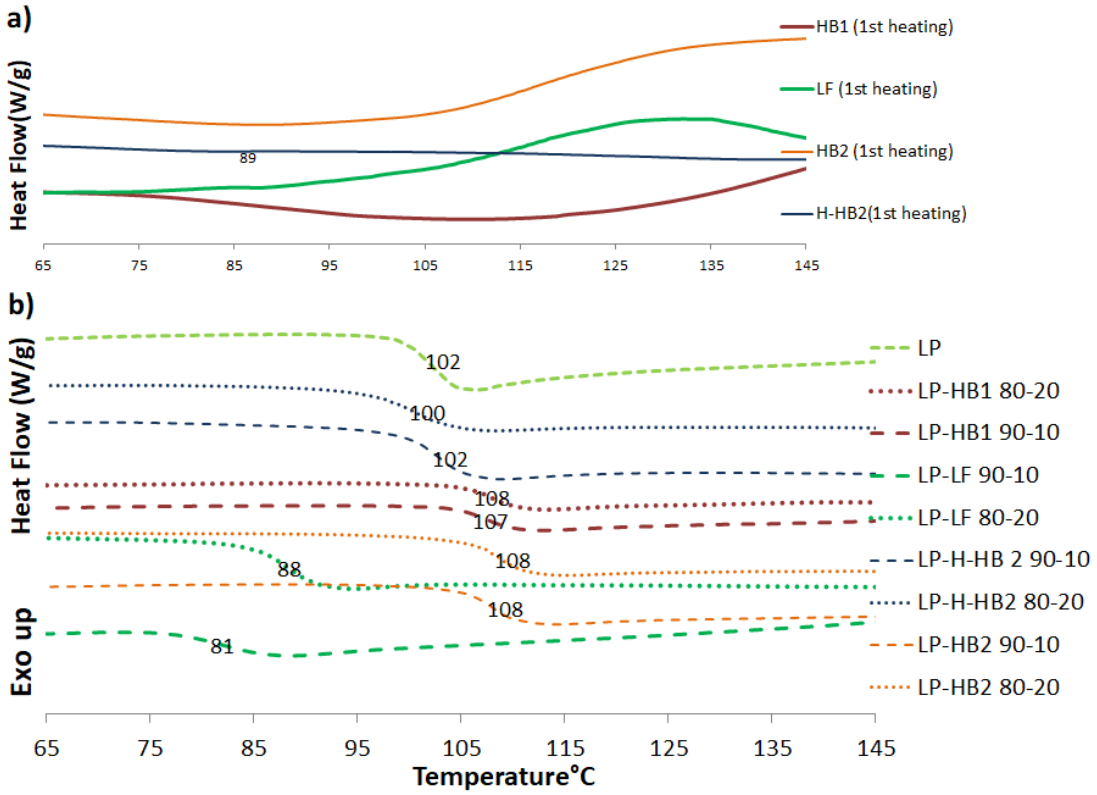

Figure 4.2: *Comparison of the DSC thermograms of a) LF, HB1, HB2 and H-HB2 (first heating cycle) polymers b) LP polymer, LP-HB1, LP-LF, LP-HB2 and LP-H-HB2 blends (second heating cycle)*

Typically, when presenting thermal data, the information detail is from the second heating cycle to allow the first heating cycle to remove any thermal history within the sample related to it physical preparation. However, in Figure 4.2a, the first heating cycles of the neat LF, HB1, HB2 and H-HB2 polymers are presented. This was because broad peaks within the temperature region of 125°C to 165°C and 110°C to 130°C were observed in the 1st heating cycle for the HB1 and HB2 materials respectively but not in the case of the hydrogenated derivative H-HB2.

The second heating cycle from the DSC scans of the polymer blends is presented in Figure 4.2b. This data showed that the LP-HB1 90-10 and 80-20 blends exhibited T_g's at higher temperature (107°C and 108°C respectively) compared to the LP polymer (102°C). Higher T_g value at 108°C in comparison to LP was also identified for LP-HB2 90-10 and 80-20 whereas for LP-H-HB2 90-10 and 80-20 the T_g value was obtained at 100°C and 102°C respectively. The lowest T_g value among blends was observed for LP-LF 90-10 and 80-20 at 81°C and 88°C respectively.

Figure 4.3 is representing the FTIR spectra of heat treated HB1 an HB2 at 200°C.

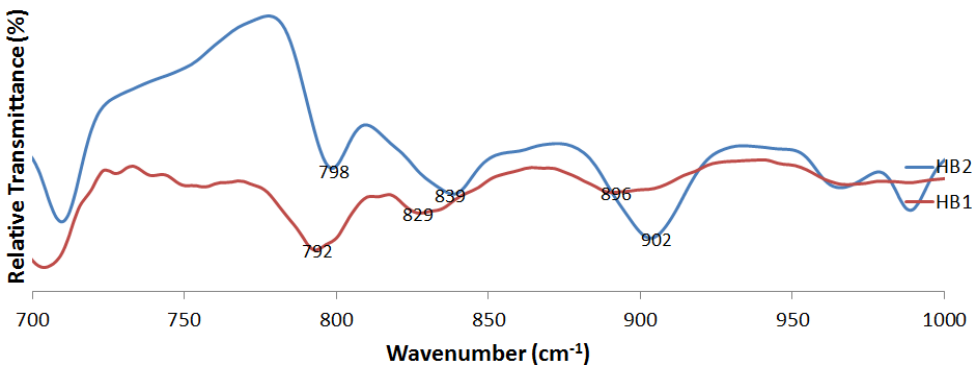

***Figure 4.3**: Comparison of the FTIR-ATR spectra of HB1 and HB2 polymer that has been heat treated at 200°C with the equivalent non-heat treated material.*

From the study of the FTIR spectra it was clear that after heat treatment the peak intensity for =C-H bending at 902 cm^{-1} was absent for HB1 whereas for HB2 the peak was still identifiable.

4.2.3 Thermogravimetric Analysis (TGA)

The thermal degradation data of LP, HB1, LF, HB2, and H-HB2 are presented in Figure 4.4 and was conducted as stated in Chapter 3 section 3.6.4.

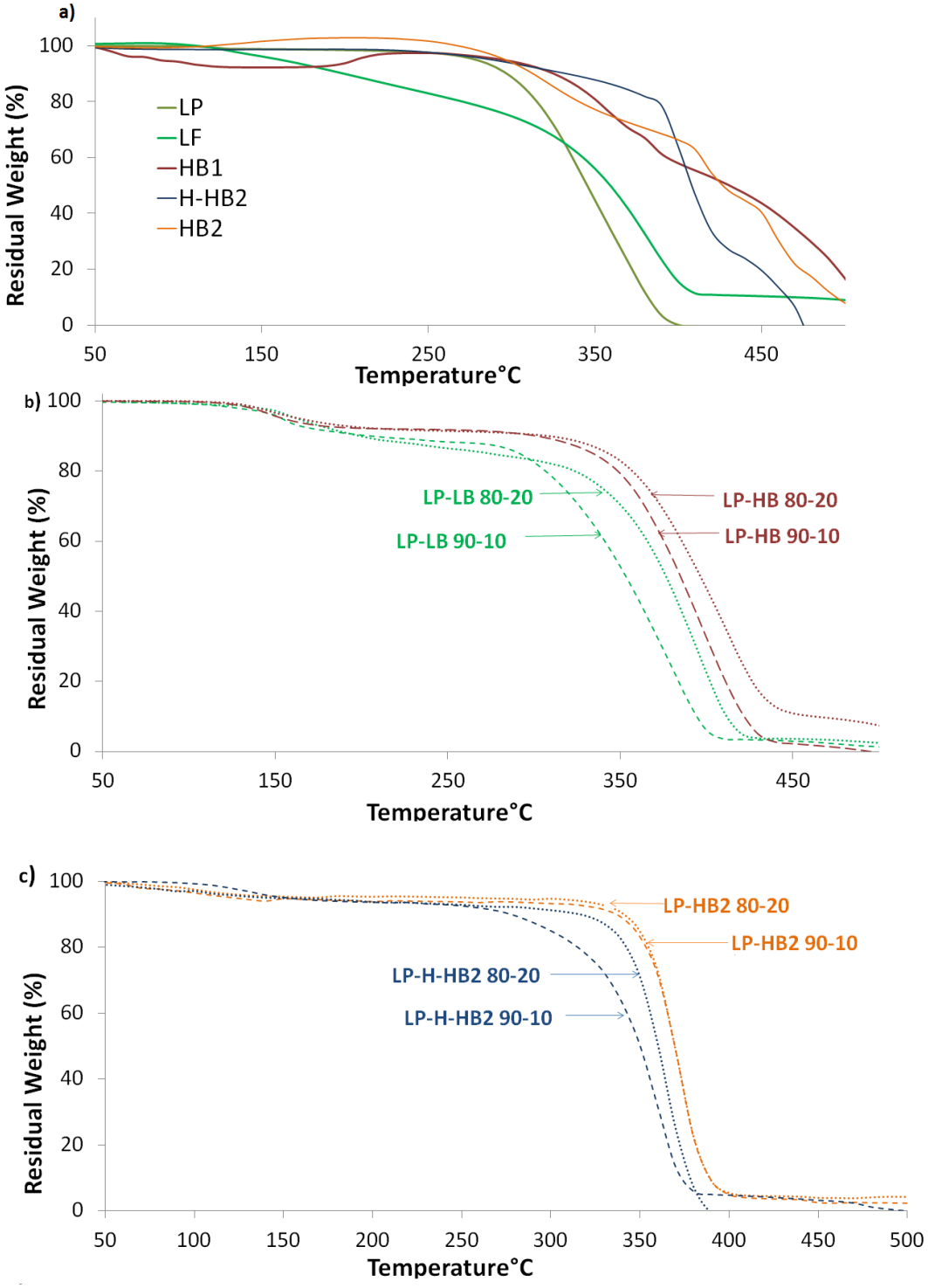

Figure 4.4: *Plot of the variation in residual sample weight versus temperature for a) LP, HB1, HB2 and H-HB2 polymers b) LP-HB1 and LP-LF blends c) LP-HB2 and LP-H-HB2 blends*

From Figure 4.4a it can be seen that LP started to thermally degrade at ~280°C, whereas the highest thermal stability was observed for H-HB2 polymer (~380°C). For HB1 and HB2 an increase in peak occurred between 225°C to ~330°C after which a multi stage major degradation was observed. LF experienced ~65% weight loss within the temperature region from 120°C to 330°C before it experienced major thermal degradation at 330°C.

Figure 4.4b and Figure 4.4c shows the TGA curve for LP-HB1, LP-LF and LP-HB2, LP-H-HB2 blends of both 90-10 and 80-20 compositions. All blends revealed 10% weight loss in the region from 130°C -180°C followed by second step of thermal degradation. LP-HB1 and LP-HB2 (Figure 4.4b and c) showed almost higher thermal stability (as for both HB1 and HB2 their 90-10 and 80-20 started to degrade ~340°C) in comparison to LP (at 280°C). Both LP-LF 90-10 and LP-H-HB2 90-10 blends showed thermal stability at ~280°C similar to LP and for LP-H-HB2 80-20 and LP-LF 80-20 thermal stability had increased to ~330°C and ~320°C respectively.

The derivative thermogravimetric curves are shown in Figure 4.5a to c, these defined the maximum decomposition temperature (T_{max}) of the neat polymers and blends of 90-10 and 80-20 compositions

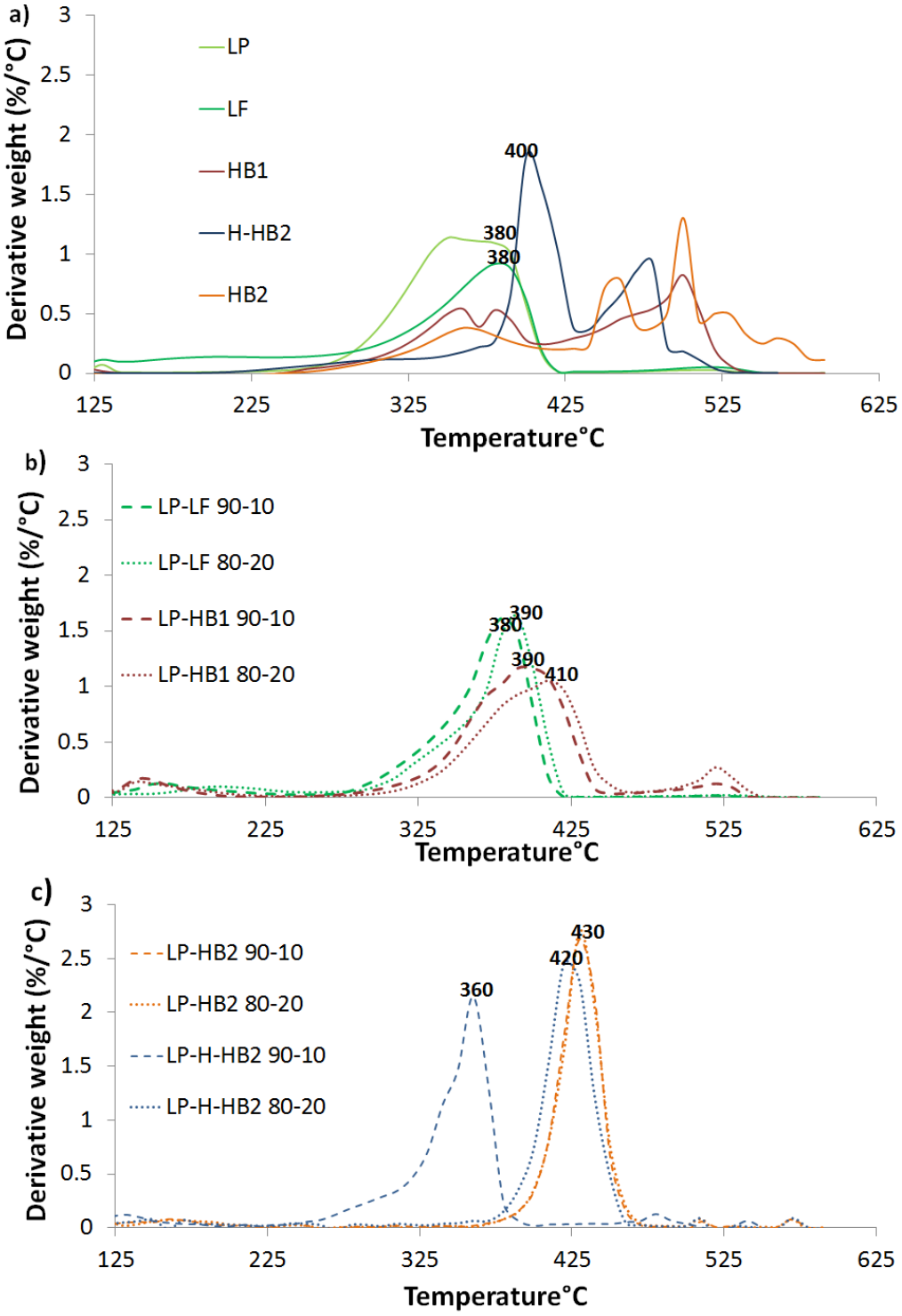

Figure 4.5: *Plot of the variation in derivative weight versus temperature for a) LP, HB1, HB2, H- HB and LF polymers b) LP-HB1, LP-HB2, LP-LF and LP-H-HB2 blends*

T_{max} is the temperature at which the major thermal degradation in the materials occurred.[37] Figure 4.5a showed the highest T_{max} for this series of polymers was exhibited by the H-HB2 polymer at 400°C. The T_{max} value identified for LP, LF at 380°C. However, no specific T_{max} was identified for the HB1 and HB2 polymers.

However, amongst the blends the higher T_{max} for LP-HB2 blends (both 90-10 and 80-20) (Figure 4.5c) increased at 430°C compared to LP-HB1 (390°C for 90-10 and 410°C for 80-20 blend) (Figure 4.5b). For LP-H-HB2 T_{max} identified for 90-10 and 80-20 blends at 360°C and 420°C respectively and for LP-LF T_{max} identified at 380°C for 90-10 and at 390°C for 80-20 respectively.

4.2.4 Dynamic-mechanical Properties (DMA)

Using DMA the storage modulus (representing the elastic portion) and the tanδ (ratio of the loss modulus to storage modulus) were investigated (see chapter 3 section 3.6.5) for the LP film, LP-HB1, LP-HB2, LP-H-HB2 and LP-LF blends (n=3) as a function of temperature and this data in shown in Figure 4.6 a and Figure 4.6b respectively**.**

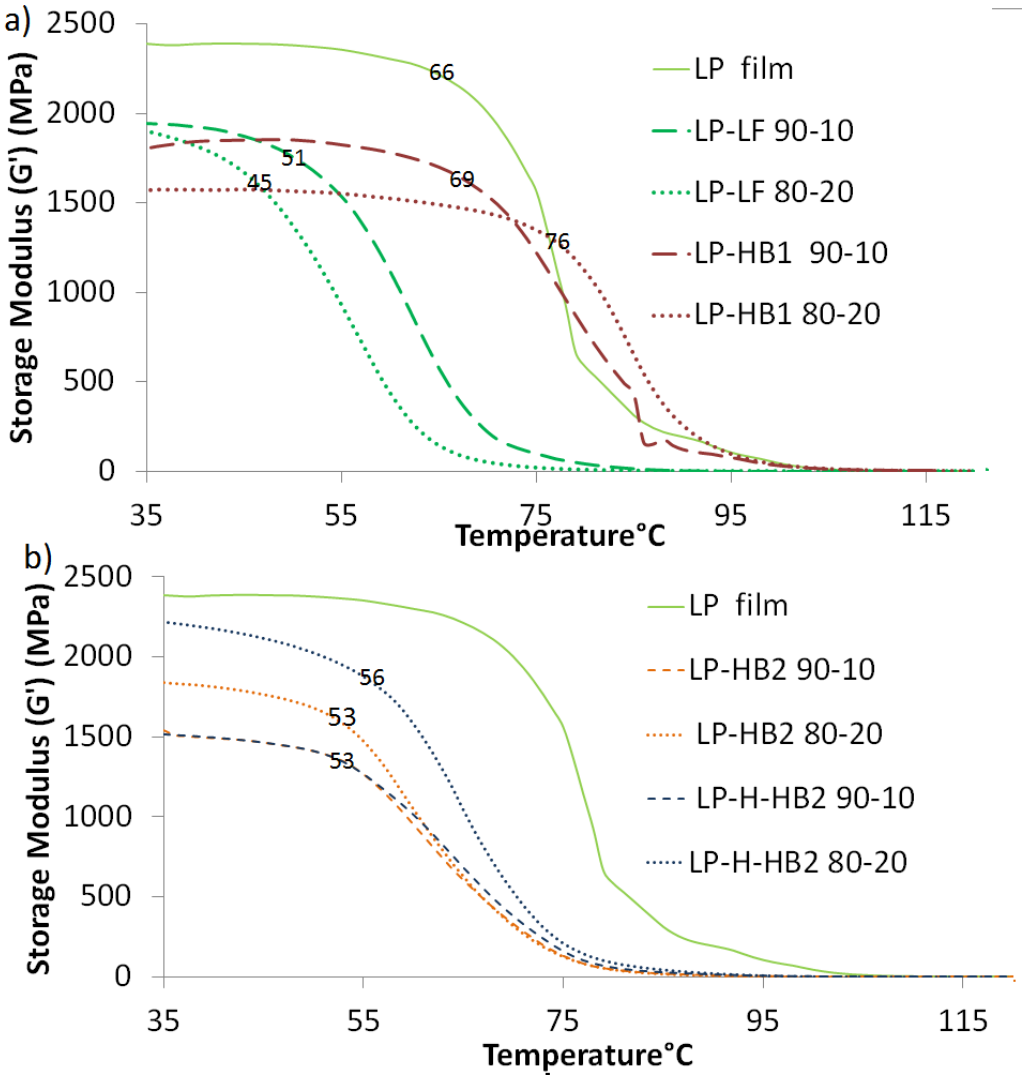

Figure 4.6: *Plot of the variation in storage modulus curves with temperature for a) LP, LP-HB1, LP-LF and b) LP-HB2 and LP-H-HB2 blend*

The DMA results presented in Figure 4.6a define how the storage modulus (*G'*) of LP, LP-LF and LP-HB1 blends varies against temperature when the sample is ramped from 30°C to 120°C. At around 35°C, the highest storage modulus (*G'*) was seen for the LP film alone (2.38 GPa) whereas for LP-HB1 the values were found at 1.7 GPa for the 90-10 blend and at 1.56 GPa for the 80-20 respectively. LP-LF films showed a modulus value of ~2 GPa for both 90-10 and 80-20 composition at around 35°C as seen from

Figure 4.7a. From Figure 4.6b it seen that the storage modulus of LP-H-HB2 (80-20) was similar (1.8 GPa) to the LP-HB2 (80-20) film (1.8 GPa) and almost the same value was obtained for LP-H-HB2 (90-10) and LP-HB2 (90-10) at (1.5 GPa) at 35°C.

From the tan delta curves (Figure 4.7) The T_g values identified for all the blended films except LP-HB2 90-10 and 80-20 were in good agreement with the T_g values measured using DSC.

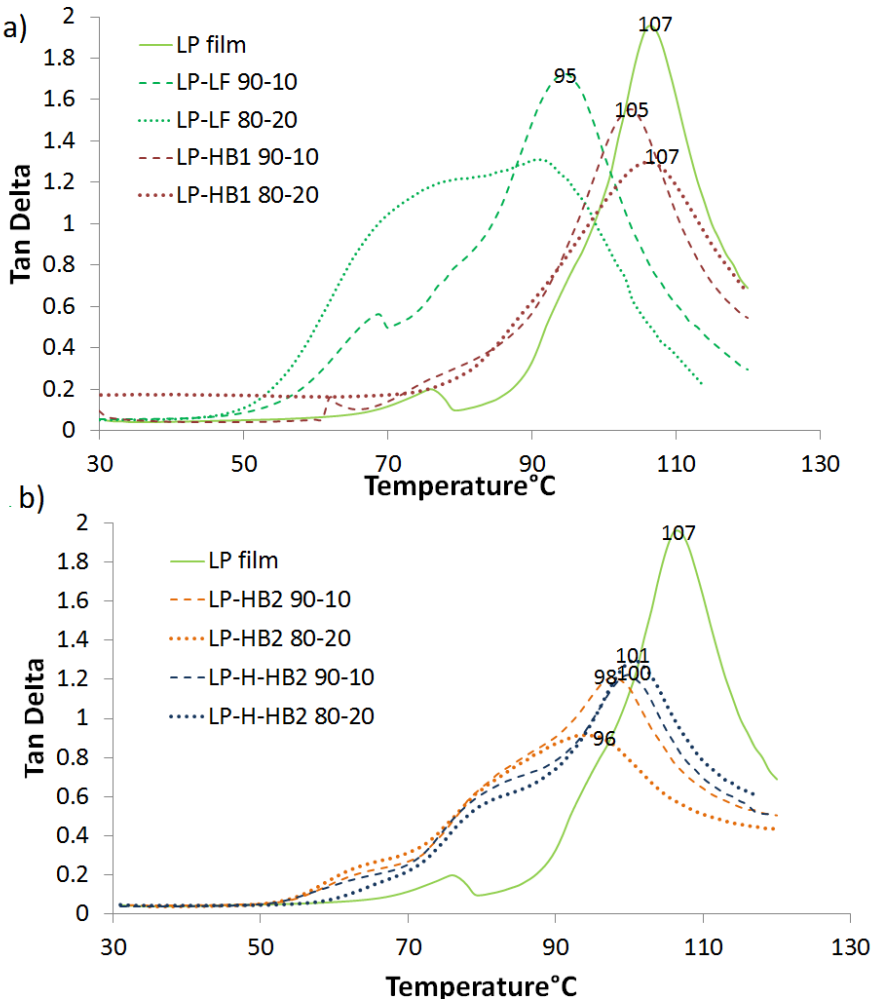

Figure 4.7: *Tan delta curves of LP, LP-HB1, LP-LF and b) LP-HB2 and LP-H-HB2 blends*

Table 4.1 is representing a comparison between the T_g value obtained by DSC and the T_g value obtained by DMA.

Table 4.1: *Comparison of the T_g value obtained from the Tan delta curve of DMA and DSC thermogram*

Samples	T_g from Tan delta (°C)	T_g from DSC (°C)
LP	107±0.04	101±0.05
LP-HB1 90-10	105±0.06	108±0.02
LP-HB1 80-20	106±0.03	107±0.03
LP-HB2 90-10	98±0.03	108±0.01
LP-HB2 80-20	96±0.02	108±0.03
LP-H-HB 90-10	100±0.05	103±0.02
LP-H-HB 80-20	102±0.01	104±0.04
LP-LF 90-10	95±0.02	88±0.02
LP-LF 80-20	91±0.03	81±0.02

4.3 Discussion

With respect to pendant/terminal vinyl species from Figure 4.1, the peaks observed for LP and LF were nearly similar, as the monomer used for LP was styrene and for LF 99% styrene with 1% divinyl benzene (DVB). However, a peak of very low intensity at 968 cm^{-1} was also identified for LF which can be attributed to the =C-H vibrations of the few vinyl groups present in LF (Figure 4.1). In contrast to LP, additional peaks were also observed for HB1, HB2 and H-HB2 polymers in the region from 700 to 1000 cm^{-1} which are the characteristic peaks for DVB.[38-40] The peaks identified for HB1 and HB2 at ~900 cm^{-1} and ~980 cm^{-1} were assigned to =C-H vibrations of the vinyl group.[41] The presence of peaks for HB1 and HB2 at =C-H indicated that no crosslinking of HB1 and HB2 had occurred at 50°C as all the polymers were kept at 50°C in an oven for 3 days before characterisation. Peaks corresponding to =C-H at ~896 cm^{-1} and ~970 cm^{-1} were also observed for the H-HB2 polymer, however, was of very low intensity which suggested that for H-HB2, some pendant/terminal vinyl double (-CH=CH_2) bonds remained non-hydrogenated to ethyl (-CH_2-CH_3).[36]

In Figure 4.2a (DSC measurement) the broad peaks identified within the temperature region of 125°C to 165°C and 110°C to 130°C for the HB1 and HB2 materials respectively could be attributed to the crosslinking of polymer chains due to the presence of reactive vinyl (-CH=CH_2) chain end groups.[42-44] Li *et al.* [42] reported a similar exothermic peak at around 165°C and did not identify any specific T_g from DSC analysis for polystyrene beads crosslinked (more than 30%) with divinylbenzene. They attributed this peak to be due to the coupling reaction (thermally initiated) of pendant double bonds/vinyl group of DVB close to each other.

Other studies have also reported on the crosslinking effect of DVB due to the presence of vinyl groups (-CH=CH_2).[36, 41, 45] This conclusion was supported by the lack of an exothermic peak being observed for the neat H-HB2 polymer (due to the presence of non-reactive ethyl -CH_2-CH_3 functional group), rather the feature found in the first heating cycle for this material (Figure 4.2a) at around 80°C was attributed to be the T_g of this polymer by comparison with the second heating data (see Figure 4.2b below). However, the T_g of the H-HB2 polymer has found to be decreased significantly in comparison to the LP, which may be attributed to the lack of polymer chain entanglement and also the increased amount of end-group free volumes of H-HB2 than LP. Barker *et al.*[2] suggested that for HB polymer, crowding increase in the molecular structure which reduce entanglements inside the branched structures and also between individual macromolecules. As a result the entanglement dominated physical properties (e,g; intrinsic viscosity, T_g value) of the HB polymer decreased. Akabori *et al.*[46] produced hydrogen terminated hyperbranched polystyrene and found that the T_g value to be 372 K for linear PS whereas this value decreased to 361K for the hyperbranched polystyrene.

The shift of the T_g of the LP-HB1 90-10 and 80-20 to 107°C and 108°C respectively could be again attributed to the crosslinking effect of HB1. Similarly, the crosslinking effect was observed with the high molecular weight HB2 polymer and again the T_g of the LP-HB2 90-10 and 80-20 was raised to 108°C. Meanwhile, the T_g did not significantly ($p<0.05$) increase for the blends containing high M_w DVB (LP-HB2). For linear polymers as M_w increases, the T_g reaches a constant value as the number of chain ends become smaller with higher M_w.[46] However, it has been reported that the T_g of HB1 and HB2 polymers are mostly affected by the branching points, chemical nature and the number of the terminal functional groups rather than the M_w.[46-48] For HB polystyrene, Akabori *et al.*[46] reported higher T_g value for HB polymer with higher number of methylene content per molecule (due to higher intramolecular crosslinking) than the one with lower number of methylene content.

To observe the effect of the crosslinking for HB1 and HB2 (of different molecular weight) on the T_g, both polymers were heat treated at 200°C for 20 min and then FTIR analysis was conducted for both polymers. For heat treated HB2 the peak at 902 cm^{-1} (due to =C-H bending) (Figure 4.3) can be identified whereas for HB1 this peak was absent.

As such, one suggested explanation for this observation was that the degree of crosslinking for the low molecular weight HB1 polymer was higher in comparison to the high molecular weight HB2 polymer. This can be related to the level of functional group of HB1 and HB2 becoming involved in crosslinking processes as they have quite different molecular weights.

Alternatively, hyper-branched polymers with increasing molecular weight may also exhibit an increased density of end groups and branching per molecule. This in turn may lead to restricted thermal molecular motion and thus a similar level of crosslinking although now with the residual functional group being present and so a similar increase the T_g for both systems.[46]

For LP-H-HB2 90-10 and 80-20 blends lower T_g was identified at 102°C and 100°C than for LP-HB2 blended films (at 108°C) of the same molecular weight. This T_g value was expected to be due to the absence of crosslinking for LP-H-HB2 from non-reactive chain ends (-CH_2-CH_3).

LF has less contribution from reactive chain end groups (-CH=CH_2) in comparison to the HB1 and HB2 polymer and will not cause a significant crosslinking effect in the LP-LF blend system (90-10 and 80-20 composition). Moreover, the branching of LF was very low compared to HB1, HB2 and H-HB2 polymers and possesses essentially linear polymeric structure like LP. In this regard, the significantly lower T_g value of LP-LF 90-10 and 80-20 blends at 81°C and 88°C respectively in comparison to the LP and other blends can be attributed to the low molecular weight (M_w: 10.3 kDa) of LF polymer. It has been reported that for lightly branched polymer molecular weight effect is predominant than for branching effect.[49] So, it can be stated that for LF polymer the lower molecular weight effect was dominant over branching and end group effect.

From Figure 4.4a (TGA thermogram) it can be seen that LP started to thermally degrade at ~280°C. The degradation of LP has been reported to be initiated at unsaturated linkages (acted as weak point) by the end chain initiation whereas for HB

at the CCTP unsaturated linkages was expected to act as the weak points along the chain.[50] Cleavage of these double bond sites produce free radicals which proceed to unzip and produce monomer (~300°C).[50] This radical depolymerisation was reported to be the dominant reaction for LP and poly DVB degradation in the temperature range of 300–600°C.[44, 51] However it was expected that CCTP polymer (HB1 and HB2) would exhibit lower thermal stability than the LP produced by standard free radical chemistry since the mechanism had introduced a cleavable double bond at the end of every chain. So, for the HB1 and HB2 polymers, the end functional groups present in the structure would be expected to be a dominant factor in determining thermal stability of these polymers. The thermogram (Figure 4.4a) for HB1 exhibited a slight decrease followed by a multi stage major degradation ~330°C. A similar ~3% weight gain was observed in the region from 125°C to 290°C, for HB2 before major degradation of polymer started. Maciejewska, *et al.* observed similar thermal degradation profile when they used DVB as a crosslinking agent for co polymer of 1-vinyl-2-pyrrolidone (filled with MCM-41 silica) in TGA measurements.[44] So, it can be said that increased thermal resistance was observed for HB1 and HB2 branched structure in comparison to LP since the higher number of branch points (CCTP vinyl group) underwent crosslinking and halted the depolymerisation process rather than acting as chain initiator site like LP.

The onset of major degradation was highest for the H-HB2 polymer (~380°C) (Figure 4.4a) and it also showed no increase in mass across the entire temperature range. This supported both the conclusion that the onset temperature is dictated by the level of CCTP end-groups as for H-HB2 as there are only saturated end groups (-CH_2-CH_3-) for hydrogenated polymer and for non-hydrogentated, it was the crosslinking

of the polymer that leads to the increase in mass observed. It has been reported that poly methyl methacrylate polymer chains which unzip at 200°C contain unsaturated groups (methacrylate), whereas polymer chains which depolymerise at higher temperatures 380°C have saturated end groups (methyl).[52]

LF polymer (Figure 4.4a) which is largely linear material possess less branching than HB polymer, however they have few DVB functional vinyl groups present and it has been made via CCTP whilst LP was made via standard free radical techniques. Thus it was proposed that the few unsaturated CCTP vinyl chain ends in LF acted as radical initiators rather crosslinking agent and promote thermal degradation at lower temperature of around 120°C than for LP (~280°C).[41, 53]

From Figure 4.4 b and c, the first step of thermal degradation (from 130°C -180°C) of all blends was attributed to either the loss of moisture or other volatiles as the blends were prepared via the solvent casting method using chloroform as solvent. [54] The second step of thermal degradation of blends, attributed to main chain degradation,[55] demonstrated the higher thermal of stability LP-HB1 and LP-HB2 (as both 90-10 and 80-20 started to degrade ~340°C) (Figure 4.4 b and c) blends was due to crosslinking effects (as both 90-10 and 80-20 started to degrade ~340°C) than the LP (at 280°C). Both LP-LF and LP-H-HB2 blends were shown to be less thermally stable in comparison to the HB1 and HB2 blends indicting that the crosslinking is an important factor in increasing thermal stability with such low levels of HB polymer addition on blends.

From Figure 4.5a similar T_{max} value identified for LP, LF at 380°C supporting the fact that LF was likely to have predominantly linear structures. However, no specific

temperature was identified for the HB1 and HB2 polymers which is likely to be due to the crosslinking of these two polymers.

However, from Figure 4.5b, the highest T_{max} observed for LP-HB2 80-20 composition in comparison to LP-HB1 80-20 can be explained in terms of the increased number of branching of high molecular weight HB2 due to its greater functional group density.[46] The higher T_{max} of the LP-H-HB2 80-20 at 420°C (Figure 4.5c) in comparison to LP at 380°C again demonstrating the presence of unsaturated terminal group increase the thermal performance. Similarly, for LP-LF (Figure 4.5c) T_{max} at 390°C did not increased significantly with addition of LF in blends than that of LP.

From Figure 4.6a, the lower modulus for LP-LF films was observed compared to LP which suggested the lower molecular weight of LF. However, with increasing temperature unlike other polymer films (LP, LP-LF 90-10 and 80-20, LP-HB1 90-10) LP-HB1 80-20 showed a constant G' value (1.4 GPa) and decreased at relatively higher temperature (~76°C). This was suggested to be due to crosslinked polymer films (LP-HB1 80-20) which had tighter and stiffer networks than un-crosslinked or lower crosslinked polymer films and showed a decrease in storage modulus at higher temperature.[56-58]

From Figure 4.6a and b it can be seen, that unlike LP-HB1 80-20, LP-HB2 80-20 blends experienced decreasing in storage modulus (G') at much lower temperature (~58°C) which again suggested lower crosslinking of HB2 compared to HB1 in the temperature range below glass transition temperature.

From the tan delta curves (Figure 4.7) the α transition (the peak temperature of the tan delta curve) represented the glass transition temperature (T_g).[29, 58, 59] For LP-

HB2 90-10 and 80-20 the T_g identified from DSC analysis was 108°C whereas from the DMA it was 98°C. It has already been reported that T_g identified by DSC and DMA can vary from as much as 5-20°C due to the difference in sample size, geometry and experimental conditions.[41] However, for LP-HB2 films in addition to the above mentioned reasons lower crosslinking effect in presence of 1 Hz constant frequency (experimental condition) may have also decreased the T_g lower than that identified using DSC analysis. For other blends the T_g value measured by DMA was in good agreement with the T_g value obtained from DSC.

4.4 Conclusions

- The crosslinking (due to the presence of reactive vinyl chain end group) of HB1 and HB2 at high temperature increased the thermal properties (T_g ~108°C and T_{max}~410°C) of blends LP-HB1 and LP-HB2 90-10 and 80-20. However, with increasing mol. wt. higher crosslinking effect was not observed for HB2 in comparison to low mol. wt. HB1.

- The H-HB2 also revealed a highly branched structure with non-reactive ethyl ($-CH_2-CH_3$) end groups caused decrease in T_g ~100°C for blend containing 20wt% of H-HB2 (LP-H-HB2 80-20). This decrease in T_g for LP-H-HB2 80-20 blend can be attributed to the lack of polymer chain entanglement in H-HB2 and also the absence of crosslinking. An increase in thermal stability was observed for LP-H-HB2 80-20 (T_{max}~420°C) due to the presence of saturated ethyl chain end group.

- The linear functional LF also caused a decrease in T_g (~ 80°C) which could be attributed to its low mol. wt.

- The storage modulus obtained for blends was found to be lower at room temperature in comparison to LP, however, for blend containing 20wt% of HB1 (LP-HB1 80-20) showed a constant storage modulus even at high temperature indicated higher crosslinking of this blend in comparison to un-crosslinked LP or comparatively lower crosslinked LP-HB2 blends.

- It can also be said that for HB1, HB2 and H-HB2 20wt% addition of this neat polymers in blend composition change the blend properties significantly, whereas for LF significant change in blend properties was observed for 10wt% addition.

4.5 References

1. *Jikei, M. and M.-a. Kakimoto, Hyperbranched polymers: a promising new class of materials. Progress in Polymer Science, 2001.* ***26****(8): p. 1233-1285.*

2. *Barker, I.A., et al., Catalytic chain transfer mediated autopolymerization of divinylbenzene: toward facile synthesis of high alkene functional group density hyperbranched materials. Macromolecules, 2012.* ***45****(23): p. 9258-9266.*

3. *Voit, B.I. and A. Lederer, Hyperbranched and Highly branched polymer architectures synthetic strategies and major characterization aspects. Chemical reviews, 2009.* ***109****(11): p. 5924-5973.*

4. *Gao, C. and D. Yan, Hyperbranched polymers: from synthesis to applications. Progress in Polymer Science, 2004.* ***29****(3): p. 183-275.*

5. *Korolev, G. and M. Mogilevich, Properties and application of hyper-branched polymers, in three-dimensional free-radical polymerization. Springer Berlin Heidelberg, 2009. p. 243-255.*

6. *Mishra, M. and S. Kobayashi, Star and hyperbranched polymers. Vol. 53. 1999: CRC Press.*

7. *Yates, C. and W. Hayes, Synthesis and applications of hyperbranched polymers. European Polymer Journal, 2004.* ***40****(7): p. 1257-1281.*

8. *Schmaljohann, D., et al., Modification with alkyl chains and the influence on thermal and mechanical properties of aromatic hyperbranched polyesters. Macromolecular Chemistry and Physics, 2000.* ***201****(1): p. 49-57.*

9. *Kwak, S.-Y., et al., Amelioration of mechanical brittleness in hyperbranched polymer. 1. Macroscopic evaluation by dynamic viscoelastic relaxation. Polymer, 2004.* ***45****(20): p. 6889-6896.*

10. *Xu, S., et al., Blending and characterizations of microbial poly (3-hydroxybutyrate) with dendrimers. Journal of Applied Polymer Science, 2006.* ***102****(4): p. 3782-3790.*

11. *Nunez, C.M., et al., Mechanical properties of blends of PAMAM dendrimers with poly (vinyl chloride) and poly (vinyl acetate). Journal of Polymer Science Part A: Polymer Chemistry, 1998.* ***36****(12): p. 2111-2117.*

12. *Ibrahim, B.A. and K.M. Kadum, Influence of polymer blending on mechanical and thermal properties. Modern Applied Science, 2010.* ***4****(9): p.157.*

13. *Kaniappan, K. and S. Latha, Certain investigations on the formulation and characterization of polystyrene/poly (methyl methacrylate) blends. International Journal of ChemTech Research, 2011.* ***3****(2): p. 708-717.*

14. *Hwang, S.-H., M.-J. Kim, and J.-C. Jung, Mechanical and thermal properties of syndiotactic polystyrene blends with poly(p-phenylene sulfide). European Polymer Journal, 2002.* ***38****(9): p. 1881-1885.*

15. *Mudigoudra, B., S. Masti, and R. Chougale, thermal behavior of poly (vinyl alcohol)/poly (vinyl pyrrolidone)/chitosan ternary polymer blend films. Research Journal of Recent Sciences ISSN, 2012.* ***2277****: p. 2502.*

16. *Zhang, J., Q. Guo, and B. Fox, Thermal and mechanical properties of a dendritic hydroxyl-functional hyperbranched polymer and tetrafunctional epoxy resin blends. Journal of Polymer Science part B: Polymer Physics, 2010.* ***48****(4): p. 417-424.*

17. *Chuai, C., K. Almdal, and J. Lyngaae-Jørgensen, Thermal behavior and properties of polystyrene/poly (methyl methacrylate) blends. Journal of Applied Polymer Science, 2004.* ***91****(1): p. 609-620.*

18. *Usmani, A., Asphalt science and technology. 1997: CRC Press.*

19. *Massa, D., et al., Novel blends of hyperbranched polyesters and linear polymers. Macromolecules, 1995.* ***28****(9): p. 3214-3220.*

20. *Bhardwaj, R., Modification of polylactide bioplastic using hyperbranched polymer based nanostructures. 2008: ProQuest.*

21. *Kim, Y.H. and O.W. Webster, Hyperbranched polyphenylenes. Macromolecules, 1992.* ***25****(21): p. 5561-5572.*

22. *Mulkern, T.J. and N.C. Tan, Polystyrene/hyperbranched polyester blends and reactive polystyrene/hyperbranched polyester blends. 1999, DTIC Document.*

23. *Mulkern, T. and N. Tan, Processing and characterization of reactive polystyrene/hyperbranched polyester blends. Polymer, 2000.* ***41****(9): p. 3193-3203.*

24. *Hong, Y., et al., A novel processing aid for polymer extrusion: rheology and processing of polyethylene and hyperbranched polymer blends. Journal of Rheology (1978-present), 1999.* ***43****(3): p. 781-793.*

25. *Diao, J.Z., et al., Mechanical properties and morphology of blends of hyperbranched polymer with polypropylene and poly (vinyl chloride). Iranian Polymer Journal, 2006.* ***15****(1): p. 91-98.*

26. *Diao, J., et al., Compatibilization effects of a hyperbranched polymer on acrylonitrile-butadiene-styrene/poly (vinylchloride) blends. Iranian Polymer Journal, 2006.* ***15****(11): p. 863-870.*

27. *Hong, Y., et al., Film blowing of linear low-density polyethylene blended with a novel hyperbranched polymer processing aid. Polymer, 2000.* ***41****(21): p. 7705-7713.*

28. *Jackson, M.B., et al., Toughening epoxy resins with polyepichlorohydrin. Journal of Applied Polymer Science, 1993.* ***48****(7): p. 1259-1269.*

29. *Kim, D.S., et al., Effects of particle size and rubber content on fracture toughness in rubber-modified epoxies. Polymer Engineering & Science, 1996.* ***36****(6): p. 755-768.*

30. *Sorensen, K., et al., Dendritic polyester macromolecule in thermosetting resin matrix. 2000, Google Patents.*

31. *Mezzenga, R., L. Boogh, and J.-A. Månson, Toughening and failure mechanisms in blends of thermosets and hyperbranched polymers. No. EPFL-CONF-179054,2000.*

32. *Xu, J., et al., A morphological investigation of thermosets toughened with novel thermoplastics. I. Bismaleimide modified with hyperbranched polyester. Journal of Applied Polymer Science, 1999.* ***72****(8): p. 1065-1076.*

33. *Varley, R.J. and W. Tian, Toughening of an epoxy anhydride resin system using an epoxidized hyperbranched polymer. Polymer International, 2004.* ***53****(1): p. 69-77.*

34. *Zhang, D. and D. Jia, Toughness and strength improvement of diglycidyl ether of bisphenol-A by low viscosity liquid hyperbranched epoxy resin. Journal of Applied Polymer Science, 2006.* ***101****(4): p. 2504-2511.*

35. *Liu, T., et al., Hyperbranched polyether as an all-purpose epoxy modifier: controlled synthesis and toughening mechanisms. Journal of Materials Chemistry A, 2015.* ***3****(3): p. 1188-1198.*

36. *Smeets, N.M., Amphiphilic hyperbranched polymers from the copolymerization of a vinyl and divinyl monomer: the potential of catalytic chain transfer polymerization. European Polymer Journal, 2013.* ***49****(9): p. 2528-2544.*

37. *Guan, Z., Control of polymer topology through transition-metal catalysis: synthesis of hyperbranched polymers by cobalt-mediated free radical polymerization. Journal of the American Chemical Society, 2002.* ***124****(20): p. 5616-5617.*

38. *Soeriyadi, A.H., et al., Synthesis and modification of thermoresponsive poly (oligo (ethylene glycol) methacrylate) via catalytic chain transfer polymerization and thiol–ene Michael addition. Polymer Chemistry, 2011.* ***2****(4): p. 815-822.*

39. *Coates, J., Interpretation of infrared spectra, a practical approach. Encyclopedia of Analytical Chemistry, 2000.*

40. *León-Bermúdez, A.-Y. and R. Salazar, Synthesis and characterization of the polystyrene-asphaltene graft copolymer by FT-IR spectroscopy. CT&F-Ciencia, Tecnología y Futuro, 2008.* ***3****(4): p. 157-167.*

41. *Workman Jr, J. and L. Weyer, Practical guide to interpretive near-infrared spectroscopy. 2007: CRC press.*

42. *He, J., et al., Crosslinking effect on the deformation and fracture of monodisperse polystyrene-co-divinylbenzene particles. Express Polymer Letters, 2013.* ***7****(4): p. 365-374.*

43. *Khutoryanskaya, O.V., V.V. Khutoryanskiy, and R.A. Pethrick, Characterisation of blends based on hydroxyethylcellulose and maleic acid-alt-methyl vinyl ether. Macromolecular Chemistry and Physics, 2005.* ***206****(15): p. 1497-1510.*

44. *Flynn, G., L. Keller, and M. Miller. FTIR detection of organic carbon in interplanetary dust particles. in Lunar and Planetary Science Conference. 1998.* ***29****: p. 1157.*

45. *Gonçalves, M.A., et al. Dynamics of network formation in aqueous suspension raft styrene/divinylbenzene copolymerization. Macromolecular Symposia. 2013. Wiley Online Library.*

46. *Umamaheswari, S. and M. Murali, FTIR spectroscopic study of fungal degradation of poly (ethylene terephthalate) and polystyrene foam. 2013.* ***64****: p. 19159-19164.*

47. *Brijmohan, S.B., et al., Synthesis and characterization of cross-linked sulfonated polystyrene nanoparticles. Industrial & Engineering Chemistry Research, 2005.* ***44****(21): p. 8039-8045.*

48. *Li, Y., Y. Fan, and J. Ma, Thermal, physical and chemical stability of porous polystyrene-type beads with different degrees of crosslinking. Polymer Degradation and Stability, 2001.* ***73****(1): p. 163-167.*

49. *Sharma, V., et al., Synthesis and characterization of styrene-co-divinylbenzene-graft-linseed oil by free radical polymerization. Express Polymer Letters, 2008.* ***2****(4): p. 265-276.*

50. *Maciejewska, M. and J. Osypiuk-Tomasik, TG/DSC studies of modified 1–vinyl-2-pyrrolidone–divinylbenzene copolymers. Journal of Thermal Analysis and Calorimetry, 2013.* ***113****(1): p. 343-350.*

51. *Kangwansupamonkon, W., S. Damronglerd, and S. Kiatkamjornwong, Effects of the crosslinking agent and diluents on bead properties of styrene–divinylbenzene copolymers. Journal of Applied Polymer Science, 2002.* ***85****(3): p. 654-669.*

52. *Akabori, K.-i., et al., Glass transition behavior of hyper-branched polystyrenes. Polymer, 2009.* ***50****(20): p. 4868-4875.*

53. *Inoue, K., Functional dendrimers, hyperbranched and star polymers. Progress in Polymer Science, 2000.* ***25****(4): p. 453-571.*

54. *Higashihara, T., et al., Synthesis of hyperbranched polymers with controlled degree of branching. Polymer journal, 2012.* ***44****(1): p. 14-29.*

55. *Lindström, A., Environmentally friendly plasticizers for pvc: improved material properties and long-term performance through plasticizer design. 2007, KTH.*

56. *Straus, S. and S.L. Madorsky, Thermal stability of polydivinylbenzene and of copolymers of styrene with divinylbenzene and with trivinylbenzene. J Res Nat Bur Stand A Phys Chem A, 1961.* ***65****: p. 243-248.*

57. *Li, Y., Y. Fan, and J. Ma, The thermal properties of porous polydivinylbenzene beads. Reactive and Functional Polymers, 2002.* ***50****(1): p. 57-65.*

58. *Chanda, M. and S.K. Roy, Plastics technology handbook. Vol. 72. 2006: CRC press.*

59. *Nakatani, H., et al., Degradation behavior of polymer blend of isotactic polypropylenes with and without unsaturated chain end group. Science and Technology of Advanced Materials, 2016.* ***9****(2): p. 024401.*

60. *Hossain, K.M.Z., et al., Physico-chemical and mechanical properties of nanocomposites prepared using cellulose nanowhiskers and poly (lactic acid). Journal of Materials Science, 2012.* ***47****(6): p. 2675-2686.*

61. *Li, C., et al., Thermal gelation of chitosan in an aqueous alkali–urea solution. Soft matter, 2014.* ***10****(41): p. 8245-8253.*

62. *Rocha, M.C.G., M.E. Leyva, and M.G.d. Oliveira, Thermoplastic elastomers blends based on linear low density polyethylene, ethylene-1-octene copolymers and ground rubber tire. Polímeros, 2014.* ***24****(1): p. 23-29.*

63. *Herrera-Kao, W. and M. Aguilar-Vega, Storage modulus changes with temperature in poly (vinyl alcohol), PVA,/poly (acrylic acid), PAA, blends. Polymer Bulletin, 1999.* ***42****(4): p. 449-456.*

64. *Spoljaric, S., et al., Thermal, optical, and static/dynamic mechanical properties of linear-core crosslinked star polymer blends. Macromolecular Chemistry and Physics, 2011.* ***212****(16): p. 1778-1790.*

65. *Stoelting, J., F. Karasz, and W. MacKnight, Dynamic mechanical properties of poly (2, 6-dimethyl-1, 4-phenylene ether)-polystyrene blends. Polymer Engineering & Science, 1970.* ***10****(3): p. 133-138.*

CHAPTER 5

5 Characterisation of composites prepared using blends of hyper, hydrogenated hyper and linear functional polymer with linear polystyrene as matrix and E-glass fibre as reinforcement

5.1 Introduction

Hyper-branched (HB) polymers have largely been used as additives for both thermoset and thermoplastic polymer matrix composites.[1]

HB polymers functionalised with reactive functional groups have been used as additives for thermoset epoxy composites.[1-5] For example, Mezzenga, *et al.* used an epoxy functionalised HB polymer to modify epoxy matrix in making epoxy based composites and reported 2.5 fold increase in fracture toughness (K_{IC}) for addition of 5phr (parts per hundred rubber) of HB and also reported this increase in properties was obtained without affecting the viscosity, processability and the glass transition temperature of the epoxy resin.[1]

For thermoplastic composites, HB polymers were investigated to improve fibre/ matrix adhesion and better filler dispersion.[6] Lu *et al.* prepared sisal fibre/poly propylene/carboxyl terminated HB polymer composites and reported a 21.5% and 9.7% increase in impact and flexural strength respectively for the HB modified composites than for unmodified polymer fibre composites.[7] An increase in interfacial shear strength from 15 MPa to 20 MPa was reported by Gustav *et al.* for polypropylene/glass fibre composites when a highly reactive HB polymer grafted polypropylene was used as matrix modifier.[8]

Other composites have also been prepared with HB polymer to exploit their unique properties. Zhou *et al.* reported on the modification of multi-wall carbon nanotube (MWCNT) with a HB polymer which contained UV reactive functional groups.[9] The resin was then cured under UV irradiation and improved tensile strength and toughness values (by 41% and 105%) of the composite were reported for only 0.1 wt.% MWCNT.[9] Henrikssonstrong *et al.* produced a nanocomposite composed of a chemically crosslinked HB matrix (Boltorn H30) with cellulosic fibres.[10]

HB polymers have also been used in making nanocoatings,[11] dental composites, [12] ion conducting membranes for better ionic conductivity.[13]

This study prepared polymer composites using E-glass fibre as reinforcement with linear polystyrene which was blended with hyper-branched poly divinyl benzene (HB2), hydrogenated hyperbrancehd poly divinyl benzene (H-HB2) and linear functional poly divinyl benzene (LF) as the matrix component. The mechanical properties of the composites prepared were evaluated.

5.2 Results

5.2.1 Rheological properties

The storage modulus, (*G'*) and loss modulus, (*G''*) were plotted against temperature for LP and the blends investigated (see Figure 5.1A-D) and was measured as described in Chapter 3 section 3.6.7.

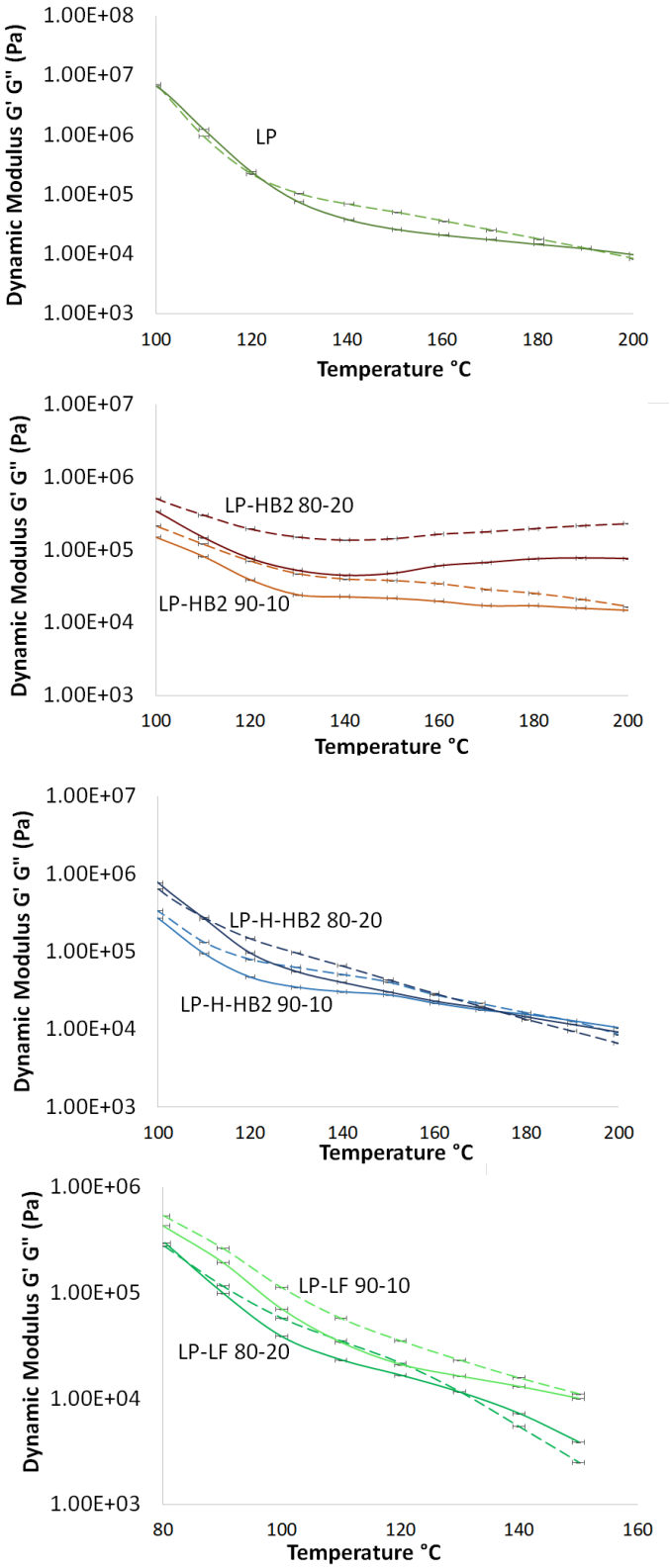

Figure 5.1: *Dynamic modulus properties for A) LP, B) LP-HB2 90-10 and 80-20, C) LP-H-HB2 90-10 and 80-20 (with temperature ramping from 90 to 200°C) and D) LP-LF 90-10 and 80-20 (with temperature ramping from 80°C to 140°C). Broken lines represent storage modulus (G') and solid lines represent loss modulus (G").*

From Figure 5.1A it can be seen that, for LP during the temperature ramp tests, the storage modulus (*G'*) was higher than the loss modulus (*G''*) up to ~190°C. However, for the hyperbranched (LP-HB2) blends (Figure 5.1B) (both 90-10 and 80-20) the storage modulus, (*G'*) was higher than the loss modulus across the temperature range from 100°C to 200°C. In addition, it was also observed that the LP-HB2 80-20 had a higher storage and loss moduli (which plateaued at around 2.3×10^5 Pa and 7.6×10^4 Pa respectively) in comparison to the LP-HB2 90-10 (both storage and loss moduli plateaued at around 1.5×10^4 Pa). However, both LP-HB2 90-10 and 80-20 did not show any flow behaviour (*G''* was lower than *G'*) across the whole temperature region.

The hydrogenated hyperbranched (LP-H-HB2) polymer blends revealed a more rapid decline in loss and storage moduli (for both the 90-10 and 80-20 blends) in comparison to the LP-HB2 blends. At approximately 100°C the LP-H-HB2 80-20 had a higher storage modulus (6.62×10^5 Pa) in comparison to LP-H-HB2 90-10 (2.41×10^5 Pa). However, the storage and loss moduli of LP-H-HB2 80-20 decreased to similar levels to the storage and loss moduli of LP-H-HB2 90-10 from between 150°C to 180°C. At around 175°C for both LP-H-HB2 90-10 and 80-20 blends the loss moduli became higher than the storage moduli and the blends started to show flow behaviour.

For the linear functional (LP-LF) polymer blends the profile observed was opposite to the LP-HB2 and LP-H-HB2 blends. Unlike the previous blends, LP-LF revealed higher storage and loss modulus for the 90-10 blend in comparison to the 80-20 across the temperature region from 80°C to 140°C. Moreover, LP-LF 80-20 started to show flow

behaviour (*G''* became higher than *G'*) around 130°C whereas for LP-LF 90-10 showed flow behaviour (*G''* became equal to *G'*) at around 140°*C.*

5.2.2 Viscosity

Figure 5.2 shows the dynamic viscosity of the LP, LP-HB2 and LP-H-HB2 blends at 200°C and LP-LF blends at 140°C was measured as described in Chapter 3 section 3.6.7.2 .

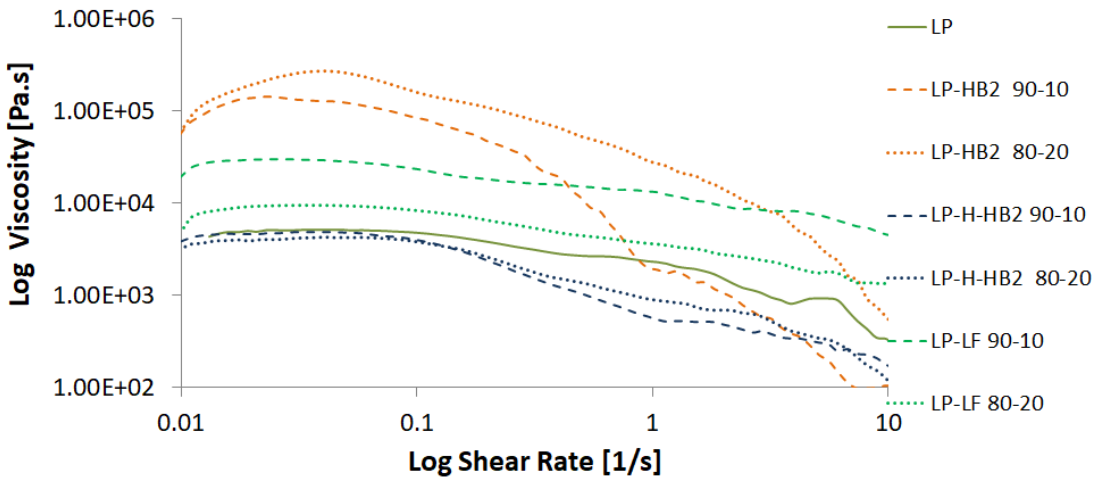

Figure 5.2*: Dynamic viscosity of LP, LP-HB2 and LP-H-HB2 polymer blends at 200°C and for LP-LF blends at 140°C.*

It was observed that at the low shear rate of 0.01 s^{-1}, the viscosity of LP-HB2 90-10 and 80-20 blends was significantly higher at 5.5×10^4 (Pa.s) and 5.9×10^4 (Pa.s) respectively, in comparison to LP at 4.0×10^3 (Pa.s). On the other hand, at the same shear rate 0.01 s^{-1} the viscosity for LP-H-HB2 90-10 at 3.8×10^3 (Pa.s) and 80-20 at 3.1×10^3 (Pa.s) was found to be slightly lower than that of LP at 4.0×10^3 (Pa.s). The viscosity of LP-H-HB2 decreased with increasing weight percentage (wt%) of H-HB2 in the blends. However, at lower temperature (140°C) and at the same shear rate the LP-LF 90-10 and 80-20 revealed higher viscosity profiles at 1.9×10^4 (Pa.s) and at

5.3×10^3 (Pa.s) in comparison to LP at 200°C. The viscosity of the LP and the blends decreased with increasing shear rate as seen in Figure 5.2.

5.2.3 Thermogravimetric Analysis

The isothermal degradation of LP, LP-HB2, LP-H-HB2 and LP-LF (both 90-10 and 80-20 blends) at 200°C and also for LP-LF 90-10 and 80-20 blends at 140°C for 20 min are presented in Figure 5.3 and was carried out as mentioned in Chapter 3 section 3.6.4.

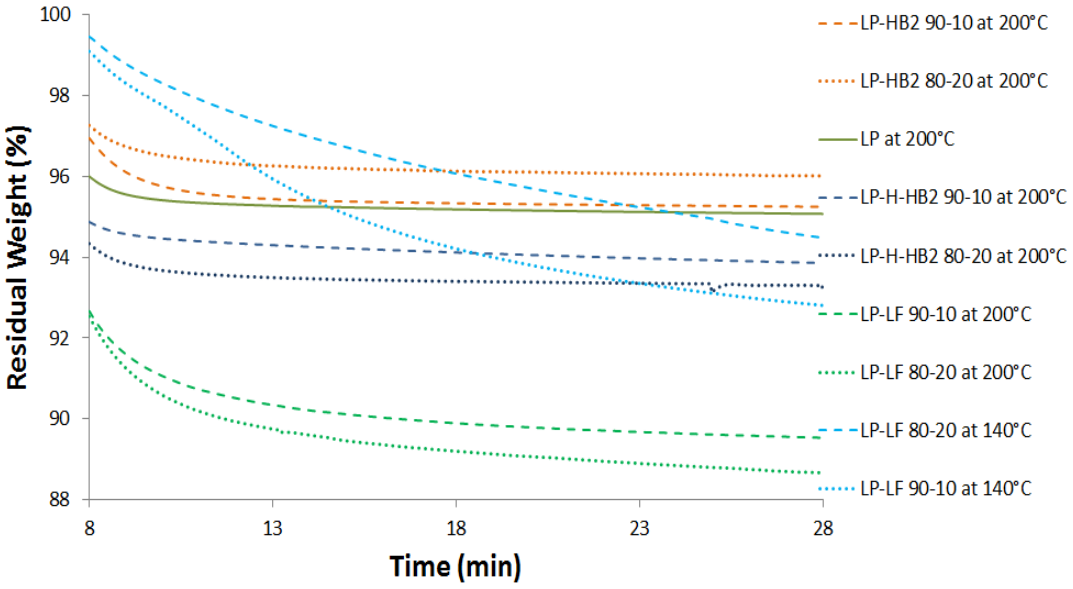

Figure 5.3: *The isothermal degradation of LP, LP-HB2, LP-H-HB2, LP-LF 90-10 and 80-20 at 200°C and also LP-LF 90-10 and 80-20 (green dotted and solid lines) at 140°C for 20 min*

The residual weight percentage (wt%) of LP, LP-HB2, LP-H-HB2 blends at 200°C and LP-LF blends at 140°C showed almost similar degradation profiles over the period of the study. However, at 200°C the LP-LF blends revealed a significantly lower residual wt% (~89% and ~88% for 90-10 and 80-20 respectively) in comparison to the residual wt% of LP (at ~96%), LP-HB2 (at ~95% and at ~96% for 90-10 and 80-20 composition

respectively), and for LP-H-HB2 (at ~95% for both 90-10 and 80-20 composition respectively). So, the LP-LF blends were heat treated at lower temperature (140°C) since this blend (due to having a lower molecular weight of LF polymer) underwent higher thermal degradation than other blends when processed at the high temperature range (200°C).

5.2.4 DSC Analysis

Figure 5.4 is representing the DSC analysis of heat treated (at 200°C for 20 min) LP-H-HB2 90-10 and 80-20 and was measured as described in chapter 3 section 3.6.3.

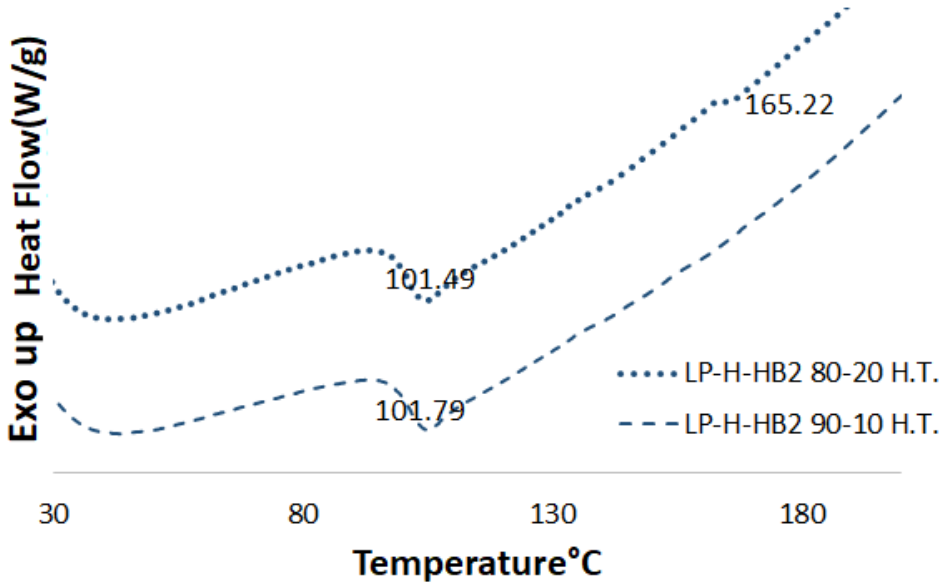

Figure 5.4: *DSC thermograms of heat treated LP-H-HB2 90-10 and LP-H-HB2 80-20*

From Figure 5.4, a peak was identified for heat treated LP-H-HB2 80-20 at 165°C whereas no such peak was found for heat treated LP-H-HB2 90-10. This peak indicated that after heat treatment at 200°C there could possibly be ethyl chain end ($-CH_2-CH_3-$) crystallisation of H-HB2 in LP-H-HB2 80-20 blends. For LP-H-HB2 90-10, absence of this peak indicated that 10wt% of H-HB2 in blend was not sufficient enough to cause any crystallisation in the blend.

5.2.5 Mechanical Properties

5.2.5.1 Tensile Tests

Figure 5.5a presents a comparison of the tensile modulus data of LP, LP-HB2, LP-H-HB2 and LP-LF blends at room temperature (R.T.) and LP, LP-HB2 and LP-H-HB2 blends heat treated (H.T) at 200°C and for LP-LF blends heat treated at 140°C respectively. This test was carried out as described in Chapter 3 section 3.6.9.1

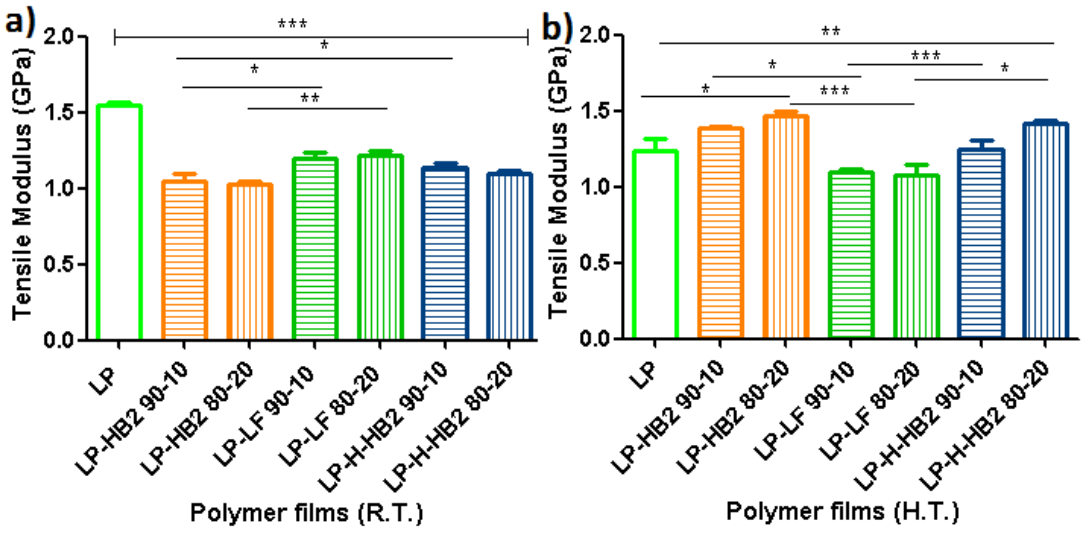

Figure 5.5: *Tensile modulus of pure LP and blends a) at room temperature and b) heat treated.*

At room temperature the tensile modulus of LP-HB2 (90-10 and 80-20 blends) decreased by 32% ($p<0.005$) and 22% ($p<0.005$) respectively as compared to LP (1.54 GPa). Similarly, the tensile modulus of LP-LF (90-10 and 80-20 blends) also decreased by 22% ($p<0.005$) in comparison to LP alone. The tensile modulus of LP-H-HB2 90-10 and LP-H-HB2 80-20 also decreased by 25% and 29% ($p<0.005$) in comparison to LP. However, after heat treatment at 200°C the tensile modulus of heat treated LP-HB2 90-10 and 80-20 revealed a 26% ($p<0.01$) and 30% ($p<0.005$) increase respectively than their tensile modulus value at room temperature. Similarly, heat treated (at 200°C) LP-H-HB2 (both 90-10 and 80-20 blends) also experienced an increase of 12%

($p>0.05$) and 27% ($p<0.005$) respectively in comparison to their tensile modulus at room temperature. On the other hand, after heat treatment (at 200°C) the tensile modulus of the LP experienced a 24% ($p<0.005$) decrease as compared to its corresponding value at room temperature. Heat treated LP-LF blends (at 140°C) (both 90-10 and 80-20) experienced a 9% and 12% decrease respectively ($p<0.05$) in tensile modulus in comparison to their room temperature values.

From Figure 5.5b it was observed that after heat treatment (at 200°C) the tensile modulus of LP-HB2 80-20 had increased statistically significantly by 21% ($p<0.05$) in comparison to LP. Similarly, the tensile modulus of LP-H-HB2 90-10 and 80-20 blends were also observed to increase by 41% ($p<0.005$) as compared to LP (1.24 GPa).

The tensile strength data of LP and blends LP-HB2, LP-H-HB2 and LP-LF (both 90-10 and 80-20 compositions) at room temperature are presented in Figure 5.6a whereas the tensile strength data for the heat treated LP, LP-HB2, LP-H-HB2 (both at 200°C) and LP-LF blends (at 140°C) are presented in Figure 5.6b.

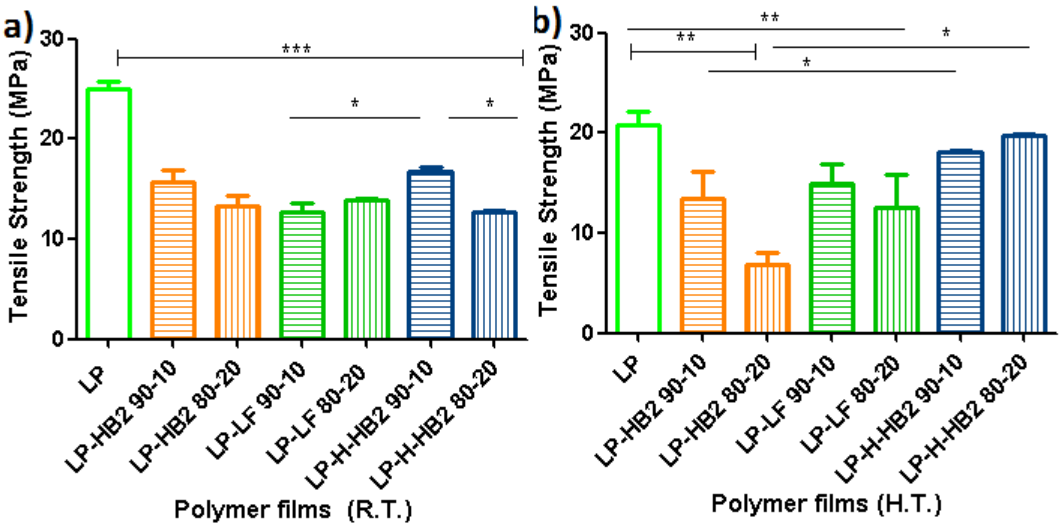

Figure 5.6: *Tensile strength of pure LP, LP-HB 90-10, LP-HB 80-20 and LP-H-HB2 90-10, LP-H-HB2 80-20 blends a) at room temperature and b) heat treated.*

For LP-HB2 90-10 and 80-20 at R.T. the tensile strength was found to be 37% and 46% ($p<0.005$) lower than the LP. Similarly, the LP-H-HB2 90-10 and 80-20 blends showed a 31% ($p<0.005$) and 51% lower ($p<0.005$) tensile strength, respectively, compared to the LP at R.T. Moreover, at room temperature the tensile strength of LP-LF 90-10 and 80-20 also decreased in comparison to LP by 49% and 41% ($p<0.005$) respectively.

A comparison table for the tensile strength of all polymer films both at room temperature and heat treated is presented in Table 5.1. From Figure 5.6b it could be observed that the lowest tensile strength was for heat treated LP-HB2 80-20 (70% lower, $p<0.005$) as compared to the heat treated LP.

Table 5.2: *A comparison of the tensile strength value of pure LP and blends (LP-HB2, LP-H-HB2 and LP-LF) for both at room temperature (R.T.) and heat treated (H.T.)*

Polymer films	Tensile Strength (R.T.) (MPa)	Tensile Strength (H.T.) (MPa)	(%) increase or decrease	P value
LP	25.01±0.2	20.8±0.6	20% decrease	(p<0.01)
LP-HB2 90-10	15.65±0.7	13.51±0.4	15 % decrease	(p>0.01)
LP-HB2 80-20	13.29±0.7	6.88±0.6	93 % decrease	(p<0.005)
LP-H-HB2 90-10	16.75±0.9	18.08±0.7	8 % increase	(p>0.05)
LP-H-HB2 80-20	12.22±0.4	19.78±0.4	61 % increase	(p<0.005)
LP-LF 90-10	12.66±0.09	14.92±0.2	15 % increase	(p>0.05)
LP-LF 80-20	14.66±0.08	11.33±0.4	29 % decrease	(p>0.01)

5.2.5.2 Flexural Test

The flexural modulus and flexural strength data of the composites produced are presented in Figure 5.7a and b respectively. This test was carried out as described in Chapter 3 section 3.6.9.2.

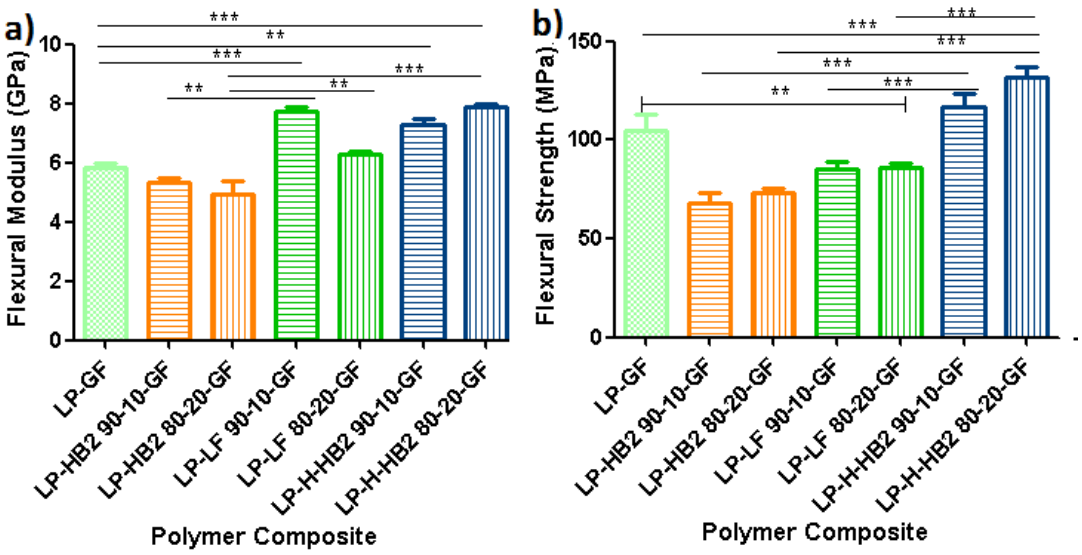

Figure 5.7: *a) Flexural modulus b) Flexural strength for composites with 21wt% E-glass fibre (woven mat) produced using LP and blends*

In comparison to the LP-GF composite the flexural modulus of the LP-H-HB2 90-10-GF and 80-20-GF was observed to have increased by 53% (p<0.005) and 21% (p<0.05) respectively. However, no statistically significant difference was observed in terms of flexural modulus for LP-HB2 90-10-GF and 80-20 respectively in comparison to LP-GF

composite. The flexural modulus of LP-LF 90-10-GF increased by 18% ($p<0.005$) in comparison to LP-GF alone. The modulus of LP-H-HB2 90-10-GF and 80-20 had also increased in comparison to LP-HB2 90-10-GF and 80-20 by 14% ($p>0.05$) and 54% ($p>0.005$) respectively. Similarly, LP-LF 90-10-GF experienced a 23% ($p>0.01$) increase in terms of flexural modulus in comparison to LP-HB2-90-10-GF.

The flexural strength (Figure 5.7b) of LP-HB2 90-10-GF and 80-20 decreased ($p<0.005$) by 36% and 29% respectively in comparison to the LP-GF composite. Similarly, the flexural strength of LP-LF-GF (both 90-10 and 80-20 blends) decreased by 18% ($p<0.05$) in comparison to LP-GF. On the other hand, the flexural strength of LP-H-HB2 90-10-GF and 80-20 increased by 15% ($p<0.05$) and 31% ($p<0.005$) respectively, in comparison to LP-GF. The flexural strength of LP-H-HB2 90-10-GF was also found to be higher by 71% ($p<0.005$) and 37% ($p<0.005$) than for LP-HB2 90-10-GF and LP-LF 90-10-GF respectively. Similarly, LP-H-HB2 80-20-GF also revealed a higher flexural strength value of 79% ($p<0.005$) compared to that of LP-HB2 80-20-GF and 52% ($p<0.005$) LP-LF 80-20-GF.

5.2.6 Scanning electron microscopy SEM

Figure 5.8a, b, c, d, e, f, g represent the fractured surface for LP-GF, LP-LF 90-10-GF and 80-20, LP-H-HB2 90-10-GF and 80-20, LP-HB2 90-10-GF and 80-20 respectively.

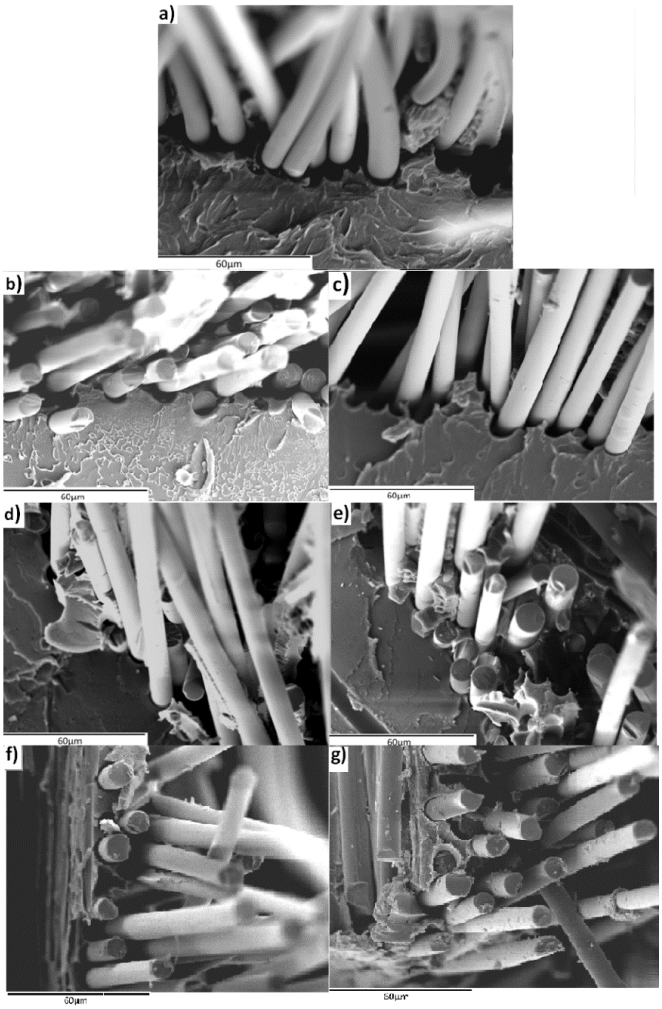

Figure 5.8: *SEM micrographs of fracture surfaces of composites a) LP-GF b) LP-HB2 90-10-GF c) LP-HB2 80-20-GF d) LP-H-HB2 90-10-GF e) LP-H-HB2 80-20-GF f) LP-LF 90-10-GF g) LP-LF- 80-20-GF.*

For LP-GF, LP-HB2-GF and LP-LF-GF the de-bonding of the fibre from matrix occurred which indicated by the poor adhesion between fibre and matrix. However, for LP-H-HB2-GF of 90-10 and 80-20 a comparatively better adhesion between the fibre and matrix was seen in comparison to the fracture surfaces of other composites.

5.3 Discussion

For LP during temperature ramping (Figure 5.1A), the storage modulus *G′* remained higher than the loss modulus to ~190°C. On heating, both *G′* and *G″* decreased with increasing temperature. Near the glass transition temperature (~100°C), the polymer chains started to show some mobility and with increasing temperature the mobility of polymer chains increased causing polymer chain disentanglements.[14] For LP this process took place gradually over a temperature range (from ~100°C to ~190°C) and at ~190°C the polymer started to show the behaviour of a flowing polymer. Above 190°C the polymer chains were flexible enough to move past each other or along their freely movable chain ends. At this point the loss modulus *G″* became higher than the storage modulus *G′* value.

For LP-HB2 blends (Figure 5.1B) as temperature increased, both *G′* and *G″* decreased. Across the whole temperature region (90°C to 200°C) the LP-HB2 polymer blends did not reach a flowing state (*G″* > *G′*) even at high temperature (~200°C). This may have been due to crosslinking effect of HB2 polymer.[14] The higher storage and loss modulus for LP-HB2 80-20 compared to LP-HB2 90-10 indicated higher crosslinking effect, which was suggested to be due to the presence of higher wt% of HB2 material in the LP-HB2 80-20 blend.

For LP-H-HB2 (Figure 5.1C) with increasing temperature *G′* and *G″* also decreased, however, for blends of both composition *G″* became higher than *G′* ~175°C. So, it can be said that both LP-H-HB2 90-10 and 80-20 blends showed flow behaviour above 175°C whereas for LP this value was above 190°C. This could be suggested to be due to the lower chain entanglements of H-HB2.[15, 16]

For LP-LF (Figure 5.1D) the *G'* was higher than *G"* up to ~140°C for 90-10 blend and ~130°C for the 80-20 blend. LF polymer possesses a linear structure with few functional groups (Figure 2.1). This blend showed flow behaviour at the lowest temperature (~140°C) in comparison to LP and other blends which may be attributed to the lower molecular weight of LF in comparison to that of LP, HB2 and H-HB2. It has been reported that above a certain average molecular weight ,M_w, the polymer chains are long enough to entangle.[17] This molecular weight is called the critical entanglement molecular weight $M_{c,}$ which for linear polystyrene is reported to be 34 kDa [18] and the molecular weight of LF used in this study was 10 kDa and LP was 192 kDa respectively. Since the molecular weight of LP used in this study was much higher than the M_c value, polymer chain entanglement of LP for all blends LP-HB2, LP-H-HB2 and LP-LF should have occurred. So, for all the blends the storage modulus was higher than the loss modulus up to a certain temperature and after that due to lack of polymer chain entanglement for H-HB2 and LF both, LP-H-HB2 and LP-LF blends started to show flow behaviour at lower temperature ~175°C and ~140°C in comparison to LP. The lack of chain entanglement in H-HB2 occurred due to its three dimensional globular structure whereas for LF the molecular weight was significantly lower than that of M_c.

The viscosity of LP and blends are presented as a function of shear rate in Figure 5.2. Both LP and the blends showed shear thinning behaviour. It has been reported that hyperbranched polymers showed Newtonian behaviour due to the absence of chain entanglement.[19, 20] The shear thinning behaviour of LP and blends was therefore attributed to the contribution of polymer chain entanglements from LP.[21] The viscosity of LP-HB2 blends was found to be the highest at 200°C at low shear rate

(0.01 s^{-1}). This behaviour could be explained taking into account the crosslinking effect of the HB2 polymer at that temperature. However, viscosity of LP-H-HB2 90-10 and 80-20 blends was found to be slightly lower in comparison to LP. Lower viscosity of LP-H-HB2 blends compared to LP was expected as there are no reactive vinyl functional groups in the chain end of H-HB2 polymer and as a result no crosslinking should have occurred. Moreover, decrease of LP-H-HB2 blend viscosities than the LP in the lower strain rate region could also be attributed to the non-entanglement of H-HB polymer chains. [22] Nunez *et al.* [21] measured solution viscosity of blends of linear poly hydroxyl methacrylate and hyperbranched polyester and reported that reduction in viscosity from 40 Pa.s to 20 Pa.s for blends containing 5wt% of hyperbranched polyester occurred due to the absence of physical entanglements in the HB polyester. LP-LF 90-10 and 80-20 at 140°C showed higher viscosity than that of LP at 200°C (Figure 5.2) since the viscosity of polymers decrease with increasing temperature.

From Figure 5.3 it can be seen that the LP-LF blends underwent higher thermal degradation at 200°C after 20 min in comparison to LP and the blends investigated. The higher thermal degradation of LP-LF blends may have been due to the lower molecular weight of LF in comparison to LP, HB2 and H-HB2.[23] However, at 140°C after 20 min LP-LF blends showed similar residual weight% to LP and the other blends, and hence why the composite with LP-LF blends were prepared at 140°C.

The tensile modulus data of LP and blends both at room temperature (R.T.) and heat treated (H.T.) are presented in Figure 5.5a and Figure 5.5b. At R.T. the tensile modulus of all polymer blends was found to be statistically significantly ($p<0.05$)

lower compared to the LP alone. The lower modulus of LP-HB2 and LP-H-HB2 blends at R.T. could also be explained in terms of the absence of crosslinking and polymer chain entanglements of HB2 and H-HB2. It has been reported that HB2 polymers possess poor mechanical properties and brittleness in comparison to their linear counterparts due to higher branching and absence of chain entanglement. [24, 25] The tensile modulus of LP-LF blends was also statistically significantly ($p<0.05$) lower than LP, which was again suggested to be due to the lower molecular weight of the LF polymer. Although LF polymer had a lower molecular weight than for HB2 and H-HB2, the tensile modulus of LP-LF 90-10 and 80-20 was statistically significantly higher ~15% ($p<0.05$) than the LP-HB2 90-10 and 80-20 respectively. At room temperature (in absence of crosslinking) both HB2 and H-HB2 possessed a globular, three-dimensional structure whereas LF possess a most likely linear structure like LP with few functional groups, since the momomer for LF was only 1% of divinyl benzene and 99% styrene. So, it can be said that the highly branched structure at R.T. may have been responsible for the statistically significantly ($p<0.05$) lower modulus value for LP-HB2 and LP-H-HB2 compared to LP-LF.[24] However, no statistical significant ($p<0.05$) difference was observed for LP-HB2 and LP-H-HB2 tensile modulus value.

After heat treatment, the tensile modulus of LP decreased by 24% ($p<0.005$). The decreased modulus value of LP could be attributed to the development of free volume and residual stress after heat treatment.[26, 27] To study the effect of thermal treatment and quenching on thermal and mechanical properties of linear polystyrene, Rouabah *et al.* [28] carried out heating and quenching of linear polystyrene to different temperatures. They reported the lowest elastic and flexural modulus for linear polystyrene after quenching, and stated that this lower modulus

was due to the development of free volume during quenching (as all polymer chains can have sufficient time to reorganise and thus free volume is induced) and residual tensile stresses developed which may have increased the total tensile stress applied to the sample.[27, 28]

Since the heating and cooling process for both LP and the blends was similar, a decrease in tensile modulus value after heat treatment was also expected for blends. However, the heat treated LP-HB2 90-10 and 80-20 blends experienced a 26% ($p<0.005$) and 30% ($p<0.005$) increase in tensile modulus respectively in comparison to LP-HB2 90-10 and 80-20 blends at R.T. This increased modulus value of heat treated LP-HB2 90-10 and 80-20 blends was attributed to the crosslinking of HB polymer at 200°C due to the presence of $-CH=CH_2$ at its chain end group.[29] Moreover, the modulus of heat treated LP-HB2 80-20 was found to have increased statistically significantly by 18% ($p<0.05$) as compared to that of heat treated LP.

H-HB2 polymer possessed non-entangled polymer chains with non-reactive ethyl ($-CH_2–CH_3$) chain end groups. The ethyl ($-CH_2–CH_3$) chain end of LP-H-HB2 80-20 may have crystallised during heat treatment and can be observed from the peak identified at 165°C (Figure 5.4) from the DSC measurement. This chain end crystallisation of H-HB2 had significantly ($p<0.005$) increased the tensile modulus value of the LP-H-HB2 80-20 blends (by 27%) than their value at R.T. However, no such peak was obtained for the LP-H-HB2 90-10 blend indicated that 10wt% amount of H-HB2 in blend was not sufficient enough to cause any significant crystallisation and no significant ($p>0.05$) improvement in mechanical properties was observed in comparison to the value of the blend at R.T.

Malmstrom *et al.* [30] investigated the effect of alkyl chain end groups on the crystallinity of hyperbranched polyester and reported the crystallisation of HB polymer chain ends with sufficiently long alkyl chain (C12-C16) length, however, they did not observe crystallisation with short alkyl chain lengths with 3-6 carbons. Schmaljohann *et al.* [31] also did not observe crystallisation for HB polymer with short alkyl chain (C4) ends, however, they reported crystallisation for polymers containing C14 and C18 long alkyl chain ends. The H-HB2 polymer used in this study contained short (C2) alkyl chain ends, however, crystallisation may have occurred since the LP-H-HB2 blends was subjected to heat treatment at 200°C for 20 min and then cooled down to below the T_g value (100°C) which could have caused reorganisation of the ethyl (-CH_2–CH_3) chain ends.

The tensile modulus value of heat treated (140°C) LP-LF 90-10 and 80-20 also decreased by 9% and 12% respectively ($p<0.05$) in comparison to the heat treated LP (at 200°C). Since LF has a linear structure with few -CH=CH_2 functional groups, the decrease in modulus may have been the same as for LP.

Figure 5.6a and Figure 5.6b presents a comparison of the tensile strength data of LP-HB2, LP-H-HB2 and LP-LF blends with LP for both at R.T. and heat treated (H.T.). At R.T. the tensile strength value of all polymer blends appeared to be statistically significantly ($p<0.005$) lower in comparison to LP. However, after heat treatment the tensile strength of LP decreased by 20% ($p<0.05$) as compared to R.T. values. The lower tensile strength of LP after heat treatment may have been due to the fact that when external load is applied the stress developed were superimposed with the tensile residual stresses (developed due to heat treatment) and the LP broke down

at a lower load.[28] LP-HB2 80-20 also experienced a decrease in tensile strength by 70% ($p<0.005$) compared to LP alone. With increase wt% of HB2 in the blend, the crosslinking density of HB2 also increased and the tensile strength decreased. Kim *et al.* [32] prepared crosslinked polymer films with hyper-branched polyglycidol containing hydroxyl (-OH) group and used carboxyl(-COOH)-terminated poly (ethylene glycol) as a crosslinking agent. They reported the lower tensile strength value at 0.139 MPa for higher crosslinking concentration (mole ratio [–COOH]/[-OH];0.75) whereas higher tensile strength value at 0.22 MPa for lower crosslinking concentration ([–COOH]/[-OH];0.25) was achieved. On the other hand, the tensile strength of heat treated LP-H-HB2 80-20 increased statistically significantly ($p<0.005$) in comparison to its value at R.T. The LP-LF 80-20 also experienced statistically significant ($p<0.005$) decrease in tensile strength value.

For the flexural modulus data of the composites (Figure 5.7A) the lower flexural modulus was observed for LP-HB2 90-10-GF and 80-20 composites at 5.5 and 5.1 GPa. However, this value was not statistically significantly lower than that of LP-GF composite (5.83 GPa). From Figure 5.1B it was clear that the storage modulus of LP-HB2 blends was higher than the loss modulus across the temperature region examined and did not show any flow behavior before being crosslinked. As a result, wetting of fibre with matrix was minimal and resulted in low a modulus value. Other studies also reported lower flexural properties for composites prepared with crosslinked hyperbranched polymer. For example, Ratna *et al.* [33] manufactured epoxy/clay nanocomposite using a matrix which was a blend of epoxy and 15wt% epoxy functional HB polymer. A crosslinking agent was used for crosslinking the HB with epoxy. They reported a significant decrease in flexural modulus value for

nanocomposites with 15wt% HB2 (2.5 GPa) in the matrix as compared to the composite without HB2 (5.0 GPa) in the matrix. They attributed this decrease in composite modulus to the lower modulus value of the HB polymer.

On the other hand, in comparison to the LP-GF composite the flexural modulus of LP-H-HB2-90-10-GF and 80-20 increased by 26% and 36% respectively. Moreover, the flexural strength for LP-H-HB2 80-20-GF was found to have increased statistically significantly by 88% compared to the LP-GF composite. This increase in modulus and strength indicated better adhesion between LP-H-HB2 matrix and the fibre due to better wettability of the fibre by the LP-H-HB2 matrix in comparison to LP matrix at the composite processing temperature (200°C). The better wettability of the LP-H-HB2 matrix can be supported by the lower viscosity at lower strain rate (0.01%) (see Figure 5.2). Hyperbranched polymers have been reported to be used as matrix modifiers for thermoplastic polymer composites due to their lower viscosity and better wettability properties. Lu *et al.* [7] used a carboxy terminated HB polymer as compatibiliser for composites with sisal fibre (as reinforcing agent) and polypropylene (as matrix) and reported an increase in flexural modulus to 2.13 GPa and flexural strength to 42.6 MPa with addition of 2% HB2 whereas for neat polymer and sisal fibre composite the values were reported to be 1.84 GPa and 35.7 MPa. They explained that this increase in flexural properties was due to the uniform distribution of sisal fibre in the HB2 modified polymer matrix.[7] Moreover, during composite manufacture alkyl chain end crystallisation was suggested to have occurred for LP-H-HB2 80-20 which contributed to the higher mechanical properties of the LP-H-HB2 80-20-GF composite.[34]

However, the flexural strength value of both LP-LF 90-10-GF and 80-20 composites decreased (by 18%, $p<0.005$) as compared to the LP-GF 90-10 composite. Although LP-LF blends melted~140°C, the viscosity of both LP-LF 90-10 and 80-20 blends was significantly higher at 140°C than LP at 200°C. The higher viscosity of the LP-LF blends may have been responsible for the comparatively poor wettability compared to the LP.[35]

Figure 5.8 shows the surface morphology of the fractured composites and in the case of LP-GF (Figure 5.8 a) and LP-HB2-GF (Figure 5.8 b,c) composites the fibres appeared to have de-bonded from the LP matrix indicated poor adhesion between the fibre and the matrix. De-bonding was also observed for LP-LF-GF composites (Figure 5.8 f,g), however, lower than LP-GF and LP-HB2-GF. For LP-H-HB2 (Figure 5.8 d,e) composites better adhesion between the fibre and matrix was observed after composite fracture in comparison to the other composites. This result was also in agreement with data from mechanical tests.

5.4 Conclusion

It can be concluded that

- From the oscillatory measurement tests, the HB2 polymer had crosslinked (*G'* > *G"*) within the LP-HB2 blends, however, the temperature at which crosslinking occurred could not be identified. Blending of H-HB2 and low mol. wt. LF caused the blends LP-H-HB2 and LP-LF to show flow behaviour at lower temperature (at ~175°C and ~140°C) compared to LP (~192°C) and LP-H-HB2 showed lower melting viscosity than LP at 200°C.

- At 200°C, the low mol. wt. LF underwent higher thermal degradation in comparison to other blends, as such the composite was prepared at 140°C whereas the other composite blends were prepared at 200°C.

- Reduction in processing temperature was obtained for LP-H-HB2 90-10 and 80-20 (at ~175°C) and LP-LF blends (~140°C) in comparison to LP (~192°C).

- For blends made at R.T. the mechanical properties were lower in comparison to LP. However, after heat treatment the tensile modulus of LP-HB2 of 90-10 and 80-20 increased significantly ($p<0.005$) due to crosslinking, however, their tensile strength properties decreased.

- For the LP-H-HB2 80-20 blends a significant ($p<0.005$) increase was observed for both tensile modulus and tensile strength value, which was suggested to be due to the ethyl chain end crystallisation of H-HB2 after heat treatment.

- For the composites the highest flexural modulus and strength was found for LP-H-HB2 80-20-GF at 7.9 GPa and 131 MPa respectively, which was

suggested to be due to the better wettability of fibre by LP-H-HB2 80-20 matrix and chain end crystallisation. This observation was also supported by SEM analysis where better adhesion between the fibre and matrix was observed for LP-H-HB2 80-20-GF.

5.5 References

1. *Mezzenga, R., L. Boogh, and J.-A.E. Månson, A review of dendritic hyperbranched polymer as modifiers in epoxy composites. Composites Science and Technology, 2001.* ***61****(5): p. 787-795.*

2. *Sorensen, K., et al., Dendritic polyester macromolecule in thermosetting resin matrix. 2000, Google Patents.*

3. *Mezzenga, R., L. Boogh, and J.-A. Månson, Toughening and failure mechanisms in blends of thermosets and hyperbranched polymers. No. EPFL-CONF-179054,2000.*

4. *Xu, J., et al., A morphological investigation of thermosets toughened with novel thermoplastics. I. Bismaleimide modified with hyperbranched polyester. Journal of Applied Polymer Science, 1999.* ***72****(8): p. 1065-1076.*

5. *Varley, R.J. and W. Tian, Toughening of an epoxy anhydride resin system using an epoxidized hyperbranched polymer. Polymer International, 2004.* ***53****(1): p. 69-77.*

6. *Boogh, L., et al. Dendritic-based additives for polymer matrix composites. in Proc. Of the ICCM-12 conference, Paris, France. July. 1999.*

7. *Lu, S., et al., Sisal fibre/polypropylene composites modified with carboxyl terminated hyperbranched polymer. Plastics, Rubber and Composites, 2013.* ***42****(9): p. 361-366.*

8. *Jannerfeldt, G., et al., Matrix modification for improved reinforcement effectiveness in polypropylene/glass fibre composites. Applied Composite Materials, 2001.* ***8****(5): p. 327-341.*

9. *Zhou, W., J. Xu, and W. Shi, Surface modification of multi-wall carbon nanotube with ultraviolet-curable hyperbranched polymer. Thin Solid Films, 2008.* ***516****(12): p. 4076-4082.*

10. *Henriksson, M., et al., Novel nanocomposite concept based on cross-linking of hyperbranched polymers in reactive cellulose nanopaper templates. Composites Science and Technology, 2011.* ***71****(1): p. 13-17.*

11. *Amerio, E., et al., Preparation and Characterization of Hyperbranched Polymer/Silica Hybrid Nanocoatings by Dual-Curing Process. Macromolecular Materials and Engineering, 2006.* ***291****(10): p. 1287-1292.*

12. *Dodiuk-Kenig, H., et al., The effect of hyper-branched polymers on the properties of dental composites and adhesives. Journal of Adhesion science and Technology, 2004.* ***18****(15-16): p. 1723-1737.*

13. *Subianto, S., N.R. Choudhury, and N. Dutta, Composite Electrolyte Membranes from Partially Fluorinated Polymer and Hyperbranched, Sulfonated Polysulfone. Nanomaterials, 2013.* ***4****(1): p. 1-18.*

14. *Mezger, T.G., The rheology handbook: for users of rotational and oscillatory rheometers. 2006: Vincentz Network GmbH & Co KG.*

15. *Hong, Y., et al., A novel processing aid for polymer extrusion: Rheology and processing of polyethylene and hyperbranched polymer blends. Journal of Rheology (1978-present), 1999.* ***43****(3): p. 781-793.*

16. *Schmaljohann, D., et al., Blends of amphiphilic, hyperbranched polyesters and different polyolefins. Macromolecules, 1999.* ***32****(19): p. 6333-6339.*

17. *Jasso-Gastinel, C.F., J.F.A. Soltero-Martínez, and E. Mendizábal, 1 - Introduction: modifiable characteristics and applications, in Modification of Polymer Properties. 2017, William Andrew Publishing. p. 1-21.*

18. *Nichetti, D. and I. Manas-Zloczower, Viscosity model for polydisperse polymer melts. Journal of Rheology (1978-present), 1998.* ***42****(4): p. 951-969.*

19. *Hsieh, T.-T., C. Tiu, and G. Simon, Melt rheology of aliphatic hyperbranched polyesters with various molecular weights. Polymer, 2001.* ***42****(5): p. 1931-1939.*

20. *Malmström, E., M. Johansson, and A. Hult, Hyperbranched aliphatic polyesters. Macromolecules, 1995.* ***28****(5): p. 1698-1703.*

21. *Nunez, C.M., et al., Solution rheology of hyperbranched polyesters and their blends with linear polymers. Macromolecules, 2000.* ***33****(5): p. 1720-1726.*

22. *Mulkern, T. and N. Tan, Processing and characterization of reactive polystyrene/hyperbranched polyester blends. Polymer, 2000.* ***41****(9): p. 3193-3203.*

23. *Funt, J.M. and J.H. Magill, Thermal decomposition of polystyrene: Effect of molecular weight. Journal of Polymer Science: Polymer Physics Edition, 1974.* ***12****(1): p. 217-220.*

24. *Salamone, J.C., Concise polymeric materials encyclopedia. Vol. 1. 1998: CRC press.*

25. *Mark, H.F., Encyclopedia of polymer science and technology, concise. 2013: John Wiley & Sons.*

26. *Broutman, L.J. and S.M. Krishnakumar, Impact strength of polymers: 1. The effect of thermal treatment and residual stress. Polymer Engineering & Science, 1976.* ***16****(2): p. 74-81.*

27. *Rouabah, F., et al., Mechanical and thermal properties of polycarbonate, part 1: influence of free quenching. Journal of Applied Polymer Science, 2008.* ***109****(3): p. 1505-1514.*

28. *Rouabah, F., D. Dadache, and N. Haddaoui, Thermophysical and mechanical properties of polystyrene: Influence of free quenching. ISRN Polymer Science, 2012.* ***2012****.*

29. *Spoljaric, S., et al., Thermal, optical, and static/dynamic mechanical properties of linear-core crosslinked star polymer blends. Macromolecular Chemistry and Physics, 2011.* ***212****(16): p. 1778-1790.*

30. *Malmström, E., M. Johansson, and A. Hult, The effect of terminal alkyl chains on hyperbranched polyesters based on 2, 2-bis (hydroxymethyl) propionic acid. Macromolecular Chemistry and Physics, 1996.* ***197****(10): p. 3199-3207.*

31. *Schmaljohann, D., et al., Modification with alkyl chains and the influence on thermal and mechanical properties of aromatic hyperbranched polyesters. Macromolecular Chemistry and Physics, 2000.* ***201****(1): p. 49-57.*

32. *Kim, B.-S., et al., Synthesis of polyglycidol hydrogel films crosslinked with carboxyl-terminated poly (ethylene glycol). Polymer Journal, 2006.* ***38****(4): p. 335-342.*

33. *Ratna, D., et al., Nanocomposites based on a combination of epoxy resin, hyperbranched epoxy and a layered silicate. Polymer, 2003.* ***44****(24): p. 7449-7457.*

34. *Lu, S., et al., The effect of hyperbranched polymer lubricant as a compatibilizer on the structure and properties of lignin/polypropylene composites. Wood Material Science & Engineering, 2013.* ***8****(3): p. 159-165.*

35. *Saliu, H.R., et al., The effect of epoxy concentration and fibre loading on the mechanical properties of ABS/epoxy-coated kenaf fibre composites. Open Journal of Composite Materials, 2015.* ***5****(02): p. 41.*

CHAPTER 6

6 Comparison of thermal and thermo-mechanical properties for star shaped poly lactic acid (SPLA) and their blends with linear PLA

6.1 Introduction

It was hypothesised that because star polymers possess physical properties which can be markedly different from their linear counterparts, blending of star and linear polymers could be a possible way to modify the resultant polymers film, blends. and also to obtain the desired properties. For example, in literature, the main reasons for linear PLA to be blended with star PLA was to enhance the plasticisation of the linear PLA [1], to form stereocomplex [2] and also to modify the crystallisation properties of linear PLA.[3]

Khajeheian and Rosling [1] blended 10 and 30wt% of star-shaped (4-arm) PLLAs with linear PLLA. They observed a significant decrease in T_g by 7°C (12% reduction) for the blends containing star PLLA (30wt%) of low molecular weight (M_n~2.5 kDa) and suggested that star PLLA acted as a plasticiser in blends with linear PLLA. In terms of crystallinity, they observed that blends containing 30wt% of high molecular weight (M_n) of star PLLA increased crystallinity by 30% in comparison to blends containing low molecular weight star PLLA. They concluded that a 4-arm star PLLA with longer branch (higher M_n value) lengths crystallised more easily during the cooling and heating process.

Phuphuak *et al.* [3] also blended 1wt% of star PLLAs with linear PLA and noticed a drastic decrease in the glass transition temperature (T_g) (from 57°C to 22°C) and an

increase in the elongation at break (30-40%) which they suggested was due to significant increases in chain mobility and plasticity. However, for blends containing short chain star PLLA, they observed rapid crystallisation rates and concluded that the short chain star PLLA acted as a good initiator of chain packing as compared to that of the long chain length star PLLA. They suggested that longer chain length star PLLA made chain packing more difficult and as a result rapid crystal formation was not observed for blends containing longer chain length star PLLAs. They concluded that the star shaped PLLA could potentially play a dual function of both plasticiser and nucleating agent.

Few evidence can be found in literature studying the properties of star and linear PLA blends. However, some of the reported results found to be contradict with one another. For example, Phuphuak *et al.*[3] reported blends containing short chain (lower M_n value~ 3370) and lower percentage (1wt%) of star 4 arm PLLA caused better crystallisation ability whereas Khajeheian and Rosling [1] reported better crystallisation ability for blends containing longer branch (higher M_n value~33,400) and higher percentage (30wt%) of 4 arm star PLLA.

In this regard, this chapter aimed to modify the thermal, crystallisation and degradation properties of linear PLA on addition of 20wt% star shaped 6 arm poly lactic acid (PDLLA) of four different molecular weights (Table 3.2). The blends containing 20wt% of the star PLA and 80wt% of linear PLA were prepared using solvent casting method (Table 3.5). The thermal, thermomechanical, crystalline and degradation properties of these blends are reported in this chapter.

Since the blends produced in this study contain same wt% of different mol. wt. SPLA rather than same mol% (same number of molecules) means blends with high mol. wt. SPLA contain longer chain length SPLA with lower number of -OH functional group whereas blends with low mol. wt. SPLA contain shorter chain length with higher number of -OH functional group.

6.2 Results

6.2.1 FTIR Analysis

FTIR analysis was conducted using the method described in Chapter 3 section 3.6.2. The FTIR spectra presented here are a comparisons of the region between 4000 cm^{-1} and 3100 cm^{-1} for linear PLA and sorbitol initiated star shaped PLA (SPLA). Figure 6.1 contains the FTIR data for linear PLA and the SPLA-3, SPLA-6, SPLA-9 and SPLA-12 stars, where the subsequent number represents the targeted molecular weight (M_n = 3, 6, 9 and 12 kDa respectively).

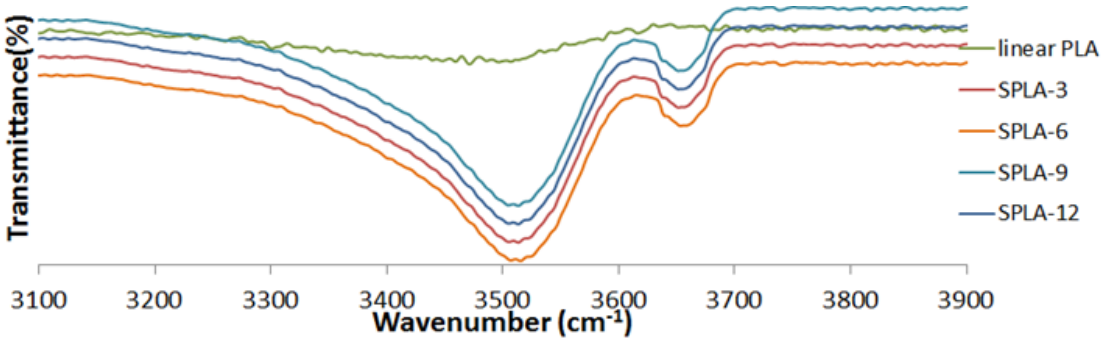

Figure 6.1: *FTIR-ATR spectra of linear PLA and SPLA polymers between 4000 and 3100 cm^{-1}*

A broad peak ~ 3500 cm^{-1} was identified for SPLA which could be attributed to the stretching of the -OH end-group (Figure 3.2) whereas no such peak was observed for linear PLA in that region.

6.2.2 DSC Analysis

DSC analysis was conducted using the method described in Chapter 3 section 3.6.3. It was used to investigate the thermal properties of the star polymers (SPLA-3, SPLA-6 and SPLA-9 and SPLA-12) (Figure 6.2) and their blends (PLA-3 80-20, PLA-6 80-20, PLA-9 80-20, PLA-12 80-20) both at room temperature (R.T.) and after being heat treated (H.T.) as stated in Chapter 3, section 3.4.2. This data is presented in Figure 6.3a and b.

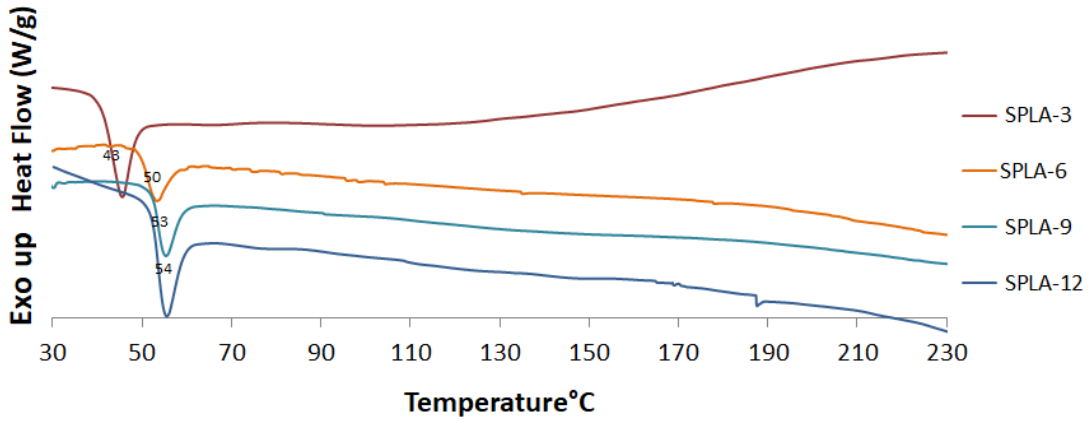

***Figure 6.2**: DSC thermogram of SPLA of different molecular weight (M_n)*

It was observed from Figure 6.2 that the T_g of the SPLA polymers ranged from 48°C, 50°C, 53°C and 54°C for SPLA-3, SPLA-6 and SPLA-9 and SPLA-12 respectively. No crystallisation and melting peaks were observed for these neat SPLA polymers (up to 230°C).

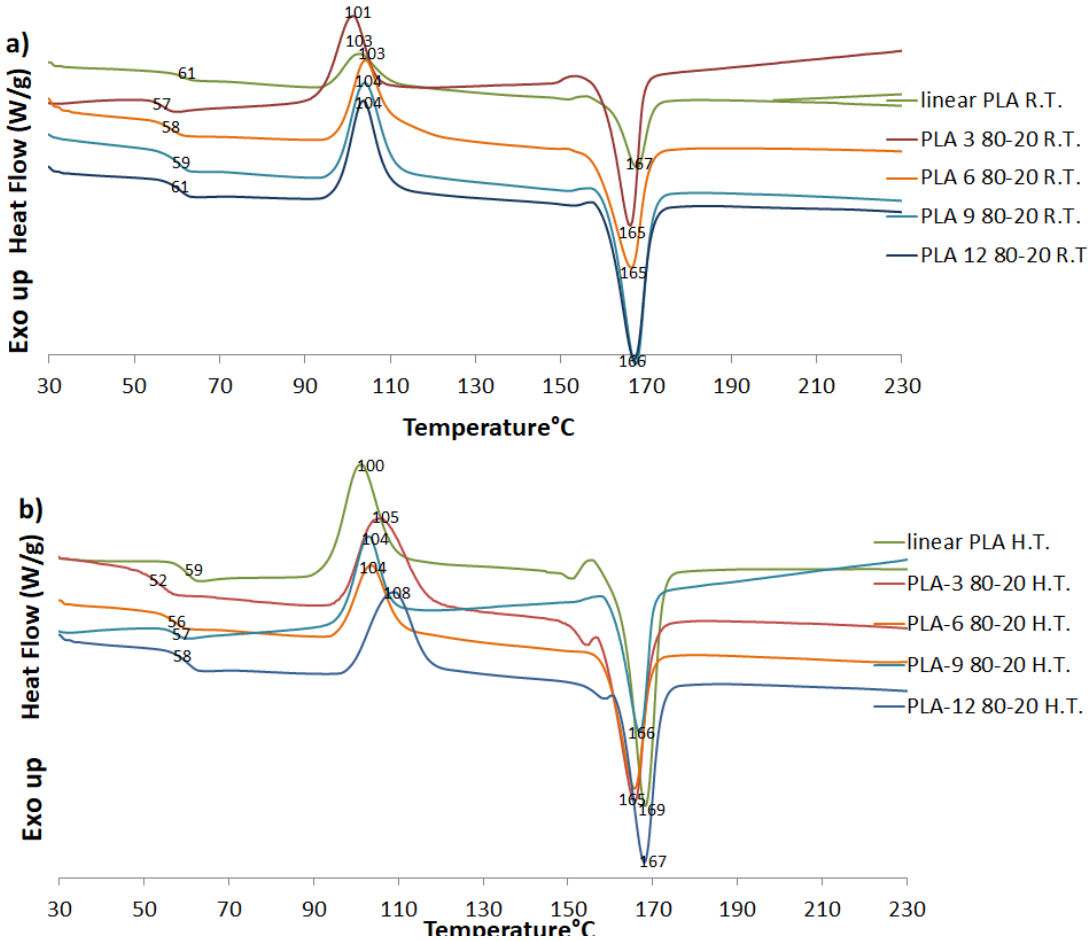

Figure 6.3: *DSC thermogram of a) linear PLA and their blends with star shaped PLA at R.T. b) heat treated (H.T.) linear PLA and blends with star shaped PLA*

Figure 6.3a and Figure 6.3b represent the DSC thermograms for linear PLA and their blends with SPLA which were produced at room temperature (R.T.) and were heat treated (H.T.) to 175°C, respectively. Unlike the neat SPLA polymers when investigated on their own, both crystallisation and melting peaks were observed for the linear PLA and the blends of linear PLA with SPLA (80-20 composition) (Table 3.5).

The crystallisation profiles for linear PLA and the blends (both at R.T. and H.T.) were also investigated using DSC analysis. The percentage crystallinity $\%X_c$ (calculated using equation 3.7 as mentioned in Chapter 3 section 3.6.3) *the* T_g (glass transition), T_c (crystalline temperature), T_m (melting temperature) values for linear PLA and the blends (both at R.T. and H.T.) are also presented in Table 6.1 below.

Table 6.1: *The percentage crystallinity, T_g, T_c and T_m values of linear PLA and blends (both at R.T. and H.T.)*

	linear PLA	PLA-3 80-20	PLA-6 80-20	PLA-9 80-20	PLA-12 80-20	Linear PLA	PLA-3 80-20	PLA-6 80-20	PLA-9 80-20	PLA-12 80-20
	R.T.					H.T.				
T_g	61	57	58	59	61	59	52	56	57	58
T_c	103	101	104	104	104	100	105	104	104	107
T_m	166	165	165	166	166	169	165	165	166	167
%X_c	13.9%	5.4%	7.3%	9.4%	11.1%	25.4%	6.9%	11.8%	12.3%	13.3%
ΔHc	21.35	27.33	21.54	21.66	22.24	18.92	21.31	22.74	19.80	15.44
ΔHm	34.33	22.27	28.35	30.48	32.80	42.62	27.76	33.80	31.87	27.75

6.2.3 Thermogravimetric Analysis (TGA)

The thermal stability (measured as stated in chapter 3 section 3.6.4) of the SPLA polymers is shown in Figure 6.4 which plots residual weight % vs. temperature.

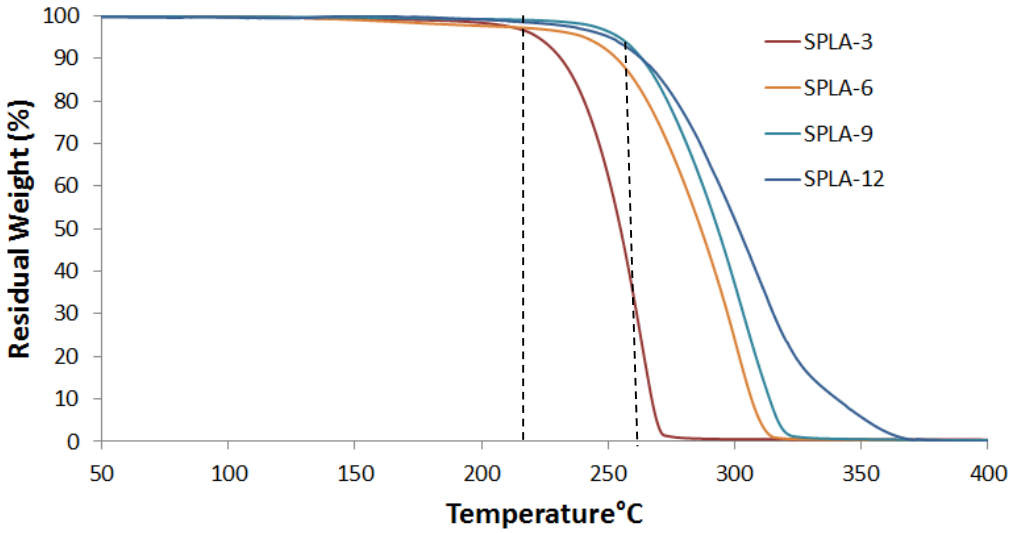

Figure 6.4: *TGA thermogram of SPLA of different molecular weight (M_n)*

From Figure 6.4 it can be seen that SPLA-3 started to degrade thermally at ~220°C, SPLA-6 at ~240°C whilst SPLA-9 and SPLA-12 underwent thermal degradation at comparatively higher temperatures in the region of 250°C. Furthermore, the fastest thermal degradation rate was observed for SPLA-3 whereas the slowest thermal

degradation rate was obtained for SPLA-12. The thermal degradation rate was similar for both SPLA-6 and S-PLA-9 (see broken straight lines added). However, the thermal degradation of all SPLAs took place in a single weight loss step which is also evidenced from the derivative thermo-gravimetric curves (DTG) curves (Figure 6.6).

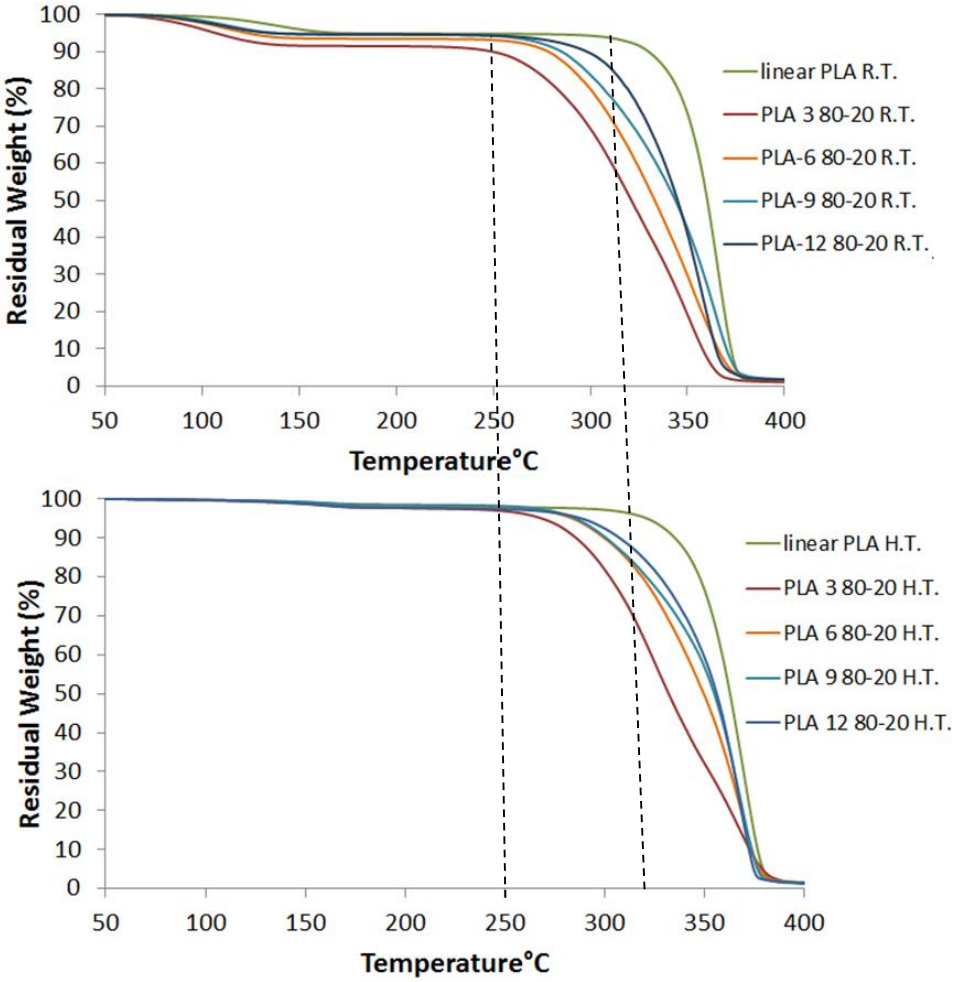

***Figure 6.5**. TGA thermogram of a) linear PLA and blends at R.T. b) heat treated (H.T.) linear PLA and blends*

Figure 6.5 a and Figure 6.5b above define the data related to the thermal stability of linear PLA and the blends (PLA-3 80-20, PLA-6 80-20, PLA-9 80-20, PLA-12 80-20) both at R.T. and H.T. respectively. Linear PLA (both R.T. and H.T.) did not exhibit significant weight loss (i.e. 95% of mass retained) up to ~320°C, whereas the blends (both at R.T.

and H.T.) were all observed to have lower thermal stabilities in comparison. PLA-12 80-20 (for both the R.T. and H.T. samples) started to degrade thermally at ~291°C. However, the thermal stability of PLA-3 80-20 (again for both R.T. and H.T.) was seen to be lower at ~254°C and ~274°C respectively. Moreover, PLA-6 80-20 and PLA-9 80-20 (both R.T. and H. T.) showed thermal stability that were between the blends of PLA-3 80-20 and PLA-12 80-20. Thus there was a definitive trend in thermal stability with weight of the SPLA used to form the blend.

Figure 6.6 below represents the derivative thermo-gravimetric (DTG) curves for the neat SPLA polymers which defines the maximum decomposition temperature (T_{max}).

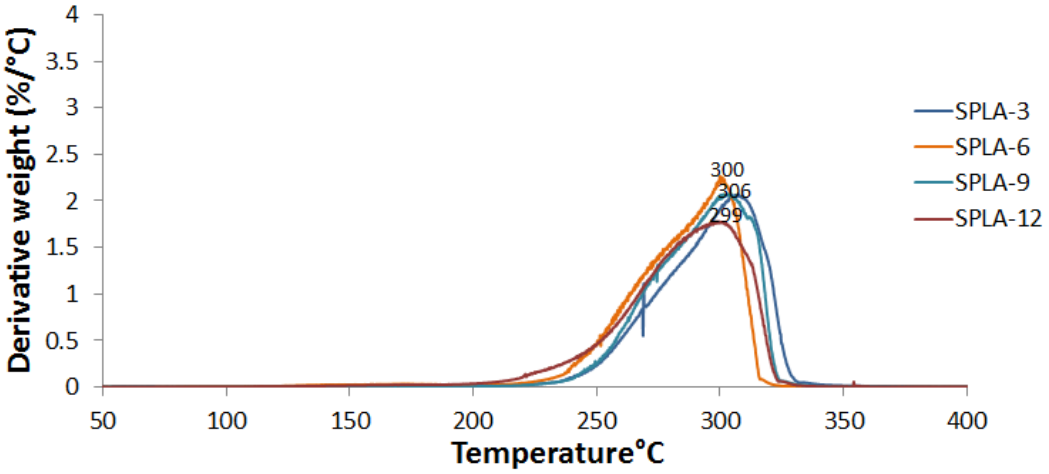

Figure 6.6: *DTG thermogram for SPLA only at different molecular weights (M_n)*

This analysis defined the maximum decomposition temperature (T_{max}) for SPLA-12 was in the region of 306°C, whilst for SPLA-3, SPLA-6 and SPLA-9 the T_{max} value were all observed to be around ~301°C. Meanwhile, Figure 6.7a and Figure 6.7b detail the maximum decomposition temperatures (T_{max}) for linear PLA and the blends.

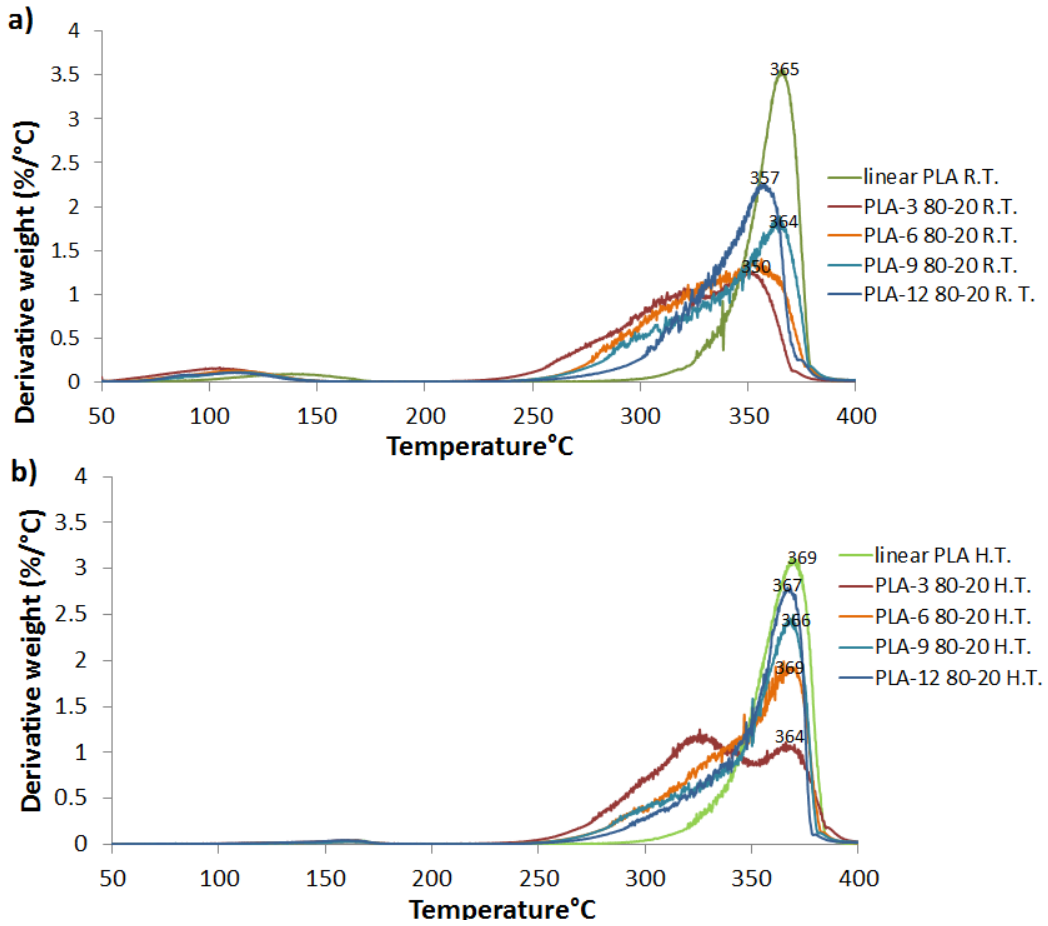

***Figure 6.7**: DTG thermogram of a) linear PLA and blends at R.T. b) heat treated (H.T.) linear PLA and blends*

The maximum decomposition temperatures (T_{max}) for linear PLA was observed to be 365°C and 369°C for R.T. and H.T. respectively. The T_{max} values identified for the H.T. blends were seen to increase slightly in comparison to their corresponding R.T. values. For the R.T. and H.T. blends the highest (T_{max}) value was obtained for the PLA-12 80-20 at 357°C and 367°C respectively. Again, the lowest (T_{max}) value was identified for blend PLA-3 80-20 R.T. and H.T. at 300°C and 364°C respectively, thus a trend with the molecular weight of the SPLA used was also defined this data. However, the maximum decomposition temperature (T_{max}) identified for H.T. films (linear PLA, PLA-3 80-20, PLA-6 80-20, PLA-9 80-20, PLA-12 80-20) at 369°C, 364°C,369°C,365°C and 367°C respectively whereas this value for the films at R.T.

(linear PLA, PLA-3 80-20, PLA-6 80-20, PLA-9 80-20, PLA-12 80-20) was identified at 365°C, 350°C, 350°C, 364°C and 357°C.

6.2.4 Thermo-mechanical Properties

Using DMA the storage modulus (i.e. the stored energy, representing the elastic portion) was investigated (as stated in Chapter 3 section 3.6.5) for the linear PLA and the blends (at both R.T. and H.T.) between temperature range of 30°C to 100°C (see Figure 6.8a and Figure 6.8 b).

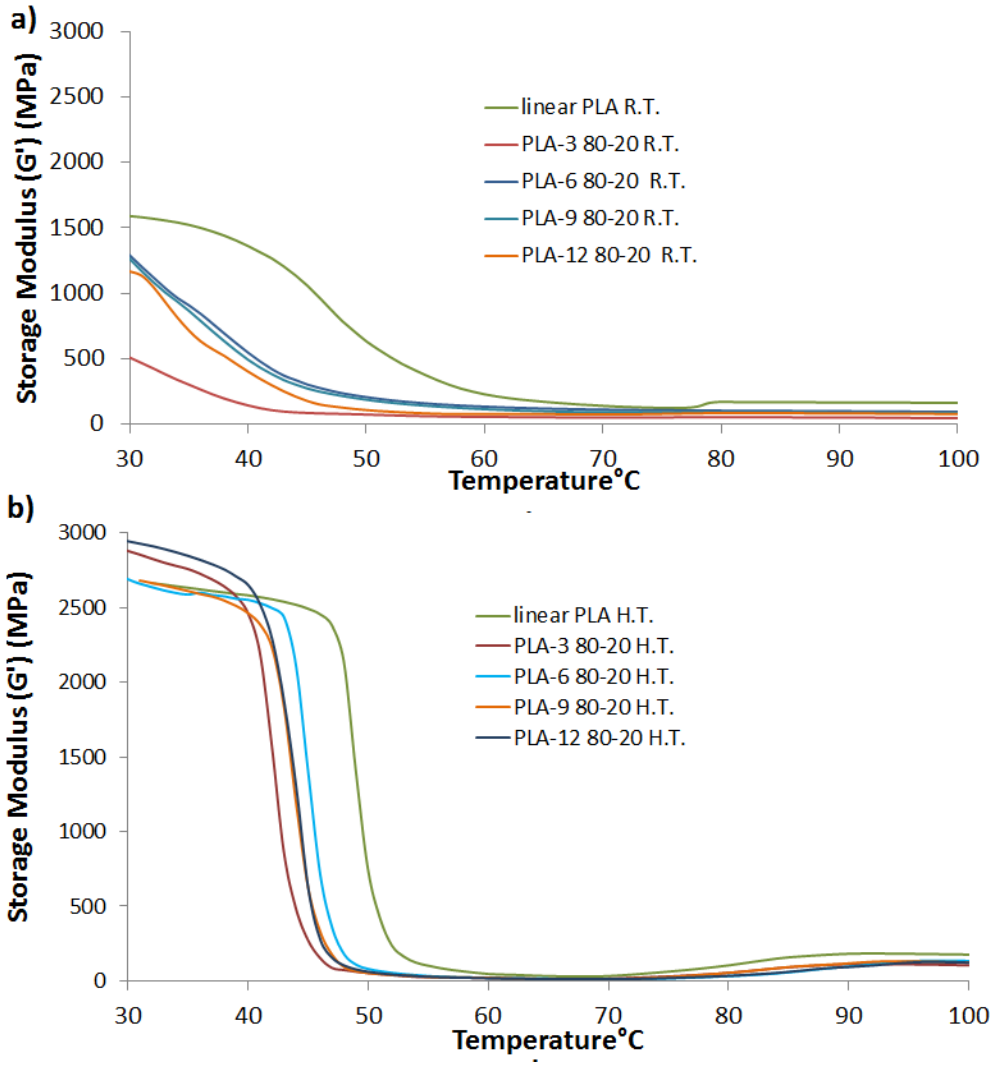

Figure 6.8: *Storage modulus curves a) linear PLA and blends at R.T. b) heat treated (H.T.) linear PLA and the blends*

For linear PLA and blends at R.T. the highest storage modulus (*G'*) was seen for linear PLA (1600 MPa) at around 30°C. However, all blends showed lower *G'* value in comparison to the linear PLA across the whole temperature range investigated. For blends at R.T. the lowest *G'* value was obtained for PLA-3 80-20 at 513 MPa whereas PLA-6, 9 and 12 exhibited similar values of 1168 MPa, 1267 MPa and 1282 MPa respectively.

Figure 6.8b revealed that higher storage modulus values were observed for the H.T. samples with PLA-12 80-20 exhibiting a value at 2947MPa. However, the *G'* value of all blends started to decrease at about 40°C whereas linear PLA retained the *G'* value up to ~50°C indicating higher crystallinity for the linear PLA in comparison to the blends.

The tan delta curves (shown in Figure 6.9a and Figure 6.9b), the α transition (the peak temperature of the tan delta curve) is also representative of the glass transition temperature (T_g).

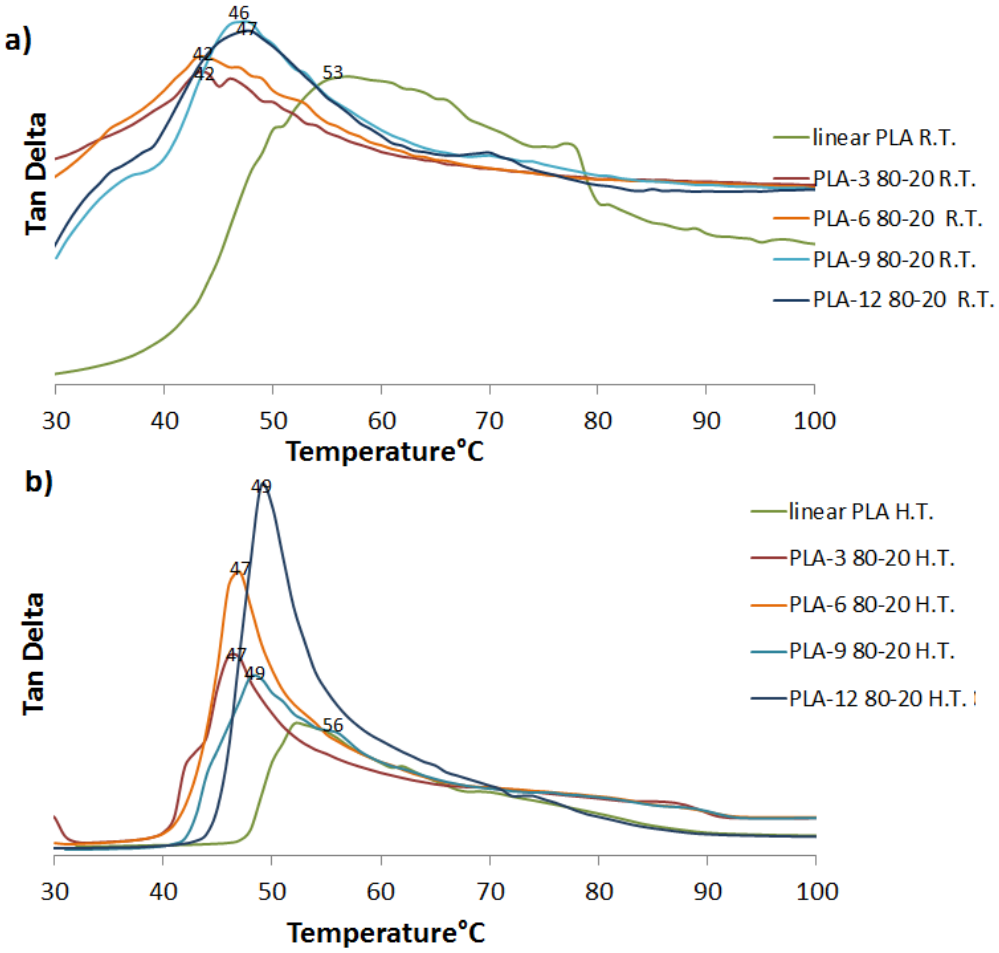

Figure 6.9: *Tan delta curves of a) linear PLA and blends at R.T. b) heat treated (H.T.) linear PLA and blends*

The T_g values identified for linear PLA and blends at H.T. were found to be higher in comparison to the T_g values for linear PLA and the blends at R.T. The tan delta peaks for linear PLA, PLA-3 80-20, PLA-6 80-20, PLA-9 80-20 and PLA-12 80-20 at R.T (Figure 6.9a) were seen at 53°C, 42°C ,42°C, 46°C and 47°C respectively whereas this value for the corresponding heat treated (Figure 6.9b) linear PLA and blends had increased to 56°C, 47°C ,47°C, 49°C and 49°C.

6.2.5 X-ray Diffraction (XRD) Analysis

The XRD analysis was carried out as described in chapter 3 section 3.6.6. Figure 6.10a and Figure 6.10b represent the main diffraction peaks for linear PLA and blends at R.T. and H.T. respectively and were identified at 2ϑ = 16.5° and 19.2°.

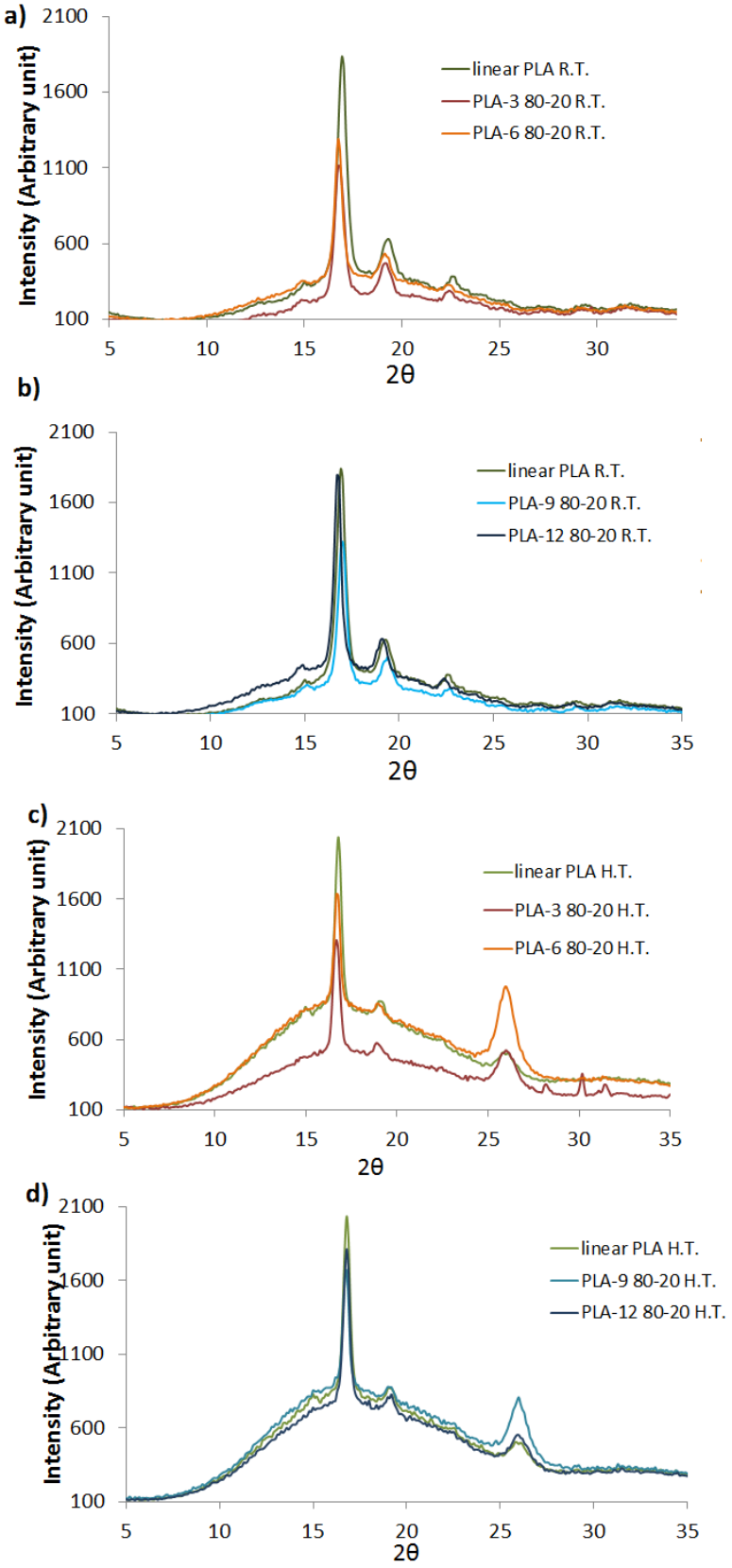

Figure 6.10: *XRD spectra of a) linear PLA, PLA-3 80-20, PLA-6 80-20 at R.T. b) linear PLA, PLA-9 80-20, PLA-12 80-20 at R.T. c) linear PLA, PLA-3 80-20, PLA-6 80-20 at H.T. d) linear PLA, PLA-9 80-20, PLA-12 80-20 at H.T. blends*

As neat SPLA was completely amorphous, (no crystalline peak was observed from DSC analysis) so the crystalline peaks identified for blends at 2ϑ position was similar to the linear PLA. However, the peak intensity observed for blends both at R.T. and H.T. was lower than the peak intensity of linear PLA at R.T. and H.T. respectively. Moreover, after heat treatment the peak intensity for linear polymer and blends increased in comparison to the linear PLA and blends at R.T. An additional peak was also identified for linear PLA and blends at H.T. at 2ϑ = 26.3°.

6.2.6 Percentage (%) wet mass loss with time

Figure 6.11a and Figure 6.11b shows the percentage wet mass loss (calculated by equation 3.6) chapter 3 3.6.12.1) for linear PLA and blends at R.T. and H.T. respectively over 35 days immersion in deionised water at 50°C to observe the accelerated degradation when held at a temperature range around the T_g.

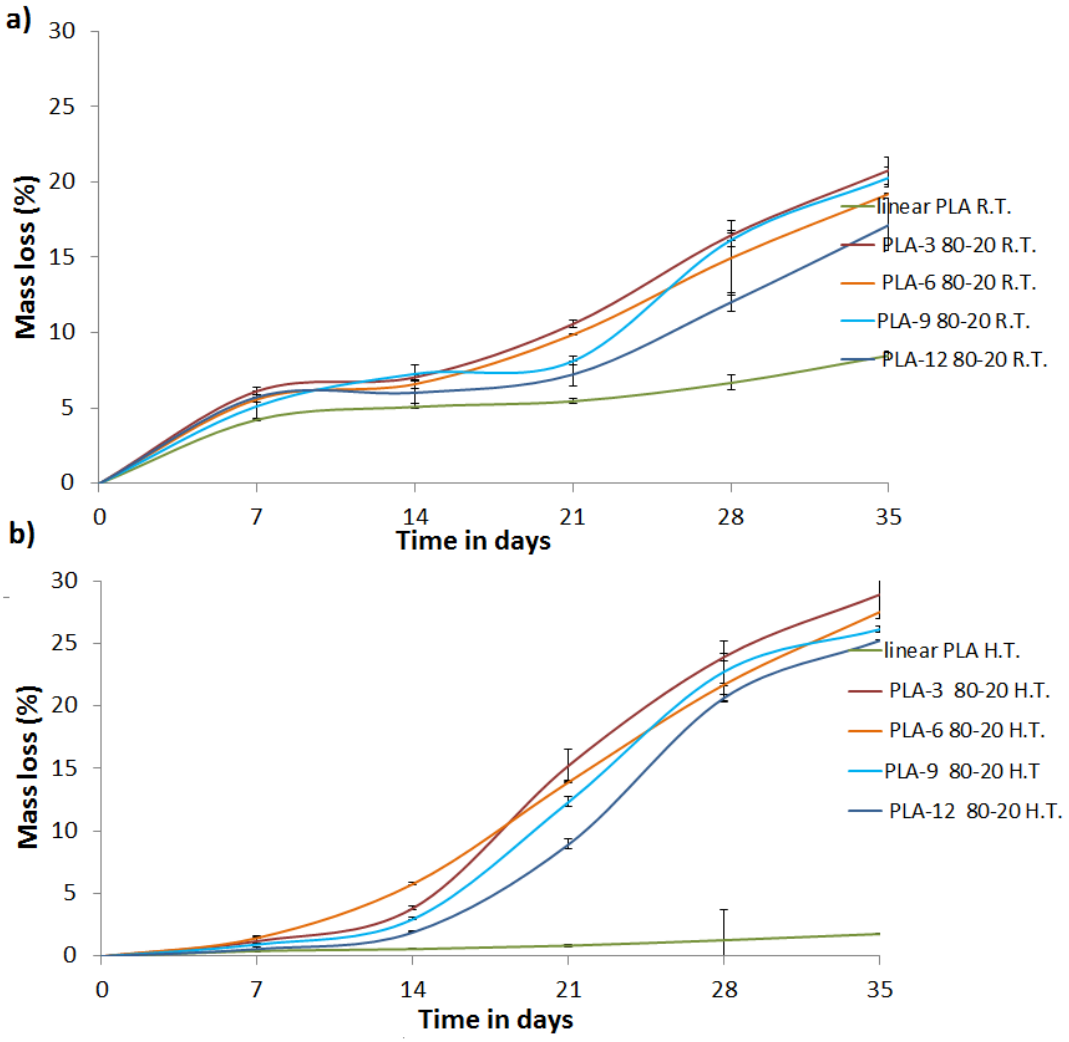

Figure 6.11: *Percentage (%) wet mass loss of a) linear PLA and blends at R.T. b) heat treated (H.T.) linear PLA and blends over 35 days of immersion in deionised water at 50°C*

The percentage wet mass loss for linear PLA at R.T. was found to be 4.25 ± 0.6 % at day 7 and then increased to 8.5± 0.3% at day 35, a difference that was shown to be statistically significant. Over the whole duration of degradation study, the blends at R.T. experienced significantly ($p<0.05$) higher % wet mass loss in comparison to the linear PLA. However, among blends least wet mass loss was observed for blends containing SPLA of high mol. wt. For example, at day 35, the percentage wet mass loss was highest for PLA-3 80-20 at 20.7± 0.2 and this value for PLA-12 80-20 was found to be the lowest at 17.1± 0.6 %.

From Figure 6.11b, which contains the data for the heat treated samples, it was observed that the % wet mass loss for linear PLA did not change statistically ($p>0.05$) until day 35. At day 35, the % wet mass loss of linear PLA increased by 66% than the value at day 7. Again, for all blends the % wet mass loss value was nearly same at day 7. However, after day 7, the % wet mass loss profile for blends started to increase significantly ($p<0.05$) in comparison to the linear PLA across the degradation study duration and reached to the maximum value by day 35. At day 35, the % wet mass loss of PLA-3 80-20, PLA-6 80-20, PLA-9 80-20 and PLA-12 80-20 was found to be 28.8± 0.9, 27.4± 0.7,26.1± 0.3, and 25.2± 0.2 respectively whereas for linear PLA the value was at 1.7± 0.4. From the reported data it can be again said that among blends at H.T. the lowest percentage of wet mass loss was again obtained for PLA-12 80-20.

Table 6.2 and Table 6.3 are representing the T_g, T_c , T_m and $\%X_c$ value from the DSC measurement for linear PLA and blends at R.T. and H.T. respectively during hydrolytic degradation study at day 35 at 50°C.

Table 6.2: *Glass trasition, crystalline, melting temperature and percentage crystallinity of linear PLA and blends at R.T. during hydrolytic degradation at day 35 at 50°C*

Polymers at R.T.	linear PLA	PLA-3 80-20	PLA-6 80-20	PLA-9 80-20	PLA-12 80-20
	Day 35	Day 35	Day 35	Day 35	Day 35
Tg	53±0.01	54±0.01	54±0.04	52±0.03	53±0.03
Tc	99±0.01	96±0.03	97±0.06	98±0.07	96±0.05
Tm	156±0.02	157±0.02	156±0.02	157±0.01	156±04
%Xc	13.9%	19.8%	2.36%	29.2%	39.4%

Table 6.3: *Glass trasition, crystalline, melting temperature and percentage crystallinity of linear PLA and blends at H.T. during hydrolytic degradation at day 35 at 50℃*

Polymers at H.T.	linear PLA	PLA-3 80-20	PLA-6 80-20	PLA-9 80-20	PLA-12 80-20
	Day 35	Day 35	Day 35	Day 35	Day 35
Tg	51±0.02	49±0.01	52±0.01	51±0.01	51±0.02
Tc	96±0.05	96±0.05	94±0.04	94±0.08	93±0.07
Tm	153±0.04	157±0.02	152±0.03	152±0.02	151±0.03
%Xc	25.5%	23.4%	26.2%	23.3%	25.3%

6.2.7 pH profiles

The pH analysis (measured as mentioned in chapter 3 section 3.6.12.2) of the degradation media (deionised water) for linear PLA and blends at R.T. and H.T. over 35 days are shown in Figure 6.12a and Figure 6.12b respectively.

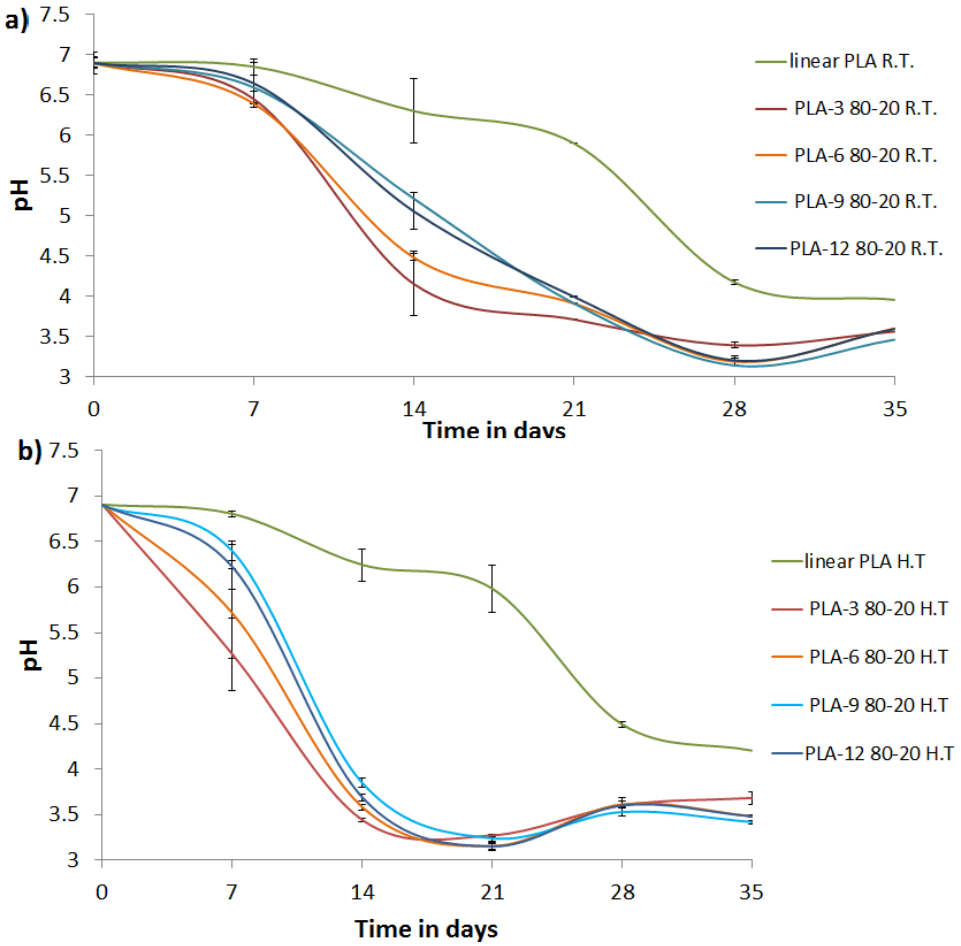

Figure 6.12: *The change in pH of deionised water a) linear PLA and blends at R.T b) heat treated (H.T) linear PLA and blends over 35 days of immersion in deionised water at 50°C*

The pH analysis of the degradation media (deionised water) for linear PLA and blends at R.T. and H.T. over 35 days are shown in Figure 6.12a and Figure 6.12b respectively. The pH of the deionised water for linear PLA both at R.T. and H.T. decreased continuously and reached at 3.96 and 4.2 respectively at day 35. For blends at R.T. the profile of pH for the PLA-9 80-20 and PLA-12 80-20 blends was similar across the whole time duration of the degradation study. PLA-3 80-20 and PLA-6 80-20 blends at R.T. showed the lowest pH among all blends up to 14 days, however all blends showed approximately same pH value ~3.6 at day 35.

For H.T. blends at day 7 the highest pH value was obtained for PLA-12 80-20 at 7.08 and lowest for PLA-3 80-20 at 5.26. However, from day 14 till day 35 all blends showed almost similar pH value and found at ~3.48 at day 35.

6.3 Discussion

Figure 6.1 represents the FTIR spectra of linear PLA and the sorbitol initiated star shaped poly lactic acid (SPLA) between 4000 cm^{-1} and 3100 cm^{-1}. A broad peak ~ 3500 cm^{-1} was found for SPLA whereas no such peak was observed for linear PLA in that region. The peaks identified for SPLA around 3500 cm^{-1} were suggested to be due to the stretching of the -OH groups.[4-6] The FTIR analysis conducted by Haque [7] and Perera [8] on sorbitol initiated linear PLA were similar to the results obtained in Figure 6.1. Both of them attributed this peak to the free hydroxyl groups on the PLA chain ends of the sorbitol stars. This confirmed the presence of -OH groups in the SPLA used in this study and also demonstrated that introducing the SPLA drastically increased the number of chain ends present in the sample when compared to the high molecular weight linear material alone.

The DSC traces of SPLA-3, SPLA-6, SPLA-9 and SPLA-12 are shown in Figure 6.2. As stated in Chapter 3 section 3.6.3, the average T_g was measured over three samples for each polymer. The T_g of the SPLA-3, SPLA-6, SPLA-9 and SPLA-12 polymers was obtained at 48°C, 50°C, 53°C and 54°C respectively. So it can be said that the glass transition temperature, T_g, of the SPLAs increased with increasing number average molecular weight (M_n) or the chain length of the polymers. This observation can be further supported by the Flory Fox equation which state that the M_n of a polymer is related to its T_g .[9]

$$T_g = T_{g\infty} - \frac{K}{M_n} \quad (6.1)$$

where M_n is the number-average molecular weight, K is a polymer-specific constant, and $T_g \infty$ is the maximum glass transition temperature that can be achieved at a theoretical infinite molecular weight. Perera [8] also synthesised sorbitol-ended PLA of three different number average molecular weight (M_n) or chain lengths and reported the increase in T_g with increasing chain length of polymers.[8] Phuphuak *et al.*[3] also observed lower T_g (at 16°C) for low mol. wt. 4 arm star PLLA (M_n=3.3 kDa) and attributed this to the presence of greater free volume on the low mol. wt. SPLA compared to the high mol. wt. SPLA.

The second heating cycle data from the DSC analysis (Figure 6.3a) of the polymer blends at R.T. showed that the T_g of the PLA-3 80-20, PLA-6 80-20, PLA-9 80-20 blends decreased (57°C ,58°C and 59°C respectively) in comparison to the linear PLA (61°C). However, the T_g of the PLA-12 80-20 was found to be in the region of 61°C. This decrease in T_g of blends due to the addition of shorter chain length or lower mol. wt. SPLA could possibly be attributed to the increased free volume associated with the short chain length SPLA which caused higher polymer chain mobility and decreased T_g than the blends containing higher M_n of SPLA. Phuphuak *et al.* also prepared blends of linear PLA containing 1wt% of SPLAs of different M_n values and reported that lowest T_g was obtained at 28°C for the blends containing shorter chain length or lower M_n value (3.3 kDa) of SPLA and the highest T_g was obtained at 47°C for blends containing SPLA of higher M_n value at 12.2 kDa or longer chain length.[3] They again attributed this decrease in T_g to the free volume associated with SPLA through the star polymer core.[3]

A non-isothermal crystallisation was also observed to take place during the DSC analysis of linear PLA and the blends. The $\%X_c$ value of linear PLA and blends (PLA-3 80-20, PLA-6 80-20, PLA-9 80-20 and PLA-12 80-20) were calculated using equation 3.8 (see chapter 3 section 3.6.3) and defined to be 13.9%, 5.4%, 7.3%, 9.4% and 11.1% respectively (Table 6.1). These indicated the slower crystallisation rate and lower crystallinity potential within the blends than that exhibited by the linear PLA. So, it was postulated that blending of SPLA into the linear PLA matrix material inhibited chain packing events and thus decreased the overall crystallinity of the linear PLA. Kim *et al.* [10] also suggested that the star-shaped PLLA possessed lower crystallinity than the linear alternatives of same molecular weight (M_w~19.7 kDa). They explained that the star-shaped PLLA contained more crystalline imperfections due to increased end groups and branching points which caused lower crystallinity and in turn lower melting temperature. Zhao *et al.* [11] also observed that star shaped PLA possessed lower T_g, T_m and crystallinity than those of linear PLA and attributed this to the crystalline imperfections due to increased free end groups and branching points in the star polymers.

Moreover, among blends lowest percentage crystallinity was observed for blends containing low mol. wt. SPLA (for PLA-3 80-20, $\%X_c$ at 5.4%) compared to the blends with high mol. wt. SPLA (PLA-12 80-20, $\%X_c$ at 11.1%). This might be attributed to the decreased free volume associated with high mol. wt. SPLA which potentially eases the reorganising of amorphous chain segments into crystalline segments during cooling process and thus increased the crystallinity. Khajeheian and Rosling [1] also reported that the 4 arm star PLLA with longer branch (or arm) length (higher M_n

value) crystallises more easily during the heating and cooling process than that of the SPLA with shorter arm length or lower M_n value.

However, the findings of this study contradicted the findings observed by Phuphuak *et al*.[3] Their group also carried out the non-isothermal crystallisation of linear PLA and blends through DSC and reported higher crystallinity at 35% for blends containing 1wt% of low mol. wt. SPLA (M_n=3.3 kDa) in comparison to the crystallinity (%X_c~29%) for blends with 1wt% of high mol. wt. SPLA (M_n=12.2 kDa). They explained that shorter chain branches of SPLA provided increased free volume and initiated rapid chain packing during cooling process from the melt (which also induced a certain level of crystalline domain to PLA main matrices) whereas for the longer chain branches SPLA the rapid formation of crystals was difficult. As stated before that they also observed lowest T_g for low mol. wt. SPLA, so they concluded that SPLA of low mol. wt. could act as both plasticising and a nucleating agent.[3]

For comparison, Figure 6.3b shows the second heating cycle of DSC for heat treated (H.T.) linear PLA and blends. During heat treatment both the linear PLA and blends were melted at 175°C and then cooled to room temperature at a rate 10°C/min. The T_g, T_c and *Tm* and %X_c data for heat treated linear PLA and blends are tabulated in Table 6.1. After heat treatment the %X_c value of the linear PLA and blends (PLA-3 80-20, PLA-6 80-20, PLA-9 80-20 and PLA-12 80-20) increased by 45%, 21%, 35%, 23% and 29% respectively when compared to the values for linear PLA and blends at R.T. It was hypothesised that this was due to the fact that some crystallinity may have developed during heat treatment of both linear PLA and blends and so increased the overall percentage crystallinity for the heat treated polymers.[12].

The thermal stability of the neat SPLAs was shown in Figure 6.4 which plots residual weight percentage vs. temperature. The thermal degradation of the SPLAs took place in a single-stage process, which was associated with the cleavage of ester groups.[13] From Figure 6.4 it could be said that with increasing molecular weight thermal stability of neat SPLAs also increased. This would suggest that the thermal cleavage of SPLA is related to the number of chain ends present in the molecule and so that the even may be located at the chain end.

Figure 6.5a and b compare the thermal stability of linear PLA and blends at R.T. and H.T. respectively. For samples at R.T., the linear PLA was found to be thermally stable at the temperature region between 50^{o}C and 309^{o}C. The lowest thermal stability was obtained for the PLA-3 80-20 blends at R.T. and started to thermally degrade ~260^{o}C. However, the reduced thermal stability of the blends both at R.T. and H.T. compared to that of linear PLA may be attributed to the lower crystallinity and the unstable hydroxyl groups (from sorbitol functionality or the increased number of chain ends present) of the star shaped PLA. [14] Teng *et al.* [14] prepared star shaped PLA from L-lactide and xylitol containing different molar ratio of L-lactide to xylitol. They reported that the thermal decomposition temperature of SPLA decreased with decreased crystallinity of SPLA or due to the increasing molar ratio of xylitol in SPLA. A similar thermal decomposition pattern was also reported by Arvanitoyannis *et al.* [15] for three-armed SPLA synthesised from L-lactide with glycerol. Zhao *et al.* [11] also reported lower thermal stability for star-shaped PLA. They attributed this to the unstable nature of the hydroxyl terminated chain ends within the molecular structure of the PLA, which they proposed decomposed to form the cyclic monomer. However, Khajeheian and Rosling [1] observed higher thermal stability for both neat SPLA (they

used pentaerythritol as co initiator to synthesise SPLA) and blends containing SPLA with linear PLA compared to the linear PLA. However, they did not include any explanation for this observation. From Figure 6.5a and b, no significant difference on thermal stability was observed for the linear PLA and blends at H.T. than that of the samples at R.T.

The peak in the DTG thermogram (Figure 6.6) was utilised to determine the maximum decomposition temperature (T_{max}) for the neat star polymers.[16] From Figure 6.6 the highest T_{max} was identified for SPLA-12 and lowest for SPLA-3 which can again be attributed to the higher molecular weight of SPLA-12. From Figure 6.7a and Figure 6.7b the highest T_{max} value was obtained for linear PLA at 365°C. The thermal degradation of PLA is proposed to occur via the cleavage of the ester bonds leading to the formation of shorter polymer chains and an increase in the number of chain ends per mass. The chain ends then promoted the depolymerisation by back-biting (intramolecular transesterification) and theorised to be the main degradation step within the temperature range of 280°C to 370°C.[17] The T_{max} value identified for blends (PLA-3 80-20, PLA-6 80-20, PLA-9 80-20 and PLA-12 80-20) at both R.T. at 350°C, 350°C, 364°C and 357°C respectively and H.T. at 364°C,369°C,365°C and 367°C respectively was found to be reduced when compared to that of linear PLA which was shown to be R.T. 365°C and H.T. at 369°C under the conditions used to determine it. However, the higher T_{max} value observed or heat treated linear PLA and blends in comparison to the linear PLA and blends at R.T can be attributed to the higher crystallinity of heat treated linear PLA and blends.[14]

The DMA results presented in Figure 6.8a determined how the storage modulus (*G'*) of linear PLA, PLA-3 80-20, PLA-6 80-20, PLA-9 80-20, PLA-12 80-20 blends at R.T. varied as temperature at it was ramped. Across the whole temperature region measured (i.e. from 30°C to 100°C), the highest storage modulus (*G'*) was seen for the linear PLA alone. In comparison, the lowest *G'* values was found at 513 MPa for PLA-3 80-20, however the storage modulus of other blends (PLA-6 80-20, PLA-9 80-20, PLA-12 80-20) was nearly the same. This result was predictable as linear PLA at R.T. possessed the highest crystallinity, whereas the PLA-3 80-20 blend contained the lowest crystallinity among blends and also was proposed to impart the highest plasticisation effect due to its shorter chain length. This latter conclusion was based on the evidence from the trend in the T_g values observed in the tan delta and DSC analysis.[18]

Figure 6.8b showed the storage modulus (*G'*) of linear PLA and blends after H.T. and this data demonstrated that the storage modulus (*G'*) of PLA-12 80-20 was found to be at 2947 MPa at around 30°C whereas the comparative value for linear PLA was found be at 2667MPa at the same temperature. The storage modulus obtained for heat treated linear PLA and blends (across the whole temperature region) was significantly ($p>0.05$) higher than the storage modulus value of linear PLA and blends at R.T. which supported the proposal that the level of crystallinity in the linear PLA and blends was increasing during heat treatment. However, for H.T. samples, the *G'* value of blends started to decrease when a temperature of around 40°C had been reached, whereas for linear PLA the *G'* decreased after around 50 °C. The decrease in *G'* value at higher temperature of linear PLA than blends may be to be due to the

reason that above T_g, the crystallinity of PLA highly affects its thermo-mechanical properties and the decrease in modulus became more significant as the percentage crystallinity decreased.[19, 20] Moreover, between 90°C and 100°C, another increase in storage modulus for both linear PLA and blends at H.T. was observed which was proposed to correspond to the range of the cold crystallisation temperature of the PLA and blends. This refers to a process where, when the materials are above the glass transition, small crystallites are formed at specific relatively low temperature range, which is then referred to as the cold crystallisation temperature. Consequently, as there is an increase in % crystallinity during cold crystallisation, this results in an increase in the rigidity of the specimen and in turn an increase the storage modulus.[20] However, the increase in storage modulus at cold crystallisation was absent for blends at R.T. and only a slight increase in linear PLA at R.T. was observed within this temperature region. This was concluded to again indicated the amorphous nature of the blends at R.T.

Figure 6.9a and Figure 6.9b shows the tan delta curves for linear PLA and blends at R.T. and H.T. respectively. Tan delta is calculated by taking the ratio of the loss to the storage moduli.[21] The peak temperature of the tan delta curve represents the glass transition temperature (T_g).[20] The tan delta peaks obtained for the heat treated linear PLA and blends (PLA-3 80-20, PLA-6 80-20, PLA-9 80-20 and PLA-12 80-20) had all shifted to the higher temperature regions compared to the values found for linear PLA and blends at R.T. The shift of tan delta peaks of H.T. samples to higher temperature by somewhere between 2 and 5^{o}C suggested that the segmental motion of polymer matrix had been restricted and reinforced the proposal that due to higher

crystallinity having been established in the heat treated samples compared to the samples at R.T.[22]

Figure 6.10a and Figure 6.10b are representing the XRD value of linear PLA and blends at both R.T. and H.T. The common peaks identified in the spectra for both R.T. and H.T. samples at the same 2ϑ (i.e. 16.5° and 19.2°) position and these are consistent with the peaks identified for linear PLA from literature.[23] After heat treatment of linear PLA and blends an increase in crystallisation peak intensity was observed which indicated higher crystallinity for heat treated samples than was exhibited by the samples at R.T. The effect of annealing of PLA specimens at different temperatures has been studied by Tabi *et al.* [24] over different time periods. They reported that the intensity of the peak increased gradually as a function of annealing time. They also noticed an additional peak appeared at 22.3° for samples annealed at temperature higher than 140°C and concluded this additional peak indicated higher crystallinity. In this study, for heat treated samples an additional peak was identified at H.T at 2ϑ = 26.3°, which indicated that crystallinity of linear PLA and blends had increased after heat treatment at 175°C.[20]

It is known that poly(L-lactic acid) (PLLA) can take more than 3 years for achieve complete degradation.[25] Moreover, when hydrolysed at 37°C, the PLLA films retained the weight for around 18 months prior to showing signs of degradation.[26] For this reason accelerated degradation at higher temperature become an accepted technique among researchers to shorten the time of degradation studies.

Mass loss profiles for the PLA samples during hydrolytic degradation are proposed to be caused by the formation of water-soluble low molecular weight oligomers and

monomers created by chain cleavage. Furthermore, their acidic character is thought to then catalyse further cleavage and so weight loss. Lyu *et al.* [25, 27] also proposed three major hydrolytic degradation steps for linear PLA which included (i) water diffuses into the polymer which then interacts/reacts polymer bonds (ii) the molecular weight of the polymer is decreased and the polymer chain ends concentration is increased, where these chain ends will interact with the polymer chain to inspire cleavage of bonds and (iii) the small polymer chains then became soluble in the testing media which are leached away creating mass loss. Therefore, the mass loss from a polymer can be used as an indicator of the fraction of water-soluble low molecular weight oligomers and monomers formed within the polymer. [12, 28] From Figure 6.11a it can be seen that the % wet mass loss of linear PLA and blends at R.T. increased significantly during the 1st week of degradation study, however, for PLA-3 80-20, PLA-6 80-20, PLA-9 80-20 and PLA-12 80-20 blends the % wet mass loss increased more significantly in comparison to the linear PLA over the whole duration of degradation. This was proposed to be due to the lower crystallinity of the blends that caused higher hydrolytic degradation of blends than linear PLA. It has been reported that during the degradation of PLA, water diffuses into the amorphous regions initially, which are less packed and allow water penetration more easily than the crystalline regions.[29] Teng *et al.* [14] also observed higher hydrolytic degradation of SPLA than linear PLA and explained that multi-arm structure of SPLA possessed improved hydrophilicity (due to the presence of -OH group in SPLA from Xylitol and/or the increased number of chain ends of the star polymer) and lower degree of crystallinity and experienced increased rate of hydrolysis. On the other hand, Tsuji and Hayashi [30] reported higher degradation rate (monitored by

decrease of M_n value) for linear 2 arm PDLLA than that of the neat 4 arm PDLLA and explained that due to the presence of more -OH end group and molecular architecture, 4 arm PDLLA underwent hydrolytic degradation by surface erosion mechanism whereas linear 2 arm PDLLA underwent hydrolytic degradation by bulk erosion mechanism.

From Figure 6.11b the % wet mass loss for heat treated linear PLA was not significant till 28 days of studies. However, H.T. blends started to degrade from day 14 and experienced significant increase in the % wet mass loss in comparison to linear PLA over the rest of the degradation period.

Moreover, from day 21, the percentage wet mass loss of H.T. blends became higher than that of the blends at R.T. and continued till the end of the study. By comparing Figure 6.11a and b, it can be seen that at the end of the study the % wet mass loss of PLA-3 80-20, PLA-6 80-20, PLA-9 80-20 and PLA-12 80-20 blends at H.T. was higher (at 28.8± 0.9, 27.4± 0.7,26.1± 0.3, and 25.2± 0.2 respectively) than that of the blends at R.T. (at 20.7± 0.2, 19.1± 1, 20.3± 0.9 and 17.1± 0.6 % respectively). This was most likely due to the fact that after degradation of most or all the amorphous regions, the water slowly penetrates into the crystalline regions, crystallinity decreased and therefore, higher percentage of wet mass loss occurred for H.T. blends than blends at R.T.[29] However, no increased mass loss was observed for linear PLA at H.T. than linear PLA at R.T.

Table 6.2 and Table 6.3 highlight the DSC data and the calculated percentage crystallinity for linear PLA and blends at R.T. and H.T. respectively during hydrolytic

degradation at day 35. By comparing Table 6.1 and Table 6.2 can be said that, after hydrolytic degradation at day 35, the percentage crystallinity of linear PLA, PLA-3 80-20, PLA-6 80-20 PLA-9 80-20, PLA-12 80-20 at R.T. increased by 26%, 73%, 69%, 68% and 71% respectively in comparison to the percentage crystallinity value of the linear PLA and the blends at R.T. prior to degradation. Similarly, from Table 6.1 and Table 6.3 it can be again said that after hydrolytic degradation, at day 35, the percentage crystallinity of PLA-3 80-20, PLA-6 80-20, PLA-9 80-20, PLA-12 80-20 at H.T increased by 69%, 54%, 47% and 52% respectively than the value before degradation study. However, for linear PLA at H.T., no increase in % crystallinity was observed at day 35 of degradation.

In both cases, after hydrolytic degradation, the comparatively higher increase in % crystallinity of the blends in comparison to the linear PLA (both R.T. and H.T.) can be again attributed to the lower crystallinity of blends than that of the linear PLA before degradation, which caused rapid degradation of the amorphous regions of the blends hence leading to increased crystallisation of PLA.[29]

From Figure 6.12a and Figure 6.12b it can be said that there was a good correlation between the % wet mass loss and the pH change against time for linear PLA and blends at both R.T. and H.T. The decrease of the pH of the degradation media was quite expected since degradation of PLA is associated with the cleavage of the ester bonds which form new acidic carboxyl end groups and resulted in acidity (lower pH value) of the degradation media.[31]

However, for blends at both R.T. and H.T. the pH change was significantly lower in comparison to linear PLA (both R.T. and H.T.) which was due to the faster hydrolytic degradation rate of the blends than linear PLA. Moreover, the lowest pH value

obtained after the degradation at day 35 for both R.T. and H.T. was ~3. Agrawal *et al.* [32] studied the degradation of a 50:50 PLA-PGA copolymer over a wide temperature range (25°C to 80°C) in PBS media. They observed significant decrease in pH value ~3 for samples tested at 54°C. They explained that an increase in the test temperature resulted in accelerated degradation. Since PLA degraded to lactic acid and released acidic by-products into the media which significantly lowered the pH.

6.4 Conclusions

The effect of blending of star PLA with linear PLA on the thermal, thermomechanical and degradation properties of linear PLA was investigated in this chapters. On the basis of the results obtained in this chapters, following points can be concluded,

- Blending of star PLA with linear PLA decreased the T_g value of the blends than that of the linear PLA. However, the lowest T_g value and % crystallinity was observed for blends containing low mol. wt. SPLA than that of high mol. wt. SPLA. This might be to be due to the greater free volume exists (causes higher chain mobility and lower T_g value) for the star PLA of low mol. wt. than that of the star PLA of high mol. wt.
- Addition of SPLA with linear PLA decreased the crystallinity of the blends than the linear PLA, however, after heat treatment the % crystallinity of the blends increased (not higher than the linear one), so possibly the amorphous segments of the amorphous star PLA has the ability to reorganise and form crystalline segments on heat treatment. However, after heat treatment lower % crystallinity was observed for blends containing low mol. wt. SPLA, which

might be again attributed to the higher free volume of low mol. wt. SPLA caused less chain packing than that of high mol. wt. SPLA.

- The hydrolytic degradation of PLA depends on both the crystallinity, the number and the nature of the chain end group. Higher hydrolytic degradation rate was observed for blends in comparison to the linear PLA which possibly due to the lower crystallinity and the presence of hydrophilic -OH chain end group on SPLA. Blends containing high mol. wt. SPLA experienced lower hydrolytic degradation than that of blends containing low mol. wt. SPLA due to higher crystallinity.

So, in short, it can be said that, addition of SPLA allowed to predictively control the crystallinity, thermal properties, hydrolytic degradation ability and potentially the degradation time of linear PLA.

6.5 References

1. *Khajeheian, M.B. and A. Rosling, Preparation and characterization of linear and star-shaped poly L-lactide blends. Journal of Applied Polymer Science, 2016.* ***133****(2).*

2. *Han, L., et al., Exclusive stereocomplex crystallization of linear and multiarm star-shaped high-molecular-weight stereo diblock poly (lactic acid) s. The Journal of Physical Chemistry B, 2015.* ***119****(44): p. 14270-14279.*

3. *Phuphuak, Y., et al., Balancing crystalline and amorphous domains in PLA through star-structured polylactides with dual plasticizer/nucleating agent functionality. Polymer, 2013.* ***54****(26): p. 7058-7070.*

4. *Coates, J., Interpretation of infrared spectra, a practical approach. Encyclopedia of analytical chemistry.*

5. *Lopes, M.S. and A.L. Jardini, Synthesis and characterizations of poly (lactic acid) by ring-opening polymerization for biomedical applications. Chemical Engineering Transactions, 2014.*

6. *Erbetta, C.D.A.C., et al., Synthesis and characterization of poly (D, L-lactide-co-glycolide) copolymer. Journal of Biomaterials and Nanobiotechnology, 2012.* ***3****(02): p. 208.*

7. *Haque, P., Oligomeric PLA coupling agents for phosphate glass fibres/PLA composites. 2011, University of Nottingham.*

8. *Perera, M.S., The use of sorbitol-initiated polylactic acid as a coupling agent in resorbable phosphate glass fibre reinforced polylactic acid composites. 2015, University of Nottingham.*

9. *O'Driscoll, K. and R.A. Sanayei, Chain-length dependence of the glass transition temperature. Macromolecules, 1991.* ***24****(15): p. 4479-4480.*

10. *Kim, E.S., B.C. Kim, and S.H. Kim, Structural effect of linear and star-shaped poly (L-lactic acid) on physical properties. Journal of Polymer Science Part B: Polymer Physics, 2004.* ***42****(6): p. 939-946.*

11. *Zhao, Y.-L., et al., Synthesis and thermal properties of novel star-shaped poly(l-lactide)s with starburst PAMAM–OH dendrimer macroinitiator. Polymer, 2002.* ***43****(22): p. 5819-5825.*

12. *Auras, R.A., et al., Poly (lactic acid): synthesis, structures, properties, processing, and applications. Vol. 10. 2011: John Wiley & Sons.*

13. *Nicolae, C.-A., M.A. Grigorescu, and R.A. Gabor, An Investigation of thermal degradation of Poly (lactic acid). Engineering Letters, 2008.* ***16****(4): p. 568-571.*

14. *Teng, L., et al., Synthesis and degradability of a star-shaped polylactide based on l-lactide and xylitol. Journal of Polymer Research, 2015.* ***22****(5): p. 1-7.*

15. *Arvanitoyannis, I., et al., Novel star-shaped polylactide with glycerol using stannous octoate or tetraphenyl tin as catalyst: 1. Synthesis, characterization and study of their biodegradability. Polymer, 1995.* ***36****(15): p. 2947-2956.*

16. *Cheerarot, O. and Y. Baimark, Thermal and mechanical properties of biodegradable star-shaped/linear polylactide stereocomplexes. Journal of Chemistry, 2015.* ***2015****: p. 9.*

17. *Al-Itry, R., K. Lamnawar, and A. Maazouz, Improvement of thermal stability, rheological and mechanical properties of PLA, PBAT and their blends by reactive extrusion with functionalized epoxy. Polymer Degradation and Stability, 2012.* ***97****(10): p. 1898-1914.*

18. *Silverajah, V., et al., A comparative study on the mechanical, thermal and morphological characterization of poly (lactic acid)/epoxidized palm oil blend. International Journal of Molecular Sciences, 2012.* ***13****(5): p. 5878-5898.*

19. *Battegazzore, D., S. Bocchini, and A. Frache, Crystallization kinetics of poly (lactic acid)-talc composites. Express Polymer Letters, 2011.* ***5****(10): p. 849-858.*

20. *Srithep, Y., P. Nealey, and L.S. Turng, Effects of annealing time and temperature on the crystallinity and heat resistance behavior of injection-molded poly (lactic acid). Polymer Engineering & Science, 2013.* ***53****(3): p. 580-588.*

21. *Menard, K.P., Dynamic mechanical analysis: a practical introduction. 2008: CRC press.*

22. *Hossain, K.M.Z., Extension of the use of cellulose nanowhiskers in composite materials. 2014, University of Nottingham.*

23. *Yasuniwa, M., et al., Crystallization behavior of poly (L-lactic acid). Polymer, 2006.* ***47****(21): p. 7554-7563.*

24. *Tabi, T., et al., Crystalline structure of annealed polylactic acid and its relation to processing. Express Polym Lett, 2010.* ***4****(10): p. 659-668.*

25. *Lyu, S., et al., Kinetics and time-temperature equivalence of polymer degradation. Biomacromolecules, 2007.* ***8****(7): p. 2301-2310.*

26. *Tsuji, H., K. Nakahara, and K. Ikarashi, Poly (L-lactide), 8. High-temperature hydrolysis of poly (l-lactide) films with different crystallinities and crystalline thicknesses in phosphate-buffered solution. Macromolecular Materials and Engineering, 2001.* ***286****(7): p. 398-406.*

27. *Lyu, S. and D. Untereker, Degradability of polymers for implantable biomedical devices. International journal of molecular sciences, 2009.* ***10****(9): p. 4033-4065.*

28. *Tsuji, H. and T. Hayashi, Hydrolytic degradation and crystallization behavior of linear 2-armed and star-shaped 4-armed poly (l-lactide) s: Effects of branching architecture and crystallinity. Journal of Applied Polymer Science, 2015.* ***132****(20).*

29. *Felfel, R.M., et al., Accelerated in vitro degradation properties of polylactic acid/phosphate glass fibre composites. Journal of Materials Science, 2015.* ***50****(11): p. 3942-3955.*

30. *Tsuji, H. and T. Hayashi, Hydrolytic degradation of linear 2-arm and branched 4-arm poly (dl-lactide) s: effects of branching and terminal hydroxyl groups. Polymer Degradation and Stability, 2014.* ***102****: p. 59-66.*

31. *Weir, N., et al., Degradation of poly-L-lactide. Part 2: increased temperature accelerated degradation. Proceedings of the Institution of Mechanical Engineers, Part H: Journal of Engineering in Medicine, 2004.* ***218****(5): p. 321-330.*

32. *Agrawal, C., et al., Elevated temperature degradation of a 50: 50 copolymer of PLA-PGA. Tissue engineering, 1997.* ***3****(4): p. 345-352.*

CHAPTER 7

7 Characterisation of composites prepared using star shaped and linear poly lactic acid blends as matrix and E-glass fibre as reinforcement

7.1 Introduction

Over the past few decades polymer blends have been studied extensively due to their potential applications and as new materials. Among the different polymer blends investigated, blending of star and linear polymer have also been studied as these materials possess some unique characteristics which were not found in their linear counterparts.[1] For example, modification of hydrolytic degradation, crystallinity, viscosity and mechanical properties have been reported to be modified for blends of linear and star shaped PLA.[2, 3]

Wang *et al.* [4] studied the zero shear viscosity (at 180 °C) of linear PLA and blends containing three arm long chain branched PLA and reported that the blends containing 16wt% of these materials showed 3.3 times higher zero shear viscosity compared to the linear PLA. They also observed significant shear thinning behaviour for the blends than linear PLA. They explained that the long chain branches caused more chain entanglements in the blends than the linear PLA which resulted in higher melt viscosity and shear thinning behaviour.

Ouchi *et al.* [5] prepared blends of linear PLLA with branched PLLA and PDLA to show the effectiveness of branched PLLA or PDLA as plasticisers. They reported a higher elongation at break at 88 % and 120% for blends of linear PLLA with branched PLLA and PDLA respectively compared to linear PLLA film at 14%. However, these blends

also revealed lower tensile strengths (24.6 and 31.9 MPa respectively) and Young's modulus (1180 MPa and 1195 MPa) compared with the tensile strength (33.1 MPa) and Young's modulus (1210 MPa) of linear PLA film. They suggested that the short chain length (M_n~6 kDa) of branched PLA caused the physical crosslinking among crystalline domains of linear PLA.

Fibre reinforced polymer composites have been widely used due to their improved mechanical as well as thermomechanical properties and excellent load transfer capacity for light-weight structural applications.[6] The mechanical properties of composites depend on the properties of both the reinforcing fibres and the polymer matrix used. Improved mechanical properties of composites can be achieved by enhancing the interfacial adhesion between the fibres and matrix.[7] Several routes have been used to explore improving the impregnation of fibres and matrix, for example using chemical coupling agents on fibre surfaces, [8] using low molecular weight oligomers of the matrix material.[9] Another method used to increase the interfacial bonding could be via the use of a thermoplastic star polymer matrix since star shaped polymers possess high fluidity in comparison to linear polymers thus potentially providing good impregnation of the reinforcing fibres.[10] Myard and Philippo [10] prepared carbon and glass fibre reinforced composites using a blend of star and linear polyamide as matrix. They reported that the mechanical properties of the composites prepared were not inferior to composites prepared using a thermoset polymer matrix.

In this study, the rheological properties (dynamic temperature ramp test) of linear PLA and blends were investigated to establish if there was any change in modulus

with temperature ramping and to also ascertain suitable temperatures for composite manufature. Viscosity measurements were also conducted included tensile testing of the linear PLA and its blends (both at R.T. and H.T.) to investigate the effect of heat treatment on the mechanical properties of these samples. The composites were produced using linear PLA and blends as the matrix with E glass fibre as reinforcement via a hot compression process by laminate stacking the matrix and fibre mats. The mechanical and degradation properties of the composites are also reported in this chapter.

7.2 Results

7.2.1 Rheological properties

The rehological measurement was carried out as described in chapter 3 section 3.6.7.1. The storage modulus, (*G*') and loss modulus, (*G*") were plotted against temperature for linear PLA with PLA-12 80-20, PLA-9 80-20, PLA-6 80-20 and PLA-3 80-20 (Table 3.5) investigated (see Figure 7.1A-D).

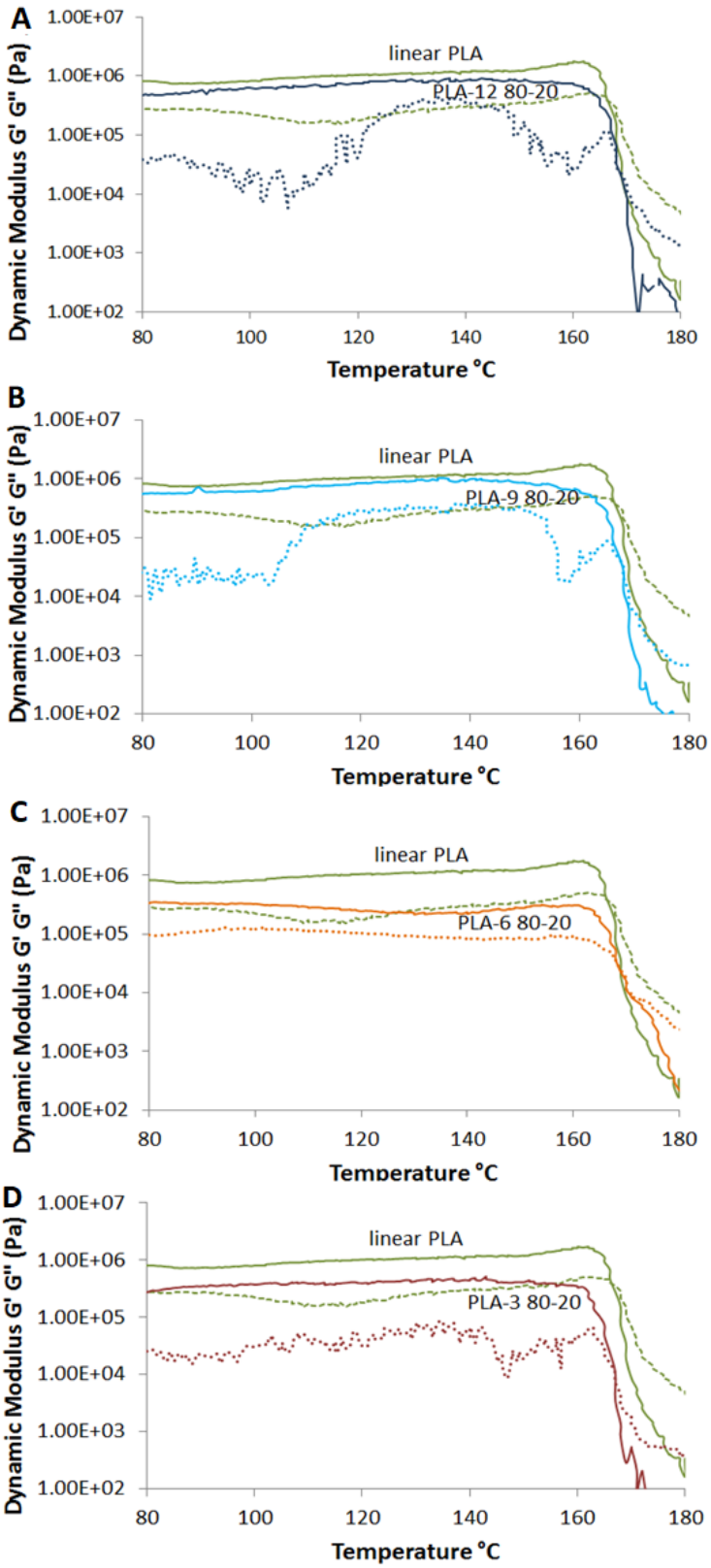

Figure 7.1: *Comparison of dynamic modulus properties for linear PLA with A) PLA-12 80-20 B) PLA-9 80-20 C) PLA-6 80-20 and D) PLA-3 80-20 with temperature ramping from 80 to 180°C. Solid lines represent storage modulus (G') and broken lines represent loss modulus (G") for linear PLA and blends during heating process.*

For both linear PLA and the blends, the storage modulus (*G'*) was higher than the loss modulus (*G''*) up to ~165°C. After ~ 165°C both storage and loss modulus for linear PLA and the 80:20 blends started to decrease, however, the storage modulus decreased faster than the loss modulus. Around 80°C the storage modulus for linear PLA was approximately 8.0×10^5 Pa whereas for PLA-3 80-20, PLA-6 80-20, PLA-9 80-20 the storage modulus was approximately 3.5×10^5 Pa, 3.2×10^5, 5.1×10^5 Pa, 4.8×10^5 Pa respectively.

7.2.2 Viscosity

Figure 7.2 shows the dynamic viscosity (measured as stated in Chapter 3 section 3.6.7.2) of the linear PLA and blends at 175°C. It was observed that at the low shear rate of 0.01 s^{-1}, the highest viscosity was found for the linear PLA at 1.0×10^3 (Pa.s) whereas the lowest viscosity was identified for PLA-3 80-20 at 116 (Pa.s).

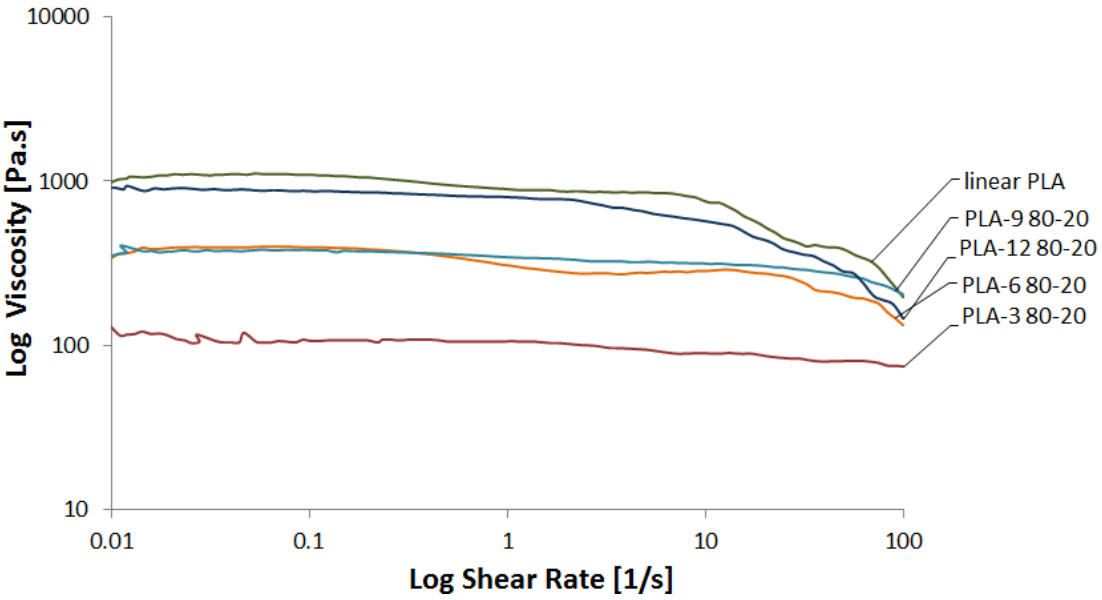

Figure 7.2: *Dynamic viscosity of linear PLA, PLA-3 80-20, PLA-6 80-20, PLA-9 80-20, PLA-12 80-20 blends at 175°C.*

The viscosity of PLA-12 80-20 at 897 (Pa.s) was found to be slightly lower than that of the linear PLA. The viscosity of PLA-6 80-20, PLA-9 80-20 was found to be similar to

each other (at 361 Pa.s) and was between the value of PLA-12 80-20 and PLA-3 80-20 at ~367 (Pa.s). The viscosity profiles of linear PLA and its blends were seen to decrease with increasing shear rate.

7.2.3 Mechanical Properties

7.2.3.1 Tensile Test

The tensile test of linear PLA and blends at R.T. and H.T. was conducted as stated in chapter 3 section 3.6.9.1. The elongation at break of linear PLA and its blends at room temperature are presented in Figure 7.3a whereas the elongation at break for the heat treated linear PLA and blends (subjected to 175°C) are presented in Figure 7.3b.

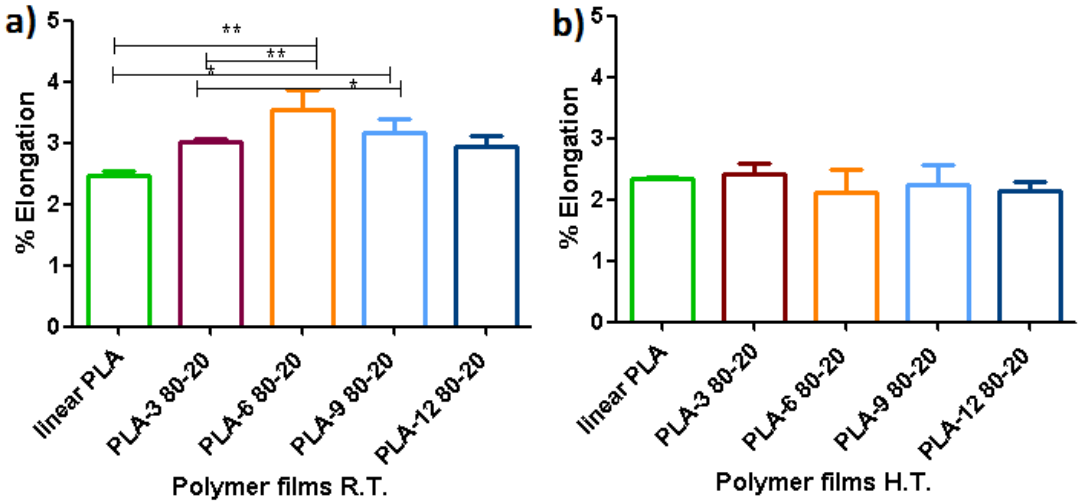

Figure 7.3: *Percentage elongation of linear PLA, PLA-3 80-20, PLA-6 80-20, PLA-9 80-20, PLA-12 80-20 blends a) at room temperature and b) heat treated at 175°C.*

For PLA-3 80-20, PLA-6 80-20, PLA-9 80-20, PLA-12 80-20 blends at R.T., the elongation at break was seen to increase by approximately 25% ($p<0.05$), 44% ($p<0.005$), 28% ($p<0.05$) and 24% ($p<0.05$) respectively in comparison to the linear PLA.

Post heat treatment at 175°C, the elongation at break of heat treated linear PLA had found to be 2.35%. Moreover, for the heat treated PLA-3 80-20, PLA-6 80-20, PLA-9

80-20 and PLA-12 80-20 blends the elongation at break had found at 2.4%, 2.1%, 2.2% and 2.1% respectively. No statistically significant difference was observed for the elongation at break for the heat treated samples.

Figure 7.4a presents a comparison of the tensile moduli data of linear PLA and blends at room temperature (R.T.) and Figure 7.4b the equivalent data for the samples heat treated (H.T.) at 175°C.

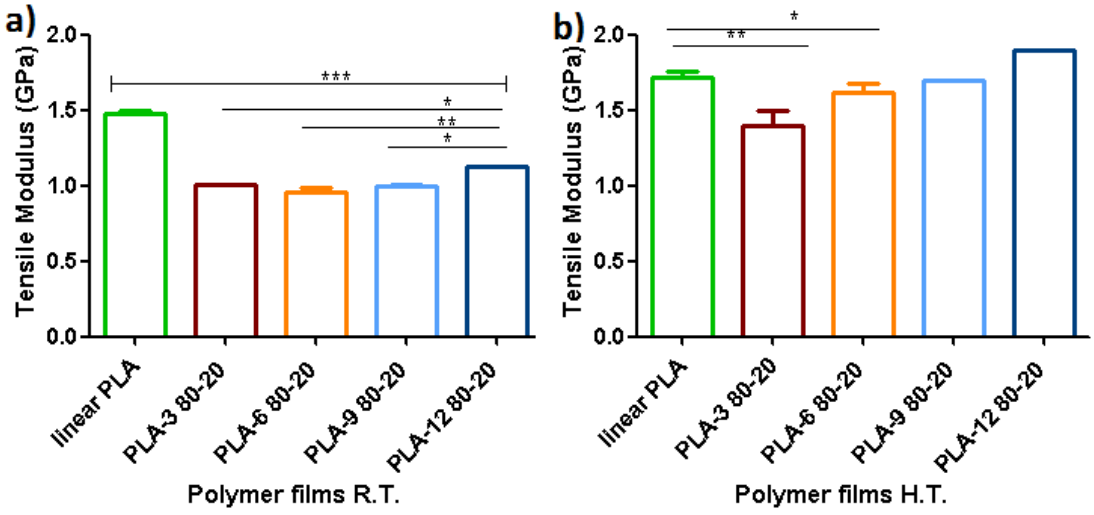

Figure 7.4: *Tensile moduli of linear PLA, PLA-3 80-20, PLA-6 80-20, PLA-9 80-20, PLA-12 80-20 blends a) at room temperature and b) heat treated at 175°C.*

At room temperature, the tensile moduli of PLA-3 80-20, PLA-6 80-20, PLA-9 80-20 and PLA-12 80-20 blends exhibited decreased values by 32% ($p<0.005$), 35% ($p<0.005$), 33% ($p<0.005$) and 25% ($p<0.005$) respectively, as compared to linear PLA (1.12 GPa). Moreover, the tensile moduli of PLA-3 80-20, PLA-6 80-20, PLA-9 80-20 had also noted to be 10% ($p<0.05$), 15% ($p<0.05$) and 11% ($p<0.05$) lower when compared to the PLA-12 80-20 blend.

Post heat treatment at 175°C, the tensile modulus of heat treated linear PLA was approximately 1.72 GPa whereas the tensile moduli of PLA-3 80-20, PLA-6 80-20, PLA-

9 80-20 and PLA-12 80-20 blends were 1.4 GPa, 1.6 GPa, 1.7 GPa and 1.8 GPa respectively. The tensile modulus value of PLA-9 80-20 and PLA-12 80-20 blends were concluded not to be statistically significantly different from that of the linear PLA.

Moreover, after heat treatment the tensile moduli of the PLA-3 80-20, PLA-6 80-20, PLA-9 80-20 and PLA-12 80-20 blends experienced a statistically significant increase of 33% ($p<0.005$), 40% ($p<0.005$), 41% ($p<0.005$) and 37% ($p<0.005$) respectively when compared to their corresponding value at room temperature. Meanwhile, for heat treated linear PLA the tensile moduli did not increase statistically significantly compared to the value for linear PLA at R.T.

The tensile strength data of linear PLA and blends at room temperature are presented in Figure 7.5a and for the heat treated linear PLA and blends (at 175°C) in Figure 7.5b.

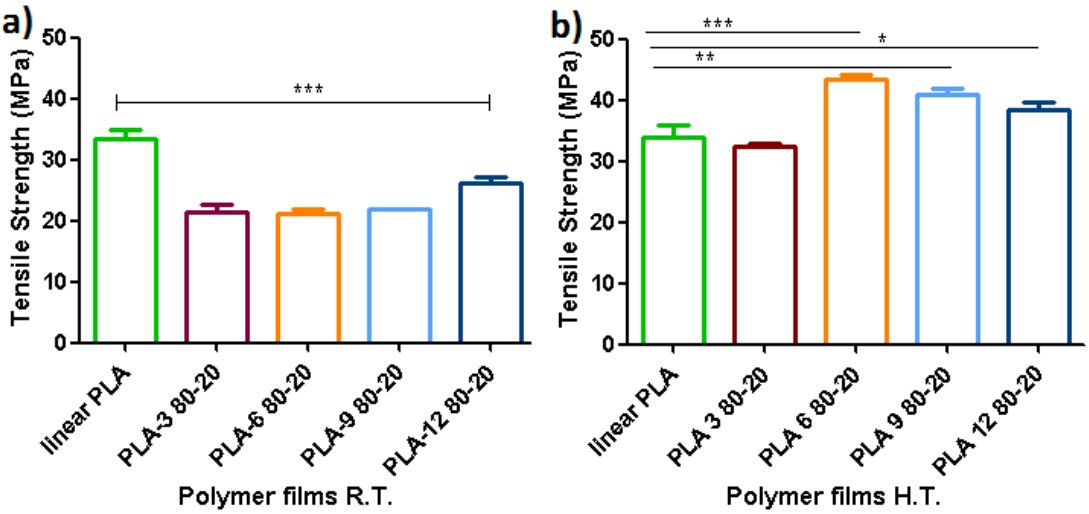

Figure 7.5: *Tensile strength of linear PLA, PLA-3 80-20, PLA-6 80-20, PLA-9 80-20, PLA-12 80-20 blends a) at room temperature and b) heat treated at 175°C.*

For PLA-3 80-20, PLA-6 80-20, PLA-9 80-20 blends at R.T. the tensile strength values 43% ($p<0.005$) lower than the linear PLA (38 MPa) values and for PLA-12 80-20 blend this value is 31% ($p<0.005$) lower than the linear PLA.

Figure 7.5b demonstrated that post heat treatment (at 175°C) the tensile strength for linear PLA was 34 MPa whereas for PLA-3 80-20, PLA-6 80-20, PLA-9 80-20 and PLA-12 80-20 blends the tensile strength was 32.5 MPa, 43.3 MPa, 39.3 MPa and 38.3 MPa respectively. These values for the heat treated blends (except PLA-3 80-20) was found to be statistically significantly higher ($p<0.005$) in comparison to the heat treated linear PLA.

A comparison table for the all the measured tensile strength values of linear PLA and blends are presented in Table 7.1

Table 7.1: *A comparison of the tensile strength value of linear PLA and blends (PLA-3 80-20, PLA-6 80-20, PLA-9 80-20 and PLA-12 80-20) at both room temperature (R.T.) and heat treated (H.T.)*

Linear PLA and blends	Tensile Strength (R.T.) (MPa)	Tensile Strength (H.T.) (MPa)	(%) increase or decrease	P value
Linear PLA	33±0.4	34±0.2	3% increase	(p>0.005)
PLA-3 80-20	21.6±0.03	32.5±0.5	33 % increase	(p<0.005)
PLA-6 80-20	21.25±0.7	43.33±0.7	50 % increase	(p<0.005)
PLA-9 80-20	21.94±0.2	39.3±0.4	44 % increase	(p<0.005)
PLA-12 80-20	26.05±0.5	38.3±0.08	32 % increase	(p<0.005)

7.2.4 X-ray Diffraction (XRD) Analysis

XRD analysis was conducted using the method described in Chapter 3 Section 3.3.5. The XRD spectra for linear PLA-GF, PLA-3 80-20-GF, PLA-6 80-20-GF, PLA-9 80-20-GF and PLA-12 80-20-GF composites prior to degradation are shown in Figure 7.6.

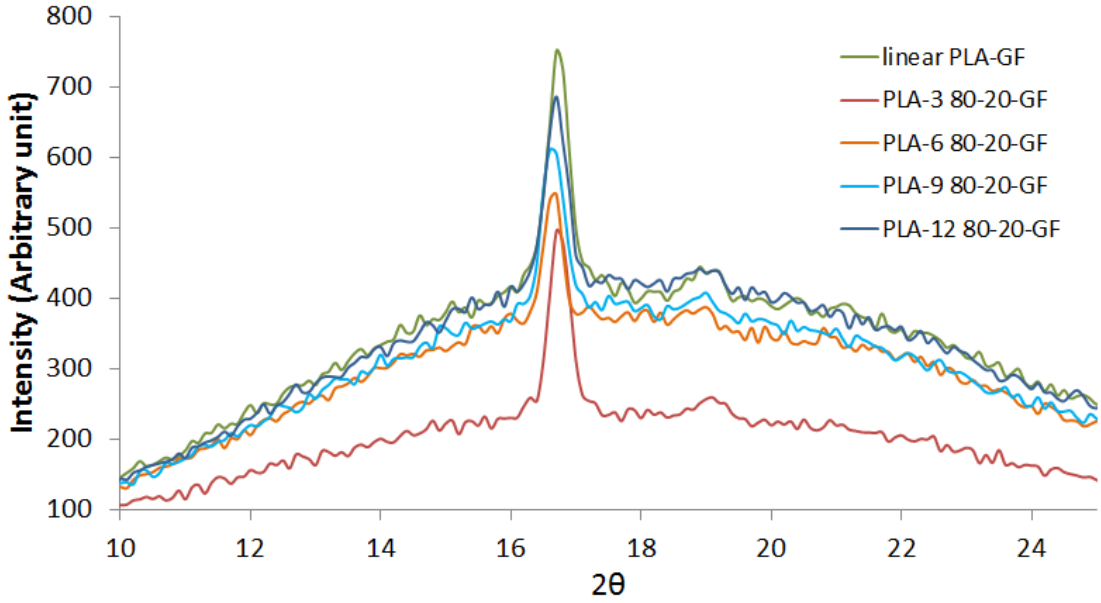

Figure 7.6: *XRD spectra of composites with E-glass fibre (GF) of linear PLA-GF, PLA-3 80-20-GF, PLA-6 80-20-GF, PLA-9 80-20-GF and PLA-12 80-20-GF composites*

It was evident from the XRD spectrum of the PLA (Polymer Grade: Nature Works 3251D) alone that some crystallinity is present in the matrix material and so it would be expected to be present in all the samples. The peak identified for these composites was at ~16.5° (Miller indices of (200).

7.2.5 Flexural Tests

Figure 7.7a shows the initial flexural moduli and strength data (measured as stated in chapter 3 section 3.6.9.2) for the composites of PLA-GF, PLA-3 80-20-GF, PLA-6 80-20-GF, PLA-9 80-20-GF and PLA-12 80-20-GF.

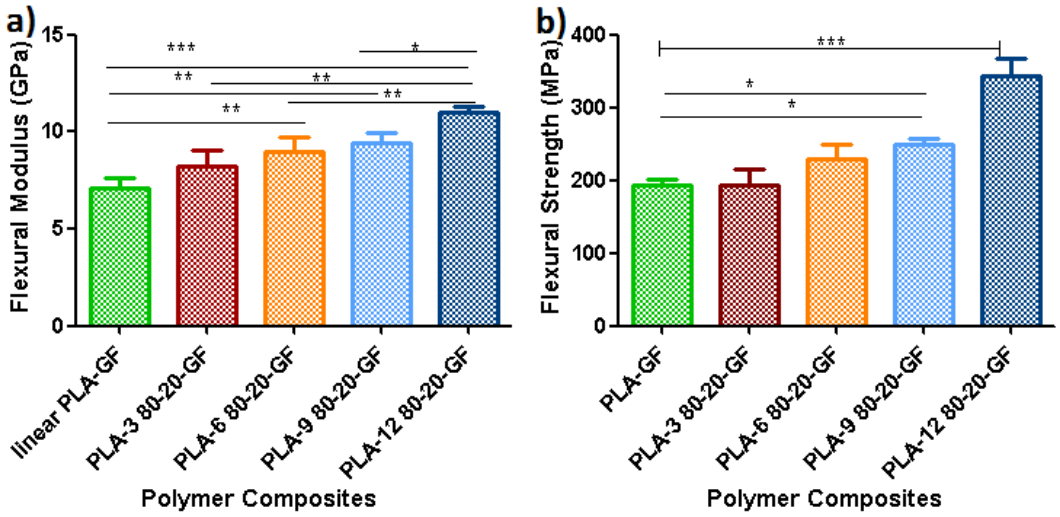

Figure 7.7: *a) The initial Flexural moduli and b) flexural strength of composites (with 21wt% E-glass fibre (woven mat)) linear PLA-GF, PLA-3 80-20-GF, PLA-6 80-20-GF, PLA-9 80-20-GF and PLA-12 80-20-GF.*

The flexural modulus for the PLA-GF composite was found to be 7.0 GPa and for blend composites with the same volume fraction of E-glass fibres the flexural modulus was observed to increase with increasing molecular weight of the SPLA in the matrix with values at 8.2 ($p>0.05$), 9.0 ($p<0.05$), 9.46 ($p<0.005$) and 11.03 ($p<0.005$) GPa for PLA-3 80-20-GF, PLA-6 80-20-GF, PLA-9 80-20-GF and PLA-12 80-20-GF respectively. Moreover, the flexural modulus of PLA-12 80-20-GF (11.03 GPa) also 33 % ($p<0.005$), 22% ($p<0.005$) and 16% ($p<0.05$) higher when compared to the flexural moduli of PLA-3 80-20-GF, PLA-6 80-20-GF, PLA-9 80-20-GF respectively. However, the flexural moduli of PLA-3 80-20-GF, PLA-6 80-20-GF, PLA-9 80-20-GF appeared to have no significant difference when compared to each other.

From Figure 7.7b it can be determined that the flexural strength of PLA-12 80-20-GF (343 MPa) to be statistically significantly higher compared to those of PLA-GF, PLA-3 80-20-GF, PLA-6 80-20-GF, PLA-9 80-20-GF by 77% ($p<0.005$), 77% ($p<0.005$), 49% ($p<0.005$), 37% ($p<0.005$) respectively. There was no significant difference between the flexural strength of linear PLA-GF, PLA-3 80-20-GF composites. There was,

however, a statistically significant increase ($p<0.05$) in the flexural strength of PLA-6 80-20-GF and PLA-9 80-20-GF composites in comparison to that of PLA-GF by 18% ($p<0.05$) and 22% ($p<0.05$) respectively.

The SEM micrographs (Figure 7.8) were taken using the method described in Chapter 3 Section 3.6.10.

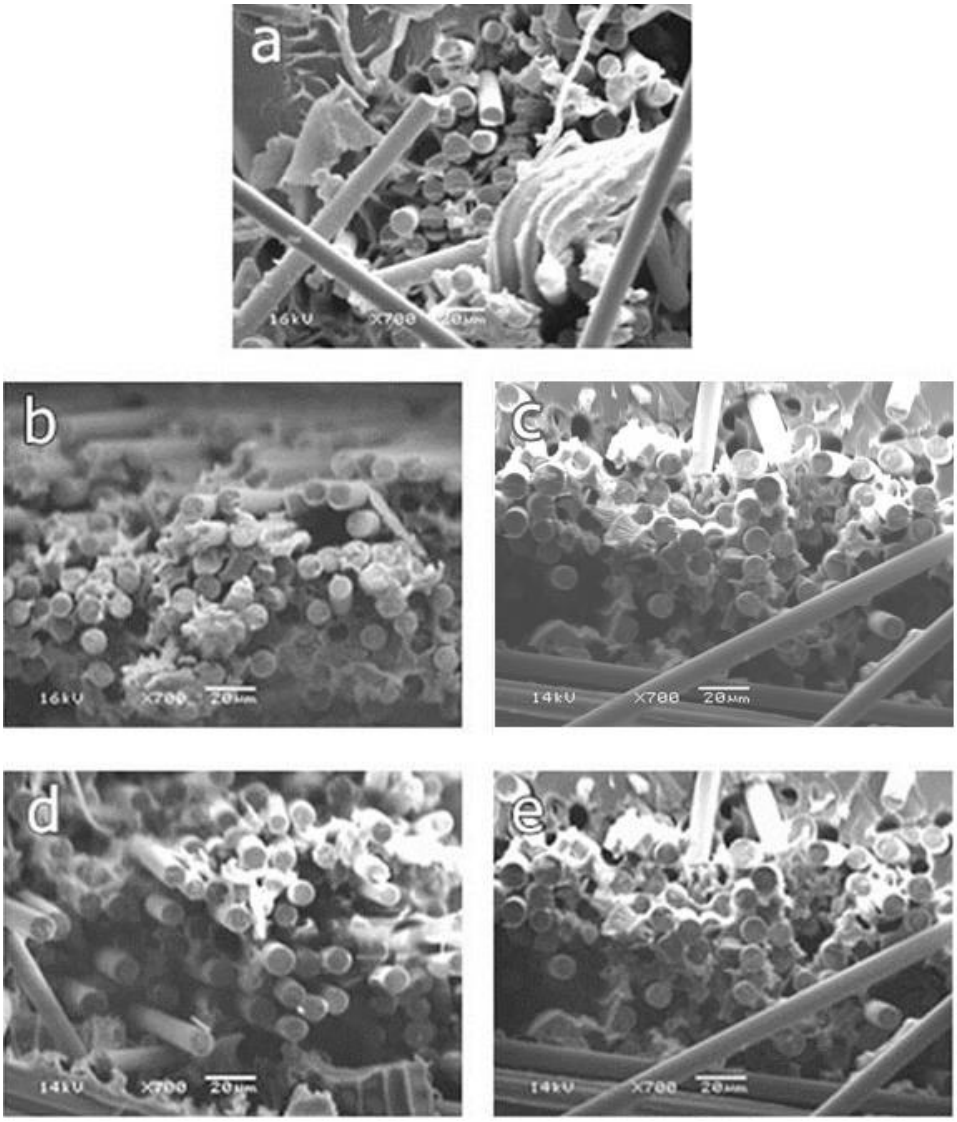

Figure 7.8: *SEM micrographs of a fractured surface of a) PLA-GF and b) PLA-3 80-20-GF c) PLA-6 80-20-GF d) PLA-9 80-20-GF e) PLA-12 80-20-GF non-degraded samples in deionised water at 50°C*

Figure 7.8(a), (b), (c), (d) and (e) is showing the fractured surface of PLA-GF, PLA-3 80-20-GF, PLA-6 80-20-GF, PLA-9 80-20-GF and PLA-12 80-20-GF composites respectively

prior to degradation. It can be seen that the fracture occurred by short fibre pull-out for all composites.

7.2.6 Degradation study

7.2.6.1 Flexural properties

Figure 7.9a shows the variation with flexural moduli of the composites over 21 days of immersion in deionised water at 50°C. Meanwhile, Figure 7.9b contains the flexural strength of the composites over 21 days of immersion in deionised water at 50°C.

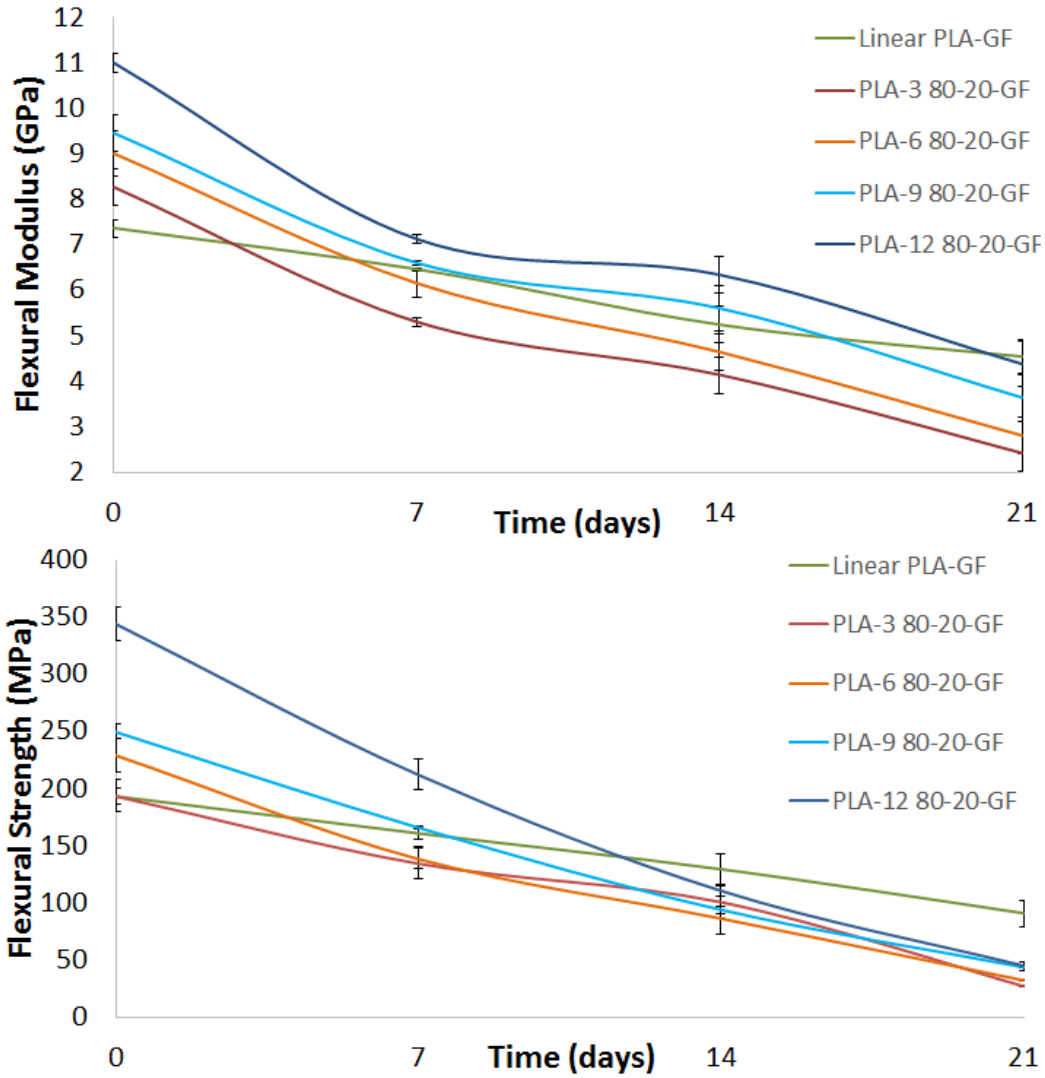

Figure 7.9: *a) The flexural moduli of PLA-GF, PLA-3 80-20-GF, PLA-6 80-20-GF, PLA-9 80-20-GF and PLA-12 80-20-GF composites* over 21 days after immersion in deionised water at 50°C b) *The flexural strength of PLA-GF, PLA-3 80-20-GF, PLA-6 80-20-GF, PLA-9 80-20-GF and PLA-12 80-20-GF composites over 21 days after immersion in deionised water at 50°C*

PLA-GF showed comparatively smaller variations in flexural modulus over the course of the 21 days of immersion compared to the blend composites. The flexural moduli of the blend composites exhibited a decrease over the 21 days of immersion in deionised water at 50°C. At day 21 of immersion, the flexural moduli of PLA-3 80-20-GF, PLA-6 80-20-GF, PLA-9 80-20-GF and PLA-12 80-20-GF composites showed a statistically significant decrease by 70% ($p<0.005$), 68% ($p<0.005$), 61% ($p<0.005$) and

60% ($p<0.005$) respectively whereas the value for PLA-GF decreased by only 37% ($p<0.05$) from an initial value of 7.0 GPa prior to degradation.

Again, the flexural strength of PLA-GF showed small differences over the course of the 21 days of immersion compared to the blend composites. The flexural strength of the blend composites decreased steadily until the end of the study. At day 21, the strength of PLA-3 80-20-GF, PLA-6 80-20-GF, PLA-9 80-20-GF and PLA-12 80-20-GF composites decreased by 86%, 85%, 82% and 85% respectively from the initial value whereas this value for the PLA-GF composite experienced a decrease in flexural strength by 53%.

7.2.6.2 Percentage (%) Mass loss

The percentage wet mass loss (measured by equation 3.6)) of PLA-GF, PLA-3 80-20-GF, PLA-6 80-20-GF, PLA-9 80-20-GF and PLA-12 80-20-GF composites over the 21 days immersion in deionised water at 50°C is shown in Figure 7.10.

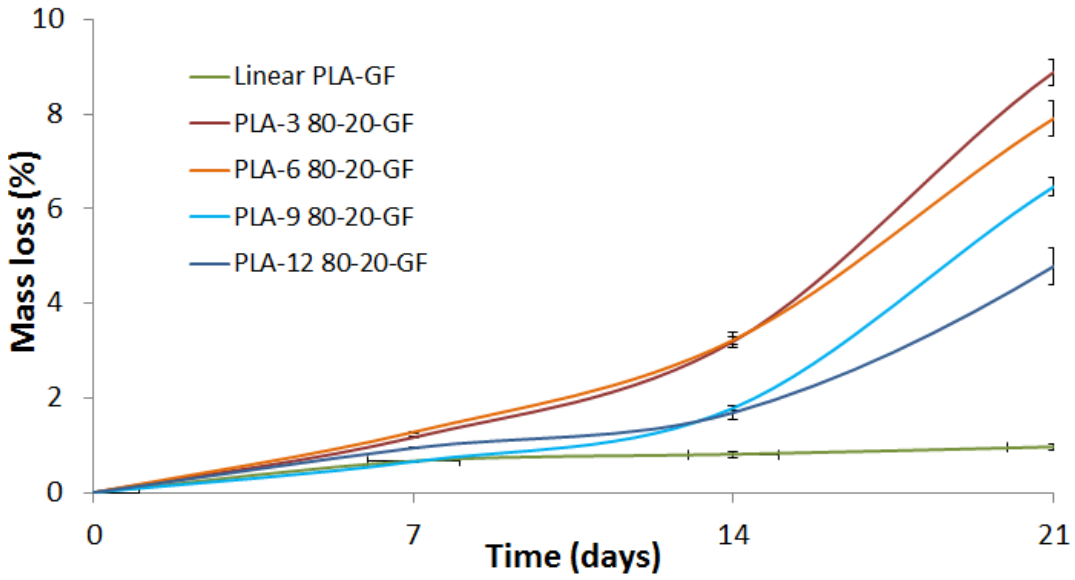

Figure 7.10: *The (%) wet mass loss of PLA-GF, PLA-3 80-20-GF, PLA-6 80-20-GF, PLA-9 80-20-GF and PLA-12 80-20-GF* composites *over 21 days of immersion in deionised water at 50°C*

After the initial day of immersion, the percentage wet mass loss increased statistically significantly for all the samples except PLA-GF over the duration of the study period. At day 21, the % wet mass loss of PLA-3 80-20-GF, PLA-6 80-20-GF, PLA-9 80-20-GF and PLA-12 80-20-GF composites increased to 8.8% ($p<0.005$), 6.4% ($p<0.005$), 7.9% ($p< 0.005$) and 4.7% ($p<0.005$) respectively. Meanwhile the PLA-GF experienced only 0.95% mass loss by day 21 of the study.

7.2.6.3 pH value

The pH analysis (as described in chapter 3 section 3.6.12.2) of the degradation media (deionised water) for linear PLA-GF and blend composites over 21 days is shown in Figure 7.11.

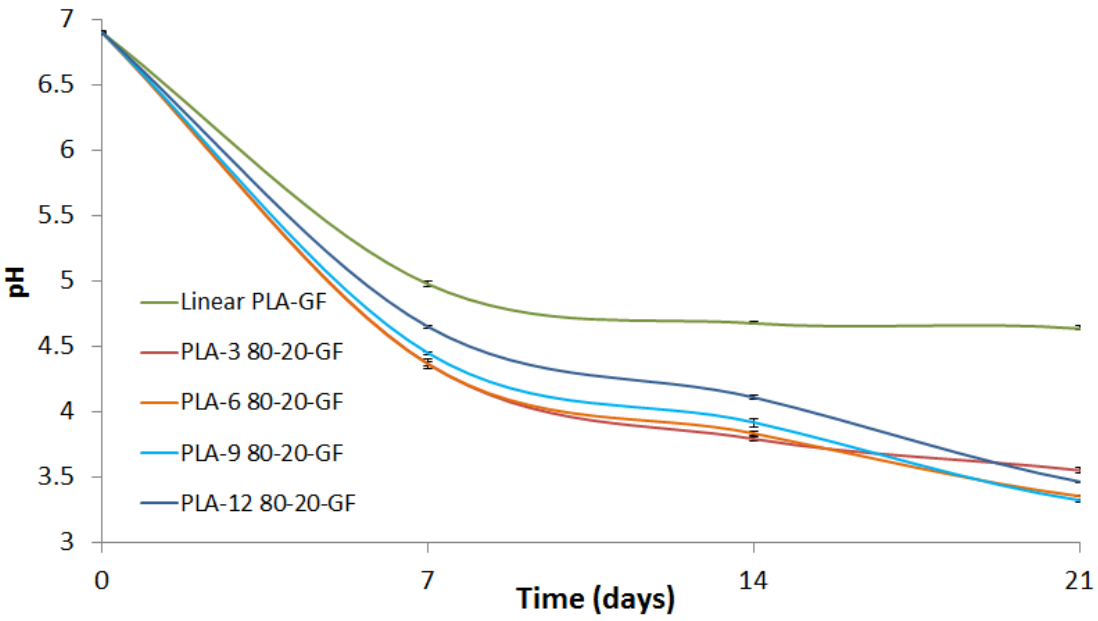

Figure 7.11: *The change in pH of PLA-GF, PLA-3 80-20-GF, PLA-6 80-20-GF, PLA-9 80-20-GF and PLA-12 80-20-GF composites over 21 days after immersion in deionised water at 50°C*

During the 1st 7days of study, the pH of the deionised water for linear PLA, PLA-3 80-20-GF, PLA-6 80-20-GF, PLA-9 80-20-GF and PLA-12 80-20-GF blend composites had decreased to 5.5, 4.3, 4.3, 4.5 and 4.7 respectively. However, from day 7 until day 21,

the pH value of blend composites started to decrease gradually whereas the pH profile for PLA-GF was found to be nearly same for the rest period of study. The pH of the deionised water was found at 3.5, 3.3, 3.4 and 3.3 for PLA-3 80-20-GF, PLA-6 80-20-GF, PLA-9 80-20-GF and PLA-12 80-20-GF respectively at day 21 of the study.

7.2.6.4 X-ray Diffraction (XRD)

The XRD spectra for the composites produced after degradation for 21 days is presented in Figure 7.12.

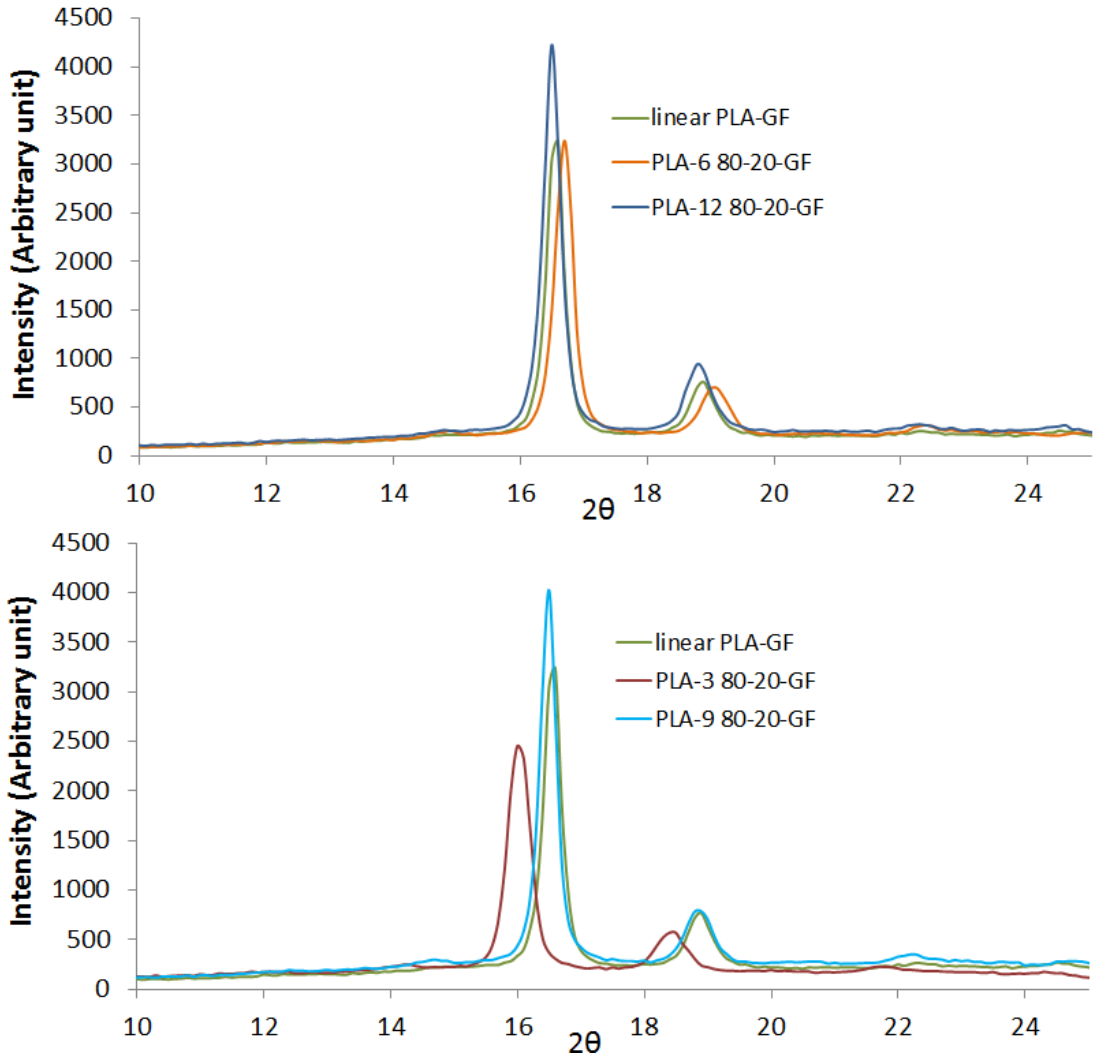

Figure 7.12: *XRD spectra of PLA-GF, PLA-3 80-20-GF, PLA-6 80-20-GF, PLA-9 80-20-GF and PLA-12 80-20-GF composites at 21 day of immersion in deionised water at 50°C*

A sharp peak was identified at ~16.5° (Miller indices of (200) and (110)) and a smaller peak at 18.5-19° (Miller index of (203)) for all composites. [11] The intensity of crystallinity peaks observed was very similar for PLA-9 80-20-GF and PLA-12 80-20-GF and was higher than that of linear PLA-GF, PLA-3 80-20-GF, PLA-6 80-20-GF composites.

7.2.6.5 Scanning Electron Microscopy (SEM)

The fractured surfaces for PLA-GF, PLA-3 80-20-GF, PLA-6 80-20-GF, PLA-9 80-20-GF and PLA-12 80-20-GF composites after 21 days of degradation are shown in Figure 7.13 (a), (b), (c), (d) and (e) respectively.

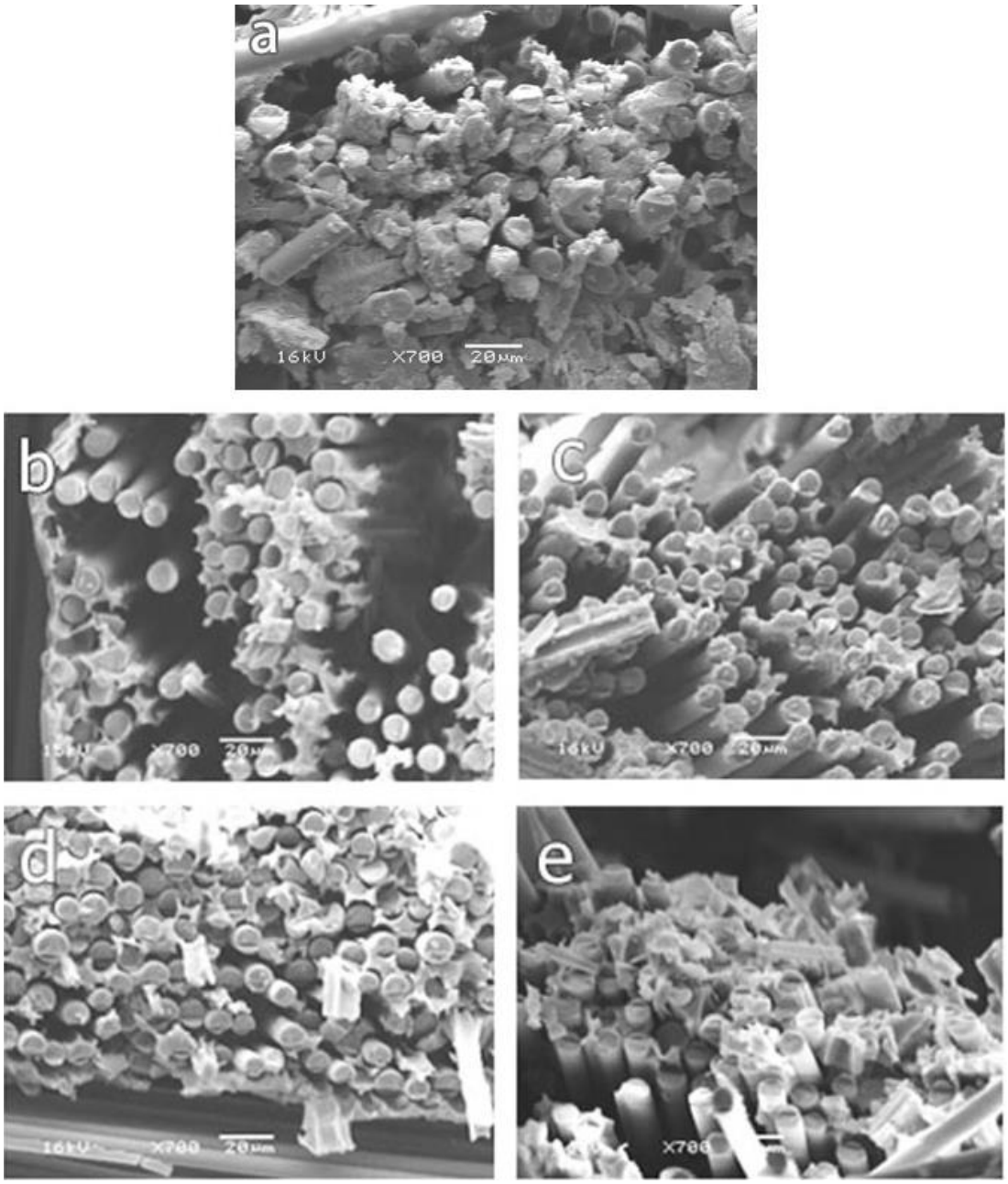

Figure 7.13: *SEM micrographs of a fractured surface of a) PLA-GF and b) PLA-3 80-20-GF c) PLA-6 80-20-GF d. PLA-9 80-20-GF e) PLA-12 80-20-GF after 21 days of immersion in deionised water at 50°C*

The SEM data collected after the degradation study, was observed to exhibit the loss of fibre matrix interface in all composites. However, for PLA-3 80-20-GF after degradation, demonstrated the greatest matrix loss observed, whilst the PLA-GF composites retained the most fibre matrix interface.

7.3 Discussion

The storage modulus, (G') and loss modulus, (G'') were plotted against temperature for linear PLA with PLA-12 80-20, PLA-9 80-20, PLA-6 80-20 and PLA-3 80-20 (see Figure 7.1A-D). Below the glass transition temperature (T_g), the molecules are thought almost immobile and to be in glassy state. Above T_g, with increasing temperature the mobility of the polymer chains is proposed to increase and so the loss modulus G'' would be increased above the storage modulus G' with increasing temperature. However, from Figure 7.1 A-D it can be seen that for both linear PLA and blends the loss modulus G'' did not increase above the storage modulus G' until the melting temperature (T_m) (~166°C). This can be explained in terms of crystallinity. For partially crystalline polymers such as PLA, as temperature increased above T_g, the polymer chains in the amorphous region started to show increased mobility. However, strong interaction forces exists between the molecules in crystalline region which caused the storage modulus to remain higher than the loss modulus value until the melting temperature.[12] This is because, on reaching the melting temperature, the molecules in crystalline zone also started to show mobility and then they lose the extended structure when the material reaches or exceeds its T_m value, at this point the loss modulus value is observed to be increased over the storage modulus value. The melting point for linear PLA and blends was identified to be in the region of 167°C and 166°C respectively (see Table 6.1). Thus the linear PLA and all blends showed the same behaviour such that the loss modulus increased over the storage modulus around ~166°C. Moreover Figure 7.1A-D demonstrated that at 80°C, when comparing the data or the blends, then the higher storage modulus was

obtained for blends containing SPLA of high mol. wt. (12 and 9 kDa) than blends containing low mol. wt. SPLA (3 and 6 kDa).

The shear viscosity of a molten polymer typically displays a constant value at very low shear rates, this is referred to as the zero shear viscosity (η_0). Moreover, if this value starts to deviate from η_0 at some characteristic shear rate this is called non-Newtonian behaviour.[13] From Figure 7.2 the viscosity of linear PLA was found to be the highest of all the samples investigated, i.e. 1.0×10^3 (Pa.s) at 175°C at low shear rate (0.01 s^{-1}). Moreover, the viscosity of the blends appeared to be lower than the viscosity of the linear PLA across the whole shear rate region. Additionally, for blends, the zero shear viscosity was observed to be decreased with decreasing mol. wt. of SPLA in blend. It was proposed that the lower viscosity of blends compared to the linear PLA could be due to molecular architecture resulting in the lower entanglement densities and fewer intermolecular interaction between branches of SPLA. [14-16].

In the shear rate region from 0.01 to 100 s^{-1}, linear PLA, PLA-12 80-20 showed shear thinning behaviour above 10 s^{-1} whereas PLA-3 80-20, PLA-6 80-20 and PLA-9 80-20 showed Newtonian behaviour. Kim *et al.* concluded that for star shaped PLA with branches long enough to entangle that the zero shear viscosity increased with branch length and exhibited more noted shear thinning behaviour than the linear PLA of comparable molecular weight.[17] So, it was proposed that because the blends PLA-3 80-20, PLA-6 80-20 and PLA-9 80-20 exhibited reduced zero shear viscosity and temperature independent/Newtonian behaviour (i.e. the viscosity values were nearly constant across the whole shear rate region) that this was due to the lower level of or complete absence of any polymer chain entanglement of low mol. wt. (M_n) SPLA

in blends. [18] Khajeheian and Rosling [13] also observed lower zero shear viscosity for blends (linear PLA with 30% of SPLA of M_n~2.4 kDa and 5.4 kDa) at ~20 Pa.s in comparison to the linear PLA at ~100 Pa.s. They attributed this to the decrease of total molecular weight of the blends due to the addition of low mol. wt. SPLA, however, they observed higher shear thinning behaviour for blends and explained that this might be to be due to the plasticising effect of low molecular weight SPLA.

From Figure 7.3a it can be seen that the elongation at break for all blends at R.T. was found to be increased statistically significantly than the elongation at break of linear PLA. So, it was concluded that blending of SPLA with linear PLA acted as plasticiser.[2, 19] Phuphuak *et al.* [2] blended SPLA with linear PLA and reported higher (~15%) elongation of break for the blend containing 20wt% SPLA whereas for linear PLA the elongation of break was reported to be 5.36% and attributed this to the plasticisation effect of SPLA. Baiardo *et al.* [20] used poly ethylene glycol to plasticise linear PLA and reported that with increasing plasticiser content, the tensile modulus and tensile strength decreased, while elongation at break increased.

However, after heat treatment the elongation at break of all the materials had decreased for all composites compared to the value of these samples at R.T. This implies that upon heat treatment the % crystallinity of linear PLA and blends increased (also see Table 6.1) and the plasticisation effect decreased.[21, 22] Chiu *et al.* [22] prepared blends of poly(lactic acid) (PLA)/poly (butylene adipate-co-terephthalate) of different compositions and heat treated at 100°C for 8hr and 24 hr and reported that the modulus and tensile strength increased, however, the elongation at break decreased due to increased crystallinity.

The tensile moduli of linear PLA and blends for R.T. and H.T. are showing in Figure 7.4a and Figure 7.4b respectively. From Figure 7.4a it can be seen that the tensile moduli of blends at R.T. had decreased statistically significantly in comparison to the linear PLA. These lower tensile moduli for blends at R.T. was expected due to lower crystallinity in comparison to linear PLA. Moreover, as it was proposed that the addition of SPLA acted as plasticiser which increased the elongation at break and decreased the tensile moduli of blends. [23] Al-Itry *et al.* [24] blended poly(butylene-adipate-co-terephtalate) with linear PLA and reported that the elongation at break increases from 14% (linear PLA) to 50% (blends) whereas the tensile modulus decreased from 1350 MPa to 820 MPa. However, Figure 7.4b it can be seen that, after heat treatment the tensile moduli value of both linear PLA and blends increased due to increased crystallinity. However, the tensile moduli of heat treated blends did not increase statistically significantly than the heat treated linear PLA.

Figure 7.5a and Figure 7.5b the tensile strength value of linear PLA and blends at R.T. and H.T. respectively. From Figure 7.5a it can be said that the tensile strength values of blends at R.T. had decreased statistically significantly ($p<0.005$) in comparison to the linear PLA. Liu *et al.* [19] prepared blends of PLA and a long-chain branched copolymer (LB-PCLA) of PLA and reported that the tensile strength of the blend (with 15wt% of block co-polymer) (46.7 MPa) was lower than that of neat PLA (57.7 MPa).

However, after heat treatment the tensile strength value of PLA-3 80-20, PLA-6 80-20, PLA-9 80-20 and PLA-12 80-20 had increased by 13 % ($p<0.05$), 54 % ($p<0.005$), 40 % ($p<0.005$) and 36 % ($p<0.05$) respectively in comparison to the linear PLA (28 MPa). No specific trend was observed in terms of increasing tensile strength with mol.

wt. of SPLA in blends. After heat treatment the statistically significantly higher tensile strength value was obtained for blends PLA-6 80-20, PLA-9 80-20 and PLA-12 80-20 in comparison to the linear PLA might be ascribed to the good balance of amorphous (causes plasticisation effect) and crystalline domains in blends since crystallinity increased after heat treatment and caused reinforcement of the amorphous phase. [2, 25] Rathi *et al*.[25] blended triblock copolymer (PDLA-PEG-PDLA) into Poly(L-Lactic Acid) (PLLA) to improve the mechanical properties. At room temperature, the blend containing 15 % triblock copolymer was ductile and after heat treatment the tensile strength increased for the blend to 72 MPa whereas for linear PLA the value observed was around 13 MPa. They concluded that the crystalline phase acted as a filler in a continuous amorphous phase and caused an increase in the tensile strength in comparison to the pure PLA.

The XRD spectra for linear PLA and SPLA blend composites (Table 3.7) prior to degradation are shown in Figure 7.6. It was evident from the XRD spectra that before hydrolytic degradation the highest crystalline peak intensity was observed for PLA-GF composite. The peak intensity of blend composites was lower than the linear PLA composite, however, the lowest peak intensity was observed for the PLA-3 80-20-GF. This observation correlated well with the heat treated linear PLA and blends XRD spectra (Figure 6.10c and d)

The flexural modulus and strength data for the composites are presented in Figure 7.7a and Figure 7.7b. From Figure 7.7a and b it can be said that the lowest flexural modulus and strength was observed for PLA-GF composite at 7.09 GPa and 193 MPa. Statistically significantly ($p<0.005$) higher flexural modulus and strength were

obtained for PLA-6 80-20-GF, PLA-9 80-20-GF and PLA-12 80-20-GF composites in comparison to the PLA-GF composite. This was attributed to improved homogeneous dispersion and better impregnation (i.e. compatibilisation with the surface of the fibre with the matrix) of the reinforcing E glass fibres by the blend matrix than the linear PLA on its own. Myard *et al.* [10] prepared a laminated composite containing glass fibres as reinforcing agent and a blend of star and linear polyamide (nylon -6) as matrix. They concluded that the high fluidity or low viscosity of the star polymer caused good impregnation of the reinforcing fibres with the matrix without declining the mechanical properties of the prepared composites. They compared the mechanical properties of the star polymer (thermoplastic) composites with the composites of thermosetting (Epoxy) matrix and reported the flexural modulus of the resultant star polymer/glass fibre composite (at 21.2 GPa) did not decrease when compared to the flexural modulus of epoxy polymer/glass fibre composite (at 21.0 GPa).

In this study, the lowest viscosity (Figure 7.2) was obtained for the PLA-3 80-20 blends at 121 (Pa.s) whereas the highest viscosity was found for the linear PLA at 1050 (Pa.s). This highest fluidity exhibited by the PLA-3 80-20 blends for the data discuss above was expected that it would achieve the highest impregnation of E-glass fibres. Thus, in turn, better mechanical (flexural modulus and strength) properties would be expected from this a blend composite when compared to composites with a matrix consisting of linear PLA alone and other blends. However, among linear PLA and blend composites the highest flexural modulus and strength was obtained for PLA-12 80-20-GF composite at 11.03 GPa and 343 MPa respectively. This result was attributed to the fact that, during preparing composites by hot pressing at 175°C, the

crystallisation of linear PLA and blends had also occurred around E glass fibre (Figure 7.6) which also played an important role in determining the mechanical properties of composites. [26] Thus, it was proposed that the PLA-12 80-20 blend possesses comparatively higher crystallinity and lower viscosity (caused better fibre impregnation) in comparison to other blends and linear PLA respectively and it is likely that a combination of both of these criterion had increased the mechanical properties of PLA-12 80-20-GF composite such that it was the highest value than other prepared composites.

Figure 7.8 contains a view of the fractured surface of PLA and blend composites prior to degradation. For all composites, similar fractured morphology was observed displaying fibre pull out of the matrix. However, for PLA-GF composite the matrix was seen to become debonded from the outer surface of the fibres, whereas for blend composites the fibres remained bonded with the matrix. This appeared to be consistent with the increase in flexural modulus and strength for blends in comparison to PLA-GF composite.

Figure 7.9a and b showed the flexural moduli and strength respectively for linear PLA and blend composites after 21 days of hydrolytic based degradation. The moduli and strength of blend composites were observed to have experienced a greater reduction in value than the PLA-GF composite during the whole period of the study. The hydrolytic degradation of PLA based composites depends on the degradation of the polymer *via* hydrolysis of the ester group in the polymer backbone.[27] The SPLA used in this study was sorbitol initiated star poly(lactic acid) with -OH chain end group which is hygroscopic/hydrophillic in nature. Thus it was proposed that these multiple

-OH group caused greater water penetration into the matrix which accelerated the hydrolysis of blend composites in comparison to linear composite. Alternatively, they may result in greater levels of water being entrained into the sample during processing, especially at the lower temperatures. [27, 28] Perera *et al.* [28] produced PLA phosphate glass fibre composites where they coated the phosphate glass fibre with sorbitol initiated linear PLA before making composite *via* a laminate film stacking process. They observed better initial longitudinal flexural modulus and strength value for composites with coated phosphate glass fibre (9 GPa and 152 MPa respectively) in comparison to uncoated phosphate glass fibre (3 GPa and 97 MPa respectively) composite which they used as control. However, after 21 days of immersion in PBS (phosphate buffer solution) at 37°C, the strengths and moduli of sorbitol PLA coated composites appeared to have experienced a greater reduction in value (74 MPa and 3 GPa respectively) than the control composite (98 MPa and 4 GPa respectively). They attributed this effect to the wicking of water along the exposed fibre ends which caused the attack of the hygroscopic sorbitol head group at the interface.

After 21 days of degradation, all blend composites have a nearly statistically similar flexural strength profile at 33 MPa, 33 MPa, 45 MPa and 45 MPa respectively, whereas for PLA-GF flexural strength was found to be at 90 MPa (Figure 7.9b). This observation suggested that blend composites experienced a loss of the fibre-matrix interface during hydrolysis degradation. This could be again attributed to the hydrolysis reaction as result of water absorbed due to the presence of -OH group in SPLA. [27-30] It was concluded that the most likely explanation for the loss of the fibre-matrix interface of blend composites was that it was caused loss of flexural strength of the composites over the whole duration of the study.

Moreover, among blend composites, after 21 days of immersion in deionised water, PLA-3 80-20-GF composite experienced the highest percentage decrease in flexural modulus and strength when compared to the other blend composites, which could be attributed to the lower crystallinity of this composite in comparison to the other composites since the degradation process of semi-crystalline polymers occurred *via* the degradation of amorphous phase.[31] Also, the processing procedures in this study were based on wt% this means that with this low mol. wt. SPLA, the highest number of chain ends (containing –OH group) are added so giving the greatest potential to increase the hydrolytic degradation.

Figure 7.10 shows the percentage wet mass loss for all the composites over 21 days' immersion in deionised water at 50°C. The percentage wet mass loss for PLA-GF composites did not differ significantly over the duration of immersion. However, for the blend composites after day 7 the percentage wet mass loss gradually increased and the maximum percentage mass loss was observed for PLA-3 80-20-GF composite (8.84 ± 0.7 %) at day 21 and the minimum percentage mass loss was observed for PLA-12 80-20-GF composite to 4.7 ± 0.2 % by day 21. The wet mass loss was suggested to be due to the continuous loss of the fibre-matrix interface caused by hydrolysis as a result of water absorption.[28, 31]

The pH analysis of the degradation media (deionised water) for all the composites over 21 days is shown in Figure 7.11. The pH of the deionised media for all composites experienced a significant decrease (from ~7 to ~4.9) in the first 7 days of immersion which correlates well with the significant decrease of mechanical (flexural) properties for all composites within the first 7 days' degradation study.

From day 7 to day 21 the pH of PLA -GF varied slightly around 4.9 to 4.6. On the other hand, the pH of the deionised water for blend composites decreased and became ~3.4 at day 21. The profile of the decrease of pH for PLA-3 80-20-GF, PLA-6 80-20-GF, PLA-9 80-20-GF and PLA-12 80-20-GF composites was statistically similar ($p>0.05$) over the whole period of degradation study. [14] The decrease in pH was most likely caused by hydrolytic degradation of PLA caused the dissociation being catalysed by the presence of the lactic acid monomer/oligomer acid end-group [-COOH] of PLA. This is created by the degradation process so is a cumulative effect and resulted in an acidic environment.[32]

In this study a significant increase in crystalline peak was observed for both linear and blend composites after hydrolytic degradation at day 21 in deionised water at 50°C (Figure 7.12). A sharp peak was found at ~16.5° and a smaller peak at 18.5-19°. [33] This indicates the preferential degradation of the amorphous matrix of linear PLA and blends during the period of hydrolytic degradation. Ndazi and Karlsson [34] also suggested that the hydrolysis of the semi-crystalline PLA started in the amorphous region and this phenomena increases with the hydrolysis temperature.

However, the intensity of crystalline peak at ~16.5° observed for PLA-12 80-20-GF and PLA-9 80-20-GF after degradation was higher in comparison to the linear PLA-GF, indicated higher crystallinity of these blend composites than that of the linear PLA-GF. This increased crystallisation of PLA-12 80-20-GF and PLA-9 80-20-GF in comparison to the linear PLA composites suggested the degradation of most of the amorphous phase of these blend composites. On the other hand, for PLA-6 80-20-GF a similar intensity of crystalline peak and for PLA-3 80-20-GF lower intensity of

crystalline peak was observed than that of the linear PLA-GF. This phenomenon again indicated that low crystalline phase present for the PLA-3 80-20-GF and PLA-6 80-20-GF composites didn't increase the crystallinity than the linear PLA-GF even after the degradation of amorphous region.

Felfel *et al.* also studied the hydrolytic degradation of PLA and phosphate glass fibre composites in PBS at different temperature 21°C, 37°C, 50°C, 65°C, 75°C and 85°C. They observed no sharp diffraction peaks after degradation in PBS at 21°C and 37°C. However, after degradation at the higher temperatures (50°C, 65°C, 75°C and 85°C) they identified two sharp peaks at 2θ = 16.5 and 19.[30] They suggested that this increasing portion of crystalline phases within the polymer chain was due to degradation of the amorphous phases at higher temperature leaving behind a higher percentage crystallinity. [31]

From the micrographs shown in Figure 7.13, the fracture morphology after degradation of 21 days was investigated and found that matrix loss occurred for all the composites. The E glass fibres were separated from each other with no matrix material around them.[28] The highest matrix loss was observed for PLA-3 80-20-GF composites (Figure 7.13b), whilst comparatively low matrix loss was observed for PLA-GF composite (Figure 7.13a). This indicated higher amount of hydrolytic degradation for PLA-3 80-20 matrix due to the presence of hydrophilic -OH chain end group of S-PLA in matrix and more amorphous regions which allowed water ingress and higher loss of fibre matrix Interface during hydrolytic degradation. This result also appeared to be consistent with composites increased crystallinity, percentage mass loss, lower pH value and loss of flexural properties after 21 days of degradation study.

7.4 Conclusions

From the above discussion it can be concluded that

- The lowest viscosity and Newtonian behaviour was observed for blend PLA-3 80-20 which had the lower mol. wt. (M_n~3 kDa) SPLA. Blends with high mol. wt. of SPLA PLA-12 80-20 (M_n~12 kDa) showed comparatively higher viscosity (lower than the linear PLA) and shear thinning behaviour which was behaved to be due to the presence of polymer chain entanglement of high mol. wt. of SPLA in the blends.
- For samples at R.T., the elongation at break observed for all blends was found to be statistically significantly higher than the linear PLA. However, the tensile modulus and tensile strength value was found to have decreased statistically significantly compared to that of linear PLA. So, it can be said that for samples at R.T. SPLA acted as plasticiser for linear PLA.
- After heat treatment, for all samples, the elongation at break decreased whereas the tensile modulus and strength increased. No specific trend was observed for the mol. wt. of SPLA with mechanical properties of the blends.
- For the composites no statistically significant improvement in mechanical (flexural modulus and strength value) properties was observed for PLA-3 80-20-GF, however, this value increased statistically significantly for the other blend composites in comparison to that of linear PLA composite. The highest flexural modulus and strength value were found for PLA-12 80-20-GF which may have attributed to the combination of higher crystallinity and lower viscosity (and better impregnation) of PLA-12 80-20 matrix in making composites.

- During degradation study the higher hydrolytic degradation of blend matrix was observed which possibly due to the presence of -OH chain end group of SPLA caused higher water penetration, greater wet mass loss, loss of fibre matrix interface and decrease in mechanical properties than linear PLA matrix. Higher hydrolysis of blend matrix also produced higher number of acidic chain end group and resulted in lower pH ~3 for degradation media of blend composite than composite with linear PLA (pH~5).
- Among blend composites, higher degradation was observed for low mol. wt. SPLA (PLA-3 80-20-GF) composite than that high mol. wt. SPLA (PLA-12 80-20-GF) composite, which possibly attributed to the lower crystallinity low mol. wt. SPLA, since the amorphous segments underwent faster degradation than the crystalline segment of PLA.

7.5 References

1. *Theodorakis, P., et al., Effective interaction parameter of linear/star polymer blends and comparison with that of linear/linear and star/star blends. The Journal of chemical physics, 2007.* ***126****(17): p. 174904.*

2. *Phuphuak, Y., et al., Balancing crystalline and amorphous domains in PLA through star-structured polylactides with dual plasticizer/nucleating agent functionality. Polymer, 2013.* ***54****(26): p. 7058-7070.*

3. *Regnell Andersson, S., et al., Customizing the hydrolytic degradation rate of stereocomplex PLA through different PDLA architectures. Biomacromolecules, 2012.* ***13****(4): p. 1212-1222.*

4. *Wang, L., et al., Blends of linear and long-chain branched poly (l-lactide) s with high melt strength and fast crystallization rate. Industrial & Engineering Chemistry Research, 2012.* ***51****(30): p. 10088-10099.*

5. *Ouchi, T., S. Ichimura, and Y. Ohya, Synthesis of branched poly (lactide) using polyglycidol and thermal, mechanical properties of its solution-cast film. Polymer, 2006.* ***47****(1): p. 429-434.*

6. *Hossain, K.M.Z., Extension of the use of cellulose nanowhiskers in composite materials. 2014, University of Nottingham.*

7. *Granda, L., et al., Fully biodegradable polylactic composites reinforced with bleached softwood fibers. Cellulose Chemistry and Technology, 2016.* ***50****(3-4): p. 417-422.*

8. *Haque, P., et al., Interfacial properties of phosphate glass fibres/PLA composites: Effect of the end functionalities of oligomeric PLA coupling agents. Composites Science and Technology, 2010.* ***70****(13): p. 1854-1860.*

9. *Gerard, P., M. Glotin, and G. Hochstetter, Composite material via in-situ polymerization of thermoplastic (meth) acrylic resins and its use. 2012, Google Patents.*

10. *Myard, P. and F. Philippon, Composite materials comprising a reinforcing material and a star polyamide as a thermoplastic matrix, the precursor compound article of said materials and the products obtained using same. 2008, Google Patents.*

11. *Iannace, S., et al., Influence of crystal and amorphous phase morphology on hydrolytic degradation of PLLA subjected to different processing conditions. Polymer, 2001.* ***42****(8): p. 3799-3807.*

12. *Mezger, T.G., The rheology handbook: for users of rotational and oscillatory rheometers. 2006: Vincentz Network GmbH & Co KG.*

13. *Khajeheian, M.B. and A. Rosling, Preparation and characterization of linear and star-shaped poly L-lactide blends. Journal of Applied Polymer Science, 2016.* ***133****(2).*

14. *Ebrahimi, T., S.G. Hatzikiriakos, and P. Mehrkhodavandi, Synthesis and Rheological Characterization of Star-Shaped and Linear Poly (hydroxybutyrate). Macromolecules, 2015.* ***48****(18): p. 6672-6681.*

15. *Gupta, R.K., Polymer and composite rheology. 2000: CRC Press.*

16. *Dorgan, J.R., J.S. Williams, and D.N. Lewis, Melt rheology of poly (lactic acid): Entanglement and chain architecture effects. Journal of Rheology (1978-present), 1999.* ***43****(5): p. 1141-1155.*

17. *Kim, E.S., B.C. Kim, and S.H. Kim, Structural effect of linear and star-shaped poly (L-lactic acid) on physical properties. Journal of Polymer Science Part B: Polymer Physics, 2004.* ***42****(6): p. 939-946.*

18. *Cifre, J.H., et al., Steady-state behavior of star polymers in dilute flowing solutions via brownian dynamics. Polymer, 2005.* ***46****(18): p. 6756-6766.*

19. *Liu, M.-J., et al., Biodegradable polylactide based materials with improved crystallinity, mechanical properties and rheological behaviour by introducing a long-chain branched copolymer. RSC Advances, 2015.* ***5****(52): p. 42162-42173.*

20. *Baiardo, M., et al., Thermal and mechanical properties of plasticized poly (L-lactic acid). Journal of Applied Polymer Science, 2003.* ***90****(7): p. 1731-1738.*

21. *El-Hadi, A., et al., Correlation between degree of crystallinity, morphology, glass temperature, mechanical properties and biodegradation of poly (3-hydroxyalkanoate) PHAs and their blends. Polymer testing, 2002.* ***21****(6): p. 665-674.*

22. *Chiu, H.-T., et al., Heat treatment effects on the mechanical properties and morphologies of poly (lactic acid)/poly (butylene adipate-co-terephthalate) blends. International Journal of Polymer Science, 2013.* ***2013****.*

23. *Al-Itry, R., K. Lamnawar, and A. Maazouz, Improvement of thermal stability, rheological and mechanical properties of PLA, PBAT and their blends by reactive extrusion with functionalized epoxy. Polymer Degradation and Stability, 2012.* ***97****(10): p. 1898-1914.*

24. *Takayama, T., M. Todo, and H. Tsuji, Effect of annealing on the mechanical properties of PLA/PCL and PLA/PCL/LTI polymer blends. Journal of the Mechanical Behavior of Biomedical Materials, 2011.* ***4****(3): p. 255-260.*

25. *Rathi, S., et al., Toughening semicrystalline poly (lactic acid) by morphology alteration. Polymer, 2011.* ***52****(19): p. 4184-4188.*

26. *Katogi, H. and K. Takemura, The effect of crystallinity on the mechanical properties of plain woven carbon reinforced composites using polypropylene. WIT Transactions on The Built Environment, 2014.* ***137****: p. 301-309.*

27. *Hasan, M.S., et al., Cytocompatibility and mechanical properties of short phosphate glass fibre reinforced polylactic acid (PLA) composites: effect of coupling agent mediated interface. Journal of Functional Biomaterials, 2012.* ***3****(4): p. 706-725.*

28. *Perera, M.S., The use of sorbitol-initiated polylactic acid as a coupling agent in resorbable phosphate glass fibre reinforced polylactic acid composites. 2015, University of Nottingham.*

29. *Hasan, M.S., Phosphate glass fibre reinforced composite for bone repair applications: investigation of interfacial integrity improvements via chemical treatments. 2012, University of Nottingham.*

30. *Felfel, R.M., et al., Accelerated in vitro degradation properties of polylactic acid/phosphate glass fibre composites. Journal of Materials Science, 2015.* ***50****(11): p. 3942-3955.*

31. *Felfel, R.M., et al., Investigation of crystallinity, molecular weight change, and mechanical properties of PLA/PBG bioresorbable composites as bone fracture fixation plates. Journal of Biomaterials Applications, 2012.* ***26****(7): p. 765-789.*

32. *Siparsky, G.L., K.J. Voorhees, and F. Miao, Hydrolysis of polylactic acid (PLA) and polycaprolactone (PCL) in aqueous acetonitrile solutions: autocatalysis. Journal of Environmental Polymer Degradation, 1998.* ***6****(1): p. 31-41.*

33. *Zhou, Z., et al., Influence of degradation of poly-L-lactide on mass loss, mechanical properties, and crystallinity in phosphate-buffered solution. Journal of Macromolecular Science®, 2009.* ***48****(2): p. 309-317.*

34. *Karlssion, S. and B.S. Ndazi, Characterization of hydrolytic degradation of polylactic acid/rice hulls composites in water at different temperatures. Express Polymer Letters, 2011.* ***5****(2): p. 119-131.*

CHAPTER 8

8 Conclusions and Future work

8.1 Conclusions

The aim of this study was to investigate the effects of including branched biopolymer structures as matrix components for use in composites and also to investigate if the effects of branched structures could be translated between non-biopolymer and biopolymer systems.

The following conclusions were drawn from the work conducted in this thesis:

- Blending of HB2 with reactive (vinyl; -CH=CH_2) chain end groups increased the T_g, thermal stability, viscosity and modulus values after they became crosslinked at high temperature. To determine the crosslinked temperature rheological study was carried out, however, no specific crosslinked temperature was identified since the storage modulus was higher than the loss modulus value from near the glass transition temperature up to~200°C.

- On the other hand, H-HB2 with non-reactive functional groups decreased the T_g, viscosity, mechanical properties of the LP-H-HB2 blend which was suggested to be due to the lack of polymer chain entanglement of the H-HB2 polymer. However, the saturated ethyl chain end group of the H-HB2 polymer caused higher thermal stability of LP-H-HB2 blends in comparison to linear LP. Crystallinity of the LP-H-HB2 80-20 blend was observed and was suggested to be due to reorganisation of ethyl chain end after heat treatment at 200°C for 20 min.

- Composites prepared using LP-HB2 and LP-H-HB2 blends showed lower and higher mechanical properties respectively in comparison to composite with LP matrix. The highest flexural modulus and strength values were obtained for composites using LP-H-HB 80-20 as matrix which was attributed to the improved wettability hence better adhesion and chain end crystallinity of LP-H-HB 80-20 matrix that increased the mechanical properties of the composite.

- Blending SPLA of four different mol. wt. with linear PLA decreased the thermal stability, T_g, crystallinity and the mechanical properties in comparison to linear PLA. However, the hydrolytic degradation of the blends was observed to have increased. Like HB polymer, the effect of SPLA was also attributed to the lack of polymer chain entanglement. Moreover, the thermal, crystallinity and mechanical properties of blends decreased mostly for the lower mol. wt. SPLA (3 kDa) and this was attributed to the greater free volume in the low mol. wt. SPLA in comparison to the high mol. wt. SPLA.

- After heat treatment the crystallinity of the blends increased in comparison to the value of the blends at R.T., however, not higher than the linear PLA. Among blends, the higher crystallinity was found for the blend (PLA-12 80-20) containing higher mol. wt. SPLA.

- The lower viscosity and Newtonian behaviour was observed for all the SPLA blends with exception of PLA-12 80-20, for which shear thinning behaviour was observed which indicated that there some chain entanglement in the high mol. wt. SPLA blend (PLA-12 80-20) may have been present.

- All blend composites with the exception of low mol. wt. SPLA (i.e. PLA-3 80-20-GF) showed significantly ($p<0.05$) higher flexural modulus and strength in comparison to linear SPLA. This was suggested to be due to the lowest crystallinity of PLA-3 80-20 blend that caused no significant ($p<0.05$) improvement in the mechanical properties of PLA-3 80-20-GF composites in comparison to composites with linear PLA (PLA-GF) although PLA-3 80-20 showed the lowest viscosity.

- On the other hand, significantly ($p<0.05$) increased flexural modulus and strength for PLA-12 80-20-GF composite was observed in comparison to the linear PLA-GF and other blend composites, which was attributed to the combination of lower viscosity of PLA-12 80-20 in comparison to linear PLA and higher crystallinity than the other blends which led to better wettability hence adhesion and increased mechanical properties.

8.2 Future work

Based on the overall summary of this project, the following points are suggested for future investigations

- Since HB1 and HB2 was found to be crosslinked just above the glass transition temperature and did not show liquid/viscous behaviour even at high temperature, further functional group modification of HB1 and HB2 or blending these polymers with other additives could be investigated to delay the crosslinking of HB1 and HB2 polymers at comparatively higher temperature. Thus a temperature range could be found at which the matrix could be in liquid/viscous state, wet the fibre better and then crosslinked at high temperature to produce composites with better mechanical properties.

- For composites with blends of H-HB2 and SPLA, the studied compositions and other blend compositions (for example 30wt% of H-HB2 and SPLA in blends with their linear analogues) could be used as coupling agents for glass fibres to improve and enhance the fibre matrix adhesion.

- Better interfacial properties of bio-composites (using phosphate glass fibre as reinforcement) could be obtained using neat SPLA as coupling agent (since this polymer as a coupling agent could be applied as a polymer solution).

- Blends of SPLA with linear PLA could be used as an alternate to linear PLA in application where lower crystallinity and higher hydrolytic degradability properties were desirable